



Design of *Pseudomonas putida* fermentations for robust biomanufacturing

Jensen, Jesper Wang

Publication date:
2023

Document Version
Publisher's PDF, also known as Version of record

[Link back to DTU Orbit](#)

Citation (APA):
Jensen, J. W. (2023). *Design of Pseudomonas putida fermentations for robust biomanufacturing*. Technical University of Denmark.

General rights

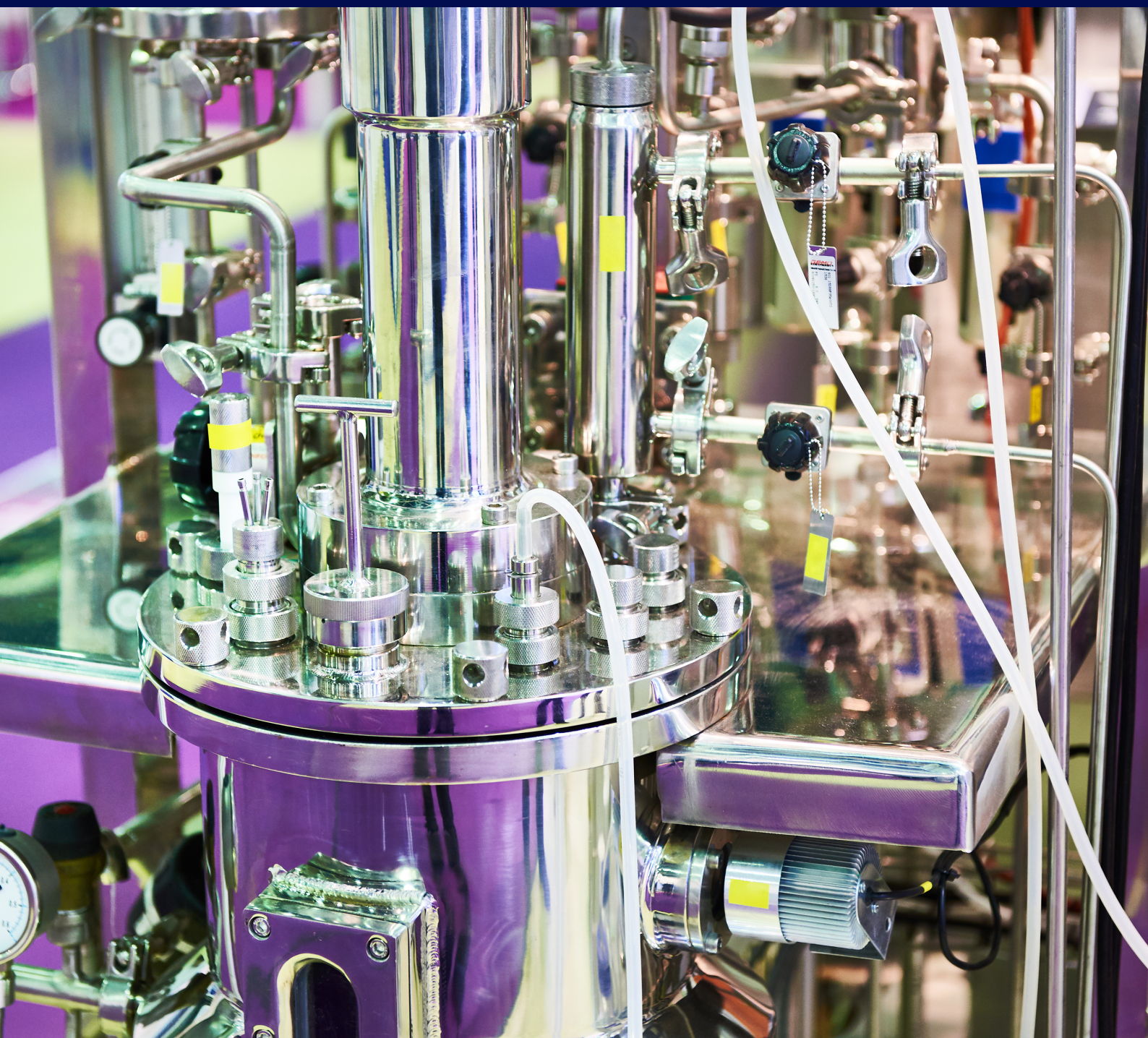
Copyright and moral rights for the publications made accessible in the public portal are retained by the authors and/or other copyright owners and it is a condition of accessing publications that users recognise and abide by the legal requirements associated with these rights.

- Users may download and print one copy of any publication from the public portal for the purpose of private study or research.
- You may not further distribute the material or use it for any profit-making activity or commercial gain
- You may freely distribute the URL identifying the publication in the public portal

If you believe that this document breaches copyright please contact us providing details, and we will remove access to the work immediately and investigate your claim.

Design of *Pseudomonas putida* fermentations for robust biomanufacturing

Jesper Wang Jensen
PhD Thesis
April 2023



Design of *Pseudomonas putida* fermentations for robust biomanufacturing

Jesper Wang Jensen

PhD Thesis
April, 2023

Process and Systems Engineering Center
Department of Chemical and Biochemical Engineering
Technical University of Denmark

Design of *Pseudomonas putida* fermentations for robust biomanufacturing

PhD Thesis

April 2023

Author:

Jesper Wang Jensen

Supervisors:

Professor John M. Woodley

Associate Professor Helena Junicke

Professor Pablo Iván Nikel

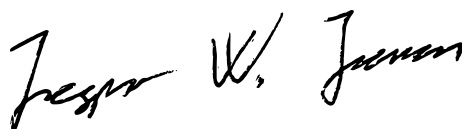
Copyright: Reproduction of this publication in whole or in part must include the customary bibliographic citation, including author attribution, report title, etc.

Cover photo: Sergey Ryzhov

Published by: DTU, Department of Chemical and Biochemical Engineering, Søtofts Plads, Building 228A, 2800 Kgs. Lyngby Denmark
www.kt.dtu.dk

Preface

This PhD thesis presents the work produced between October 2019 and April 2023 at the Process and Systems Engineering Center at the Department of Chemical and Biochemical Engineering, Technical University of Denmark. The work was performed in collaboration with the Systems Environmental Microbiology Group of the Novo Nordisk Foundation Center for Biosustainability, Technical University of Denmark. The work was supervised by Professor John M. Woodley, Associate Professor Helena Junicke and Professor Pablo I. Nikel. The project was granted as a part of the Fermentation Based Biomanufacturing Initiative funded by the Novo Nordisk Foundation (grant number NNF17SA0031362).

A handwritten signature in black ink, reading 'Jesper W. Jensen' in a cursive script.

Jesper Wang Jensen

Abstract

The ability of microorganisms to convert renewable resources to biobased chemicals as an alternative to traditional fossil-based chemical production has been the primary driver of the increased focus on industrial biotechnology. Generally, a small set of microorganisms such as *Escherichia coli* and *Saccharomyces cerevisiae* have been the center of attention in the early phases of industrial biotechnology. Nonetheless, they may not be the most suitable production hosts for any given product or production environment. Therefore, research has lately focused on developing alternative species such as *Pseudomonas putida* to broaden the range of microorganisms matured for industrial application. The bacterium is characterized by robustness and a versatile metabolism that allows it to adapt and cope with high demands of reducing power, well suited for producing highly reduced or toxic chemicals. This thesis sought to investigate the effect of industrial production conditions such as oxygen supply and medium components on the genome reduced *P. putida* SEM10 strain and benchmark it against the wild type strain KT2440.

The *P. putida* wild type strain KT2440 and the genome reduced strain SEM10 were subjected to different oxygen partial pressures (pO_2) in the aeration gas to study the effect of low oxygen availability on their growth characteristics. Both strains showed an 8-10 % increase in $Y_{X/S}$ during exponential growth at low pO_2 (0.0525 atm) compared to growth at high pO_2 (0.21 atm), despite showing a slightly lower growth rate. However, yields diminished as dissolved oxygen became limiting during growth at low pO_2 , reaching overall biomass yields similar to growth at high pO_2 . At the end of the cultivation at low pO_2 , KT2440 achieved an overall $Y_{X/S}$ of $0.352 \pm 0.027 \text{ g} \cdot \text{g}^{-1}$, similar to the $Y_{X/S}$ of $0.383 \pm 0.016 \text{ g} \cdot \text{g}^{-1}$ at high pO_2 . Likewise, SEM10 achieved a similar overall $Y_{X/S}$ at both high and low pO_2 of $0.432 \pm 0.015 \text{ g} \cdot \text{g}^{-1}$ and $0.434 \pm 0.008 \text{ g} \cdot \text{g}^{-1}$, respectively. This showed that the genome reduced strain, SEM10, retained its advantageous growth characteristics regardless of the applied pO_2 .

A medium for high cell concentration fed-batch cultivation of *P. putida* was developed and the inhibitory effects of the medium components were investigated for KT2440 and

SEM10. Ammonium salts, phosphate buffer, glucose, and slightly acidic pH showed inhibitory effects. Growth inhibition was pronounced for both ammonium sulfate and ammonium chloride concentrations exceeding 0.121 M nitrogen, and growth was absent above 0.969 M and 0.484 M, respectively. Phosphate buffer concentrations above 0.108 M showed inhibition. Uninhibited growth was observed for glucose concentrations up to 25 g·L⁻¹, and growth was absent at glucose concentrations exceeding 125 g·L⁻¹. Lastly, the optimum medium pH was between pH 7.0 and 8.0. Both strains showed similar inhibitory trends across the tested conditions.

The wild type KT2440 and genome reduced SEM10 strains were applied in the designed fed-batch medium to evaluate the genome reduced strain under industrially relevant cultivation conditions. During DO limitation and glucose in excess, SEM10 more efficiently compared to KT2440. However, the growth of SEM10 diminished later in the feeding phase, and the strains obtained comparable final biomass concentrations of 26.15±1.04 g·L⁻¹ and 28.15±0.39 g·L⁻¹ for SEM10 and KT2440, respectively. The growth profiles indicated that the genome reduced strain experienced a demanding dual limitation of glucose and DO in the late feeding phase, which diminished the improved growth characteristics of SEM10. Moreover, SEM10 showed a 53% and 29% increased viability, compared to KT2440, in the batch and stationary phases, respectively.

In summary, the genome reduced *P. putida* strain SEM10 showed promise when benchmarked against the wild type KT2440 under industrially relevant conditions such as oxygen limitation and fed-batch cultivation.

Resumé

Mikroorganismers evne til at omdanne vedvarende ressourcer til biobaseret kemikalier, som et alternativ til traditionel fossilbaseret kemikalieproduktion, har været en af de primære drivkræfter for den øgede opmærksomhed på industriel bioteknologi. Generelt har et begrænset udvalg af mikroorganismer, som for eksempel *Escherichia coli* og *Saccharomyces cerevisiae*, været fokuspunktet i de tidlige stadier for industriel bioteknologi. Ikke desto mindre, er de ikke nødvendigvis de mest velegnede produktionsværter til hvilken som helst produkt eller produktionsmiljø. Derfor har nylig forskning fokuseret på at udvikle og modne *Pseudomonas putida* og andre arter for udvide udvalget af mikroorganismer til industriel bioteknologi. *P. putida* er kendetegnet ved dens robusthed og alsidige metabolisme som lader den tilpasse sig og håndtere behov for store mængder reduceringskraft, hvilket gør den velegnet til produktion af kraftigt reducerede eller giftige kemikalier. Denne afhandling bestræbte sig på at undersøge effekten af industrielle procesforhold, såsom iltforsyning og medie komponenter, på den genom reducerede *P. putida* SEM10 stamme samt sammenligne den med vildtype stammen, KT2440.

P. putida vildtype stammen KT2440 og den genom reducerede stamme SEM10 blev udsat for forskellige partielle ilt tryk (pO_2) i luftningsgassen for at undersøge effekten af lav iltforsyning på deres vækst. Begge stammer oplevede en 8-10% forhøjet $Y_{X/S}$ under eksponentielt vækst ved lav pO_2 (0.0525 atm) sammenlignet med vækst ved høj pO_2 (0.21 atm), det til trods for en lavere vækstrate. Udbyttet blev imidlertid mindre da iltten blev begrænsende under vækst ved lav pO_2 , hvorfor de samlede biomasse udbytter var tilsvarende biomasse udbyttet ved høj pO_2 . Ved afslutningen af kultiveringen ved lav pO_2 havde KT2440 opnået en samlet $Y_{X/S}$ på $0.352 \pm 0.027 \text{ g} \cdot \text{g}^{-1}$ tilsvarende $Y_{X/S}$ ved høj pO_2 på $0.383 \pm 0.016 \text{ g} \cdot \text{g}^{-1}$. Ligeledes opnåede SEM10 tilsvarende $Y_{X/S}$ ved høj og lav pO_2 , på henholdsvis $0.432 \pm 0.015 \text{ g} \cdot \text{g}^{-1}$ and $0.434 \pm 0.008 \text{ g} \cdot \text{g}^{-1}$. Dette viste at den genom reducerede stamme, SEM10, bibeholdt dens fordelagtige vækst egenskaber uanset pO_2 .

Et medie til høje celle koncentrationer fed-batch kultivering af *P. putida* blev udviklet og

medie komponenternes væksthæmning på KT2440 og SEM10 blev undersøgt. Ammoniumsalte, fosfatbuffer, glukose og mildt syrligt pH udviste væksthæmning. Væksthæmning var udpræget ved koncentrationer af ammoniumsulfat og ammoniumklorid der overskred 0.121 M nitrogen, og ingen synlig vækst over henholdsvis 0.969 M og 0.484 M. Fosfatbuffer koncentrationer over 0.108 M udviste væksthæmning. Uhæmmet vækst kunne observeres for glukose koncentrationer op til $25 \text{ g} \cdot \text{L}^{-1}$, hvorimod ingen synlig vækst kunne observeres ved koncentrationer over $125 \text{ g} \cdot \text{L}^{-1}$. Derudover blev pH optimum bestemt til at være mellem pH 7.0 og 8.0. Begge stammer udviste lignende tendenser for væksthæmning under de testede forhold.

Vildtype stammen KT2440 og den genom reducerede stamme SEM10 blev kultiveret i det designed fed-batch medie for at evaluere den genom reducerede stamme under industrielt relevante kultiveringsforhold. Under ilt begrænsning men med overskud af glukose, voksede SEM10 hurtigere og mere effektivt sammenlignet med KT2440. Senere i fodringsfasen faldt væksten af SEM10 og stammerne opnåede lignende endelige biomasse koncentrationer på $26.15 \pm 1.04 \text{ g} \cdot \text{L}^{-1}$ og $28.15 \pm 0.39 \text{ g} \cdot \text{L}^{-1}$ for henholdsvis SEM10 og KT2440. Vækstprofilerne indikerede at den genom reducerede stamme oplevede en krævende dobbelt begrænsning af glukose og ilt i den sene fodringsfase, hvilket mindskede SEM10s forbedrede vækst egenskaber. I øvrigt udviste SEM10 53% og 29% højere overlevelsessevne, sammenlignet med KT2440, i henholdsvis batch og stationære faser.

Sammenfattende udviste den genom reducerede *P. putida* stamme, SEM10, potentiale ved sammenligning med vildtypen, KT2440, under industrielt relevante forhold som ilt begrænsning og fed-batch kultivering.

Acknowledgements

First and foremost, I would like to thank my supervisors Helena Junick, John M. Woodley and Pablo I. Nikel, who have helped shape my PhD in each their way. I appreciate all you have taught me and our giving discussions, Thank you for giving me the opportunity! In addition, I would like to thank everyone at PROSYS for making my time here incredible. Especially, Aliyeh and Pascal, for all the good times we've spent in and outside the office!

To my family, thank you for supporting me all the way through my PhD journey, no matter if I was sometimes talking jibberish!

To all of my friends for enduring all my talks about bacteria and my failure to yell out impressive equations on command!

To my flatmates for keeping up my spirits while writing!

List of contributions

Conference participation

6th BioProScale Symposium, Online (2021).

Jensen, J. W., Woodley, J. M., Nikel, P. I. and Junicke, H.

Design and Upscaling of *Pseudomonas putida* Fermentations for Robust Biomanufacturing (Poster)

7th BioProScale Symposium, Berlin, Germany (2022).

Jensen, J. W., Woodley, J. M., Nikel, P. I. and Junicke, H.

Influence of oxygen levels on a genome reduced *Pseudomonas putida* strain (Poster)

1st FBM Symposium: "Innovation for Biomanufacturing - Next Generation Cell-Factories and Process Development", Kgs. Lyngby, Denmark (2022).

Jensen, J. W., Nikel, P. I., Woodley, J. M. and Junicke, H.

Influence of oxygen levels on *Pseudomonas putida* fermentations (Poster)

Abbreviations and Nomenclature

Abbreviations

A.U.	Arbitrary unit
ATP	Adenosine triphosphate
CDW	Cell dry weight
CFU	Colony forming units
CFD	Computational fluid dynamics
EDTA	Ethylenediaminetetraacetic acid
FDA	U.S. Food and Drug Administration
<i>gcd</i>	Glucose dehydrogenase
HPLC	High pressure liquid chromatography
HV1	Host vector safety level 1
IFC	Impedance flow cytometry
LB	Lysogeny broth
<i>P. putida</i>	<i>Pseudomonas putida</i>
PHA	Polyhydroxyalkanoate
PI	Proportional Integral controller
RQ	Respiratory quotient
SI	Saturation index
TE	Trace element
TEB	Trace element booster solution
UV	Ultra violet

Nomenclature

ϵ	Control error [g·L ⁻¹]
μ	Specific growth rate [h ⁻¹]
c_{CO_2}	Dissolved CO ₂ concentration [g·L ⁻¹]

$c_{\text{CO}_2, \text{feed}}$	Dissolved CO_2 concentration in feed [$\text{g}\cdot\text{L}^{-1}$]
$c_{\text{CO}_2}^*$	Solubility of CO_2 in water [$\text{g}\cdot\text{L}^{-1}$]
c_{NH_4}	Ammonium concentration [$\text{g}\cdot\text{L}^{-1}$]
$c_{\text{NH}_4, \text{feed}}$	Ammonium concentration in feed [$\text{g}\cdot\text{L}^{-1}$]
c_{O}	Dissolved oxygen concentration [$\text{g}\cdot\text{L}^{-1}$]
$c_{\text{O}, \text{feed}}$	Dissolved oxygen concentration in feed [$\text{g}\cdot\text{L}^{-1}$]
$c_{\text{O}, \text{set}}$	DO control set point [$\text{g}\cdot\text{L}^{-1}$]
$c_{\text{O}_2}^*$	Solubility of oxygen in water [$\text{g}\cdot\text{L}^{-1}$]
c_{S}	Glucose concentration [$\text{g}\cdot\text{L}^{-1}$]
$c_{\text{S}, \text{feed}}$	Glucose concentration in feed [$\text{g}\cdot\text{L}^{-1}$]
c_{X}	Biomass concentration [$\text{g}\cdot\text{L}^{-1}$]
CTR	CO_2 transfer rate [$\text{g}\cdot(\text{L}\cdot\text{h})^{-1}$]
CER	CO_2 emission rate [$\text{g}\cdot\text{h}^{-1}$]
DO	Dissolved oxygen [%]
F_{in}	Feed rate [$\text{L}\cdot\text{h}^{-1}$]
$F_{\text{in}, 0}$	Initial feed rate [$\text{L}\cdot\text{h}^{-1}$]
$F_{\text{gas}, \text{in}}$	Gas flow rate into bioreactor [$\text{mol}\cdot\text{h}^{-1}$]
$F_{\text{gas}, \text{out}}$	Gas flow rate out of bioreactor [$\text{mol}\cdot\text{h}^{-1}$]
F_{sample}	Sample withdrawal [$\text{L}\cdot\text{h}^{-1}$]
IAP	Ion activity product [M]
K	Solubility constant [M]
K_{c}	Proportional gain [-]
K_{i}	Integral gain [h^{-1}]
K_{O}	Oxygen affinity constant [$\text{g}\cdot\text{L}^{-1}$]
K_{S}	Glucose affinity constant [$\text{g}\cdot\text{L}^{-1}$]
$k_{\text{L}}a$	Volumetric mass transfer coefficient [h^{-1}]
m_{S}	Glucose maintenance coefficient [$\text{g}\cdot(\text{g}\cdot\text{h})^{-1}$]

n_{CO_2}	Mole of CO_2 gas [mol]
n_{O_2}	Mole of O_2 gas [mol]
n_{total}	Total mole of gas [mol]
OD_{600}	Optical density at 600 nm [A.U.]
OTR	Oxygen transfer rate [$\text{g} \cdot (\text{L} \cdot \text{h})^{-1}$]
OUR	Oxygen uptake rate [$\text{g} \cdot \text{h}^{-1}$]
p	Pressure [atm]
p_{O_2}	Partial pressure of O_2 [atm]
q_{CO_2}	Biomass-specific CO_2 production rate [$\text{g} \cdot (\text{g} \cdot \text{h})^{-1}$]
q_{NH_4}	Biomass-specific NH_4 consumption rate [$\text{g} \cdot (\text{g} \cdot \text{h})^{-1}$]
q_{O_2}	Biomass-specific oxygen consumption rate [$\text{g} \cdot (\text{g} \cdot \text{h})^{-1}$]
q_s	Biomass-specific glucose consumption rate [$\text{g} \cdot (\text{g} \cdot \text{h})^{-1}$]
R	Ideal gas constant [$\text{L} \cdot \text{atm} \cdot (\text{K} \cdot \text{mol})^{-1}$]
T	Temperature [K]
V	Volume [L]
V_{gas}	Volume of gas in the bioreactor headspace [L]
$Y_{\text{X/CO}_2}$	Yield of biomass on CO_2 [$\text{g} \cdot \text{g}^{-1}$]
$Y_{\text{X/Mg}}$	Yield of biomass on Mg [$\text{g} \cdot \text{g}^{-1}$]
$Y_{\text{X/NH}_4}$	Yield of biomass on NH_4 [$\text{g} \cdot \text{g}^{-1}$]
$Y_{\text{X/O}_2}$	Yield of biomass on O_2 [$\text{g} \cdot \text{g}^{-1}$]
$Y_{\text{X/PO}_4}$	Yield of biomass on PO_4 [$\text{g} \cdot \text{g}^{-1}$]
$Y_{\text{X/S}}$	Yield of biomass on glucose [$\text{g} \cdot \text{g}^{-1}$]
$Y_{\text{X/S}}^{\text{true}}$	True yield of biomass on glucose [$\text{g} \cdot \text{g}^{-1}$]

Contents

Preface	v
Abstract	vii
Acknowledgements	xi
List of contributions	xii
Abbreviations	xiii
Nomenclature	xiii
1 Introduction	1
1.1 Background	1
1.2 Aim and Motivation of the Thesis	2
1.3 Thesis Outline	3
References	4
2 The soil bacterium <i>Pseudomonas putida</i>	9
References	16
3 Genome reduced <i>Pseudomonas putida</i> SEM10 strain tolerates oxygen depletion	25
3.1 Introduction	25
3.2 Materials and Methods	27
3.3 Results and discussion	30
3.4 Conclusions	38
References	39
4 Medium Design for <i>Pseudomonas putida</i> fed-batch cultivation	43
4.1 Introduction	43
4.2 Materials and Methods	44
4.3 Results and Discussion	46
4.4 Conclusions	67
References	68
5 Application of a genome reduced <i>Pseudomonas putida</i> strain in fed-batch cultivation	75
5.1 Introduction	75
5.2 Materials and Methods	77
5.3 Mathematical Model	80
5.4 Results and Discussion	84
5.5 Conclusions	96
References	97
6 Conclusions	101
7 Future work	105
References	107

1 Introduction

1.1 Background

Industrial biotechnology is a field that comprises a broad range of products, from bulk and commodity chemicals to pharmaceuticals and vaccines. The wide range of products has resulted in the application of biotechnology in both the chemical and health industries, highlighting the importance of the field. Consequently, it has seen immense growth over the past decades. That trend continues into the future due to greater emphasis on environmental considerations in the chemical industry and the development of new biological pharmaceuticals [1, 2].

The production of chemicals is one sub-field of industrial biotechnology that has garnered attention in the quest to reduce our reliance on petroleum-derived chemicals [2, 3]. The production of bio-based chemicals is an attractive alternative to traditional chemical production, as it is characterized by milder process conditions and based on renewable raw materials [4]. Furthermore, as the production of chemicals from petroleum is, in comparison, an old and established industry, focus on cost saving and optimization is paramount in the development of industrial biotechnology as a competitive alternative [2, 4].

The foundation of industrial biotechnology is the fermentation, where microorganisms convert substrates, like glucose, into a range of valuable products. Some of the earliest and most established fermentations have been performed using a set of traditional microorganisms like *Saccharomyces cerevisiae*, *Escherichia coli* and *Corynebacterium glutamicum*, though other microorganisms are receiving increased attention lately [5, 6]. An alternative microorganism is the bacterium *Pseudomonas putida*, which has risen to prominence due to its innate robustness and versatile metabolism [7, 8]. The metabolism of glucose through an oxidative pathway in the periplasm and further through a circular upper carbon metabolism enables excellent tuning of energy and redox levels [9–11]. The versatile metabolism allows the bacterium to cope with high demands for reducing

power, which is beneficial to withstand, for example, oxidative stress or produce highly reduced or toxic chemicals [12]. This is reflected in the range of applications investigated in the literature, ranging from biosurfactants and biopolymers to the conversion of aromatic compounds and even bioremediation [13–16]. Furthermore, *P. putida* has shown an exceptional ability to endure temporal limitations of both glucose and dissolved oxygen (DO), characteristics of an industrial scale production [17, 18]. Lastly, the *P. putida* wild type strain KT2440 has been genetically streamlined by deleting expendable genomic regions, such as prophage DNA and the flagellar operon, thereby reducing futile energy spending and producing a more substrate-efficient strain, SEM10 [19, 20].

The development of a new fermentation process starts in a well-controlled bench-top bioreactor of 1 - 10 L, followed by a pilot scale of 100 - 10,000 L, before being commercialized at industrial scale of 10 - 100 m³ [21]. However, successfully bridging the gap between scales while retaining the bench top performance might be a challenging, if not impossible, endeavor, even when employing traditional microorganisms. Typically, scale-up experiences a 10-30% drop in performance compared to bench-top scale [22]. These challenges usually arise from the lack of spatial homogeneity of large-scale aerobic fermentations [23, 24].

The spatial heterogeneity, or gradients, occurring in large-scale bioreactors is the result of mass transfer constraints [24, 25]. Gradients expected to occur during large-scale fermentations are, for example, glucose, DO and pH, exposing microorganisms to an ever-changing environment [26–28]. Such gradients have been the topic of much research in recent years, utilizing computational fluid dynamics as an alternative to costly large-scale fermentations to predict and evaluate such gradients [29, 30]. Knowledge obtained, both experimentally and through predictive modeling, has shown gradients to significantly affect microbial behavior and performance in industrial scale bioreactors [31].

1.2 Aim and Motivation of the Thesis

This thesis aims to elaborate on the knowledge of *P. putida* growth on glucose under industrially relevant conditions. To this end, the streamlined strain (SEM10) will be evalu-

ated, for the first time, under industrially relevant conditions and its performance compared to the wild type strain (KT2440). Accordingly, the thesis aimed to:

- Assess the influence of high and low oxygen availability on both strains during batch cultivation in high-throughput microbioreactors, shake flasks, and lab-scale stirred tank bioreactors.
- Theoretically design a medium for high cell concentration fed-batch cultivations of *P. putida* and experimentally evaluate the effects of the individual compound concentrations on both strains.
- Design and model a high cell concentration fed-batch cultivation of *P. putida* and experimentally evaluate the applicability of *P. putida* SEM10 for industrially relevant fed-batch cultivation.

1.3 Thesis Outline

The thesis is organized into five chapters introducing the biotechnology field, *P. putida* and addressing the aims defined earlier.

Chapter 1 and 2 introduces the thesis and provides a brief overview of *P. putida*, its metabolism, genome streamlining and applications.

Chapter 3 presents and discusses the influence of oxygen availability on *P. putida* KT2440 and SEM10 during batch cultivation..

Chapter 4 proposes a fed-batch medium design and evaluates the applicability of its components in *P. putida* cultivations.

Chapter 5 applies KT2440 and SEM10 strains in the fed-batch setting and evaluates the applicability of the genome reduced strain in this environment.

Chapter 6 and 7 summarizes and concludes on the thesis findings and offers a perspective on future work.

References

- [1] Lokko, Y., Heijde, M., Schebesta, K., Scholtès, P., Montagu, M. V., and Giacca, M. “Biotechnology and the bioeconomy—Towards inclusive and sustainable industrial development”. In: *New Biotechnology* 40 (2018), pp. 5–10. DOI: 10.1016/j.nbt.2017.06.005.
- [2] Tang, W. L. and Zhao, H. “Industrial biotechnology: Tools and applications”. In: *Biotechnology Journal* 4 (12 2009), pp. 1725–1739. DOI: 10.1002/biot.200900127.
- [3] Becker, J., Lange, A., Fabarius, J., and Wittmann, C. “Top value platform chemicals: Bio-based production of organic acids”. In: *Current Opinion in Biotechnology* 36 (2015), pp. 168–175. DOI: 10.1016/j.copbio.2015.08.022.
- [4] Burk, M. J. and Dien, S. V. “Biotechnology for Chemical Production: Challenges and Opportunities”. In: *Trends in Biotechnology* 34 (3 2016), pp. 187–190.
- [5] Becker, J. and Wittmann, C. “Advanced biotechnology: Metabolically engineered cells for the bio-based production of chemicals and fuels, materials, and health-care products”. In: *Angewandte Chemie - International Edition* 54 (11 2015), pp. 3328–3350. DOI: 10.1002/anie.201409033.
- [6] Calero, P. and Nikel, P. I. “Chasing bacterial chassis for metabolic engineering: a perspective review from classical to non-traditional microorganisms”. In: *Microbial Biotechnology* 12 (1 2019), pp. 98–124. DOI: 10.1111/1751-7915.13292.
- [7] Nikel, P. I. and Lorenzo, V. de. “Pseudomonas putida as a functional chassis for industrial biocatalysis: From native biochemistry to trans-metabolism”. In: *Metabolic Engineering* 50 (May 2018), pp. 142–155. DOI: 10.1016/j.ymben.2018.05.005.
- [8] Weimer, A., Kohlstedt, M., Volke, D. C., Nikel, P. I., and Wittmann, C. “Industrial biotechnology of Pseudomonas putida: advances and prospects”. In: *Applied Microbiology and Biotechnology* 104 (18 2020), pp. 7745–7766. DOI: 10.1007/s00253-020-10811-9.
- [9] Castillo, T. D., Ramos, J. L., Rodríguez-Herva, J. J., Fuhrer, T., Sauer, U., and Duque, E. “Convergent peripheral pathways catalyze initial glucose catabolism in

- Pseudomonas putida*: Genomic and flux analysis". In: *Journal of Bacteriology* 189 (14 2007), pp. 5142–5152. DOI: 10.1128/JB.00203-07.
- [10] Tlemçani, L. L., Corroler, D., Barillier, D., and Mosrati, R. "Physiological states and energetic adaptation during growth of *Pseudomonas putida* mt-2 on glucose". In: *Archives of Microbiology* 190 (2 2008), pp. 141–150. DOI: 10.1007/s00203-008-0380-8.
- [11] Nikel, P. I., Chavarría, M., Fuhrer, T., Sauer, U., and Lorenzo, V. de. "Pseudomonas putida KT2440 Strain Metabolizes Glucose through a Cycle Formed by Enzymes of the Entner-Doudoroff, Embden-Meyerhof-Parnas, and Pentose Phosphate Pathways". In: *Journal of Biological Chemistry* 290 (43 2015), pp. 25920–25932. DOI: 10.1074/jbc.M115.687749.
- [12] Nikel, P. I., Chavarría, M., Danchin, A., and Lorenzo, V. de. "From dirt to industrial applications: *Pseudomonas putida* as a Synthetic Biology chassis for hosting harsh biochemical reactions". In: *Current Opinion in Chemical Biology* 34 (2016), pp. 20–29. DOI: 10.1016/j.cbpa.2016.05.011.
- [13] Poblete-Castro, I., Acuña, J. M. B.-d., Nikel, P. I., Kohlstedt, M., and Wittmann, C. "Host Organism: *Pseudomonas putida*". In: Wiley-VCH Verlag GmbH & Co. KGaA, 2016, pp. 299–326. DOI: 10.1002/9783527807796.ch8.
- [14] Tiso, T., Ihling, N., Kubicki, S., Biselli, A., Schonhoff, A., Bator, I., Thies, S., Karmainski, T., Kruth, S., Willenbrink, A. L., Loeschke, A., Zapp, P., Jupke, A., Jaeger, K. E., Büchs, J., and Blank, L. M. "Integration of Genetic and Process Engineering for Optimized Rhamnolipid Production Using *Pseudomonas putida*". In: *Frontiers in Bioengineering and Biotechnology* 8 (2020). DOI: 10.3389/fbioe.2020.00976.
- [15] Poblete-Castro, I., Rodriguez, A. L., Lam, C. M. C., and Kessler, W. "Improved production of medium-chain-length polyhydroxyalkanoates in glucose-based fed-batch cultivations of metabolically engineered *Pseudomonas putida* strains". In: *Journal of Microbiology and Biotechnology* 24 (1 2014). Look at cites, pp. 59–69. DOI: 10.4014/jmb.1308.08052.

- [16] Hudcova, T., Halecky, M., Kozliak, E., Stiborova, M., and Paca, J. "Aerobic degradation of 2,4-dinitrotoluene by individual bacterial strains and defined mixed population in submerged cultures". In: *Journal of Hazardous Materials* 192 (2 2011), pp. 605–613. DOI: 10.1016/j.jhazmat.2011.05.061.
- [17] Ankenbauer, A., Schäfer, R. A., Viegas, S. C., Pobre, V., Voß, B., Arraiano, C. M., and Takors, R. "Pseudomonas putida KT2440 is naturally endowed to withstand industrial-scale stress conditions". In: *Microbial Biotechnology* 13 (4 2020), pp. 1145–1161. DOI: 10.1111/1751-7915.13571.
- [18] Demling, P., Ankenbauer, A., Klein, B., Noack, S., Tiso, T., Takors, R., and Blank, L. M. "Pseudomonas putida KT2440 endures temporary oxygen limitations". In: *Biotechnology and Bioengineering* 118 (12 2021), pp. 4735–4750. DOI: 10.1002/bit.27938.
- [19] Martínez-García, E., Nikel, P. I., Aparicio, T., and Lorenzo, V. de. "Pseudomonas 2.0: Genetic upgrading of P. putida KT2440 as an enhanced host for heterologous gene expression". In: *Microbial Cell Factories* 13 (1 2014), pp. 1–15. DOI: 10.1186/s12934-014-0159-3.
- [20] Volke, D. C., Friis, L., Wirth, N. T., Turlin, J., and Nikel, P. I. "Synthetic control of plasmid replication enables target- and self-curing of vectors and expedites genome engineering of Pseudomonas putida". In: *Metabolic Engineering Communications* 10 (January 2020), e00126. DOI: 10.1016/j.mec.2020.e00126.
- [21] Crater, J. S. and Lievens, J. C. "Scale-up of industrial microbial processes". In: *FEMS Microbiology Letters* 365 (13 2018). DOI: 10.1093/femsle/fny138.
- [22] Lara, A. R., Galindo, E., Ramírez, O. T., and Palomares, L. A. "Living With Heterogeneities in Bioreactors 355 MOLECULAR BIOTECHNOLOGY Living With Heterogeneities in Bioreactors Understanding the Effects of Environmental Gradients on Cells". In: *Molecular Biotechnology* (2006).
- [23] Hewitt, C. J. and Nienow, A. W. "The Scale-Up of Microbial Batch and Fed-Batch Fermentation Processes". In: vol. 62. 2007, pp. 105–135. DOI: 10.1016/S0065-2164(07)62005-X.

- [24] Villadsen, J., Nielsen, J., and Lidén, G. *Bioreaction Engineering Principles*. Springer US, 2011. DOI: 10.1007/978-1-4419-9688-6.
- [25] Garcia-Ochoa, F. and Gomez, E. “Bioreactor scale-up and oxygen transfer rate in microbial processes: An overview”. In: *Biotechnology Advances* 27 (2 2009), pp. 153–176. DOI: 10.1016/j.biotechadv.2008.10.006.
- [26] Bylund, F., Collet, E., Enfors, S.-O., and Larsson, G. “Substrate gradient formation in the large-scale bioreactor lowers cell yield and increases by-product formation”. In: *Bioprocess Engineering* 18 (1998), pp. 171–180.
- [27] Spann, R., Glibstrup, J., Pellicer-Alborch, K., Junne, S., Neubauer, P., Roca, C., Kold, D., Lantz, A. E., Sin, G., Gernaey, K. V., and Krühne, U. “CFD predicted pH gradients in lactic acid bacteria cultivations”. In: *Biotechnology and Bioengineering* 116 (4 2019), pp. 769–780. DOI: 10.1002/bit.26868.
- [28] Nadal-Rey, G., McClure, D. D., Kavanagh, J. M., Cassells, B., Cornelissen, S., Fletcher, D. F., and Gernaey, K. V. “Development of dynamic compartment models for industrial aerobic fed-batch fermentation processes”. In: *Chemical Engineering Journal* 420 (2021). DOI: 10.1016/j.cej.2021.130402.
- [29] Haringa, C., Noorman, H. J., and Mudde, R. F. “Lagrangian modeling of hydrodynamic–kinetic interactions in (bio)chemical reactors: Practical implementation and setup guidelines”. In: *Chemical Engineering Science* 157 (2017), pp. 159–168. DOI: 10.1016/j.ces.2016.07.031.
- [30] Kuschel, M. and Takors, R. “Simulated oxygen and glucose gradients as a pre-requisite for predicting industrial scale performance a priori”. In: *Biotechnology and Bioengineering* 117 (9 2020), pp. 2760–2770. DOI: 10.1002/bit.27457.
- [31] Blöbaum, L., Haringa, C., and Grünberger, A. “Microbial lifelines in bioprocesses: From concept to application”. In: *Biotechnology Advances* 62 (2023). DOI: 10.1016/j.biotechadv.2022.108071.

2 The soil bacterium *Pseudomonas putida*

The gram-negative bacterium *Pseudomonas putida* is isolated from soil environments, particularly polluted soils. In the 1960s, an m-toluate degrading strain of the bacterium was isolated as strain mt-2 [1]. The strain was later cured of the toluene degrading TOL plasmid to yield the model strain KT2440, which is certified as host-vector safety level 1 (HV1) by US Food and Drug Administration (FDA) [2, 3]. Since then, research on and application of the microorganism, especially the KT2440 strain, has gained traction due to its robustness and ease of handling [4]. The versatile metabolism allows it to tune the co-factor production to match the current environment [5, 6]. In 2002, the full genome of KT2440 was sequenced as the first *P. putida* strain, and subsequently, genome-scale metabolic models were developed [7–9]. Furthermore, extensive work has focused on developing genetic engineering tools for *P. putida* and streamlining the genome [10–13].

The use of specific platform microorganisms for different products and environments is an alternative to the use of model microorganisms such as *Escherichia coli* and *Saccharomyces cerevisiae*, which have a limited product and environmental scope. By applying an appropriate platform microorganism, one can utilize the microorganism's natural proficiency [14]. The aforementioned versatile metabolism and robustness, in addition to the advances in the genetic engineering toolbox, have been highlighted as the main advantages of using *P. putida* as a platform microorganism. This is exemplified by the broad range of applications, including the production of cis,cis-muconic acid, medium chain length polyhydroxyalkanoates (PHA), enzymes and biosurfactants [15–18].

Glucose metabolism of *P. putida* KT2440

A common feature of *Pseudomonas* species, and *P. putida* KT2440, is the ability, in addition to direct phosphorylation, to convert glucose to gluconate and 2-ketogluconate via

oxidation in the periplasm [19, 20]. In addition, the strain utilizes a cyclic upper central carbon metabolism consisting of the Entner-Doudoroff (ED) pathway, pentose phosphate (PP) pathway and an incomplete Embden-Meyerhof-Parnas (EMP) pathway. The incomplete EMP pathway, which lacks 6-phosphofructo-1-kinase, forces the characteristic use of the PP and ED pathways for glucose degradation by *P. putida* KT2440 [6, 21]. Figure 2.1 illustrates the upper central carbon metabolism of *P. putida* KT2440 and the conversion of glucose in the periplasm. In the first step of the oxidative pathway in the periplasm, glucose is converted into gluconate by glucose dehydrogenase (*gcd*) and in the second step, gluconate is converted into 2-ketogluconate by gluconate dehydrogenase (*gad*). Both molecules can be taken up by the cell. Each enzymatic step releases two electrons used to drive ATP generation via the respiratory chain [5]. Furthermore, the conversion of glucose through the oxidative pathway bypasses the ATP-consuming glucose transport but also the NADPH-generating conversion of glucose-6-phosphate to gluconate-6-phosphate by *zwf* [5]. The latter molecule is the convergence point for gluconate and 2-ketogluconate before it enters the ED pathway and subsequently either the tricarboxylic acid cycle or is recycled back through the EMP pathway. The metabolic recycling is believed to stimulate growth and to enable tuning of NADPH production at the expense of ATP production, which can help protect the bacteria against oxidative stress [21]. The latter may also be utilized as a source of redox co-factors required to produce highly reduced bio-chemicals.

Innate tolerance of *P. putida* towards environmental stresses

P. putida is endowed with a natural ability to combat a range of environmental stresses experienced in polluted sites, from where it has often been isolated [6, 21]. The *P. putida* strain KT2440 metabolizes glucose in a cyclic fashion believed to enhance its tolerance towards oxidative stress. The cyclic layout of the metabolism allows *P. putida* to increase the NADPH production, at the expense of ATP production, to cope with increased oxidative stress [21, 22]. Furthermore, the species is known for its robustness towards a range of other physicochemical stresses such as heavy metals and many organic solvents [23–25]. The solvent tolerant *P. putida* strain DOT-T1 could not only thrive at concentra-

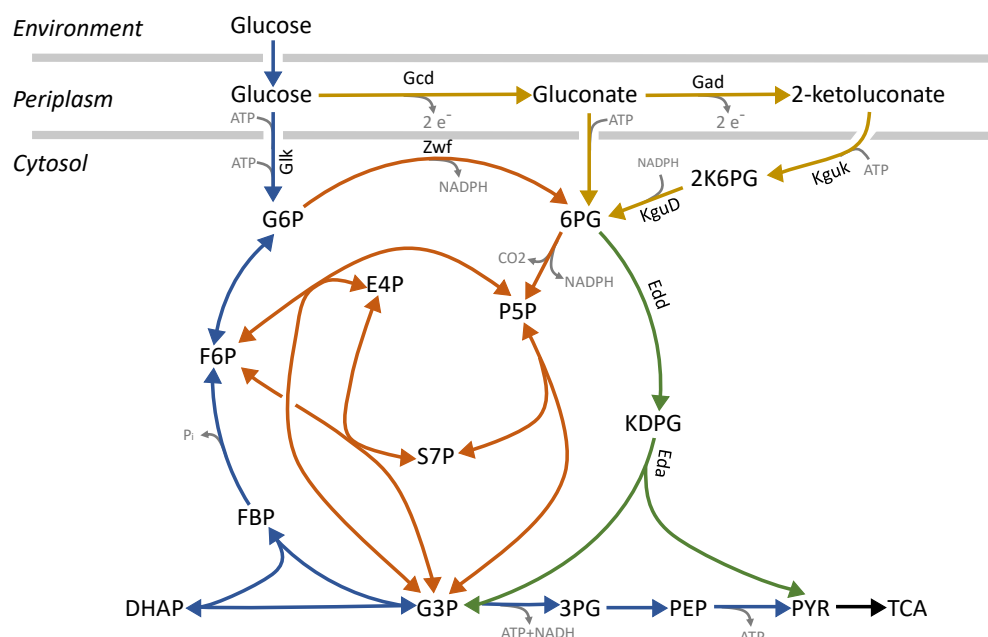


Figure 2.1: The upper central carbon metabolism of *Pseudomonas putida* KT2440 presented with lumped reactions. Glucose enters the metabolism through the oxidative path in the periplasm (yellow) or by direct phosphorylation. Glucose is then metabolized through a cycle consisting of the pentose phosphate (PP) pathway (orange), the Entner-Doudoroff (ED) pathway (green) and an incomplete Embden-Meyerhof-Parnas (EMP) pathway (blue). Due to the incomplete EMP pathway, the majority of glucose is metabolized through the PP and ED pathways. Depending on the environmental demands, metabolites can be funneled into the tricarboxylic acid (TCA) cycle and oxidative phosphorylation to generate ATP or recycled through the EMP pathway to generate NADPH [21]. Metabolites: 2-Ketogluconate 6-P (2K6PG), gluconate 6-P (6PG), glucose 6-P (G6P), 2-keto-3-deoxy-gluconate 6-P (KDPG), glyceraldehyde 3-P (G3P), dihydroxyacetone phosphate (DHAP), fructose 1,6-P (FBP), fructose 6-P (F6P), erythrose 4-P (E4P), pentose 5-P (P5P), sedoheptulose 7-P (S7P), 3-phosphoglyceric acid (3PG), phosphoenolpyruvate (PEP) and pyruvate (PYR). Enzymes related to the initial glucose metabolism: Glucose dehydrogenase (Gcd), gluconate 2-dehydrogenase (Gad), gluconate kinase (GnuK), 2-ketogluconate kinase (KguK), 2-ketogluconate-6-P reductase (KguD), glucose-6-P 1-dehydrogenase (Zwf), 6-phosphogluconate dehydratase (Edd) and 2-keto-3-deoxy-6-phosphogluconate aldolase (Eda).

tions otherwise lethal towards other microorganisms but also utilize it as the sole carbon source [26, 27]. Such high tolerance towards a range of toxic chemicals is a result of an expansive repertoire of tools to counteract physicochemical stresses that range from an overproduction of NADPH to efflux pumps and alteration of the cell membrane [21, 28, 29]. In several cases, the natural tolerance towards organic solvents has been applied for two-phase cultivations of *P. putida* to enhance product titers [30, 31].

Growth under industrially relevant conditions

The industrial production environment is often characterized by mass transfer limitations, resulting in gradients of substrate and oxygen [32]. Gradients in the cultivation environment expose the microorganisms to ever-changing substrate concentrations, oxygen or a combination of both [32, 33]. The effect of glucose gradients on *P. putida* KT2440 has been investigated both experimentally and computationally [34, 35]. A study on the Lagrangian lifelines of *P. putida* KT2440 in a simulated 54 m³ cultivation showed that exposure to a glucose gradient significantly affected the bacterium. In general, the bacterial population presented a high degree of heterogeneity in growth and an increased cell maintenance demand [35]. *P. putida* KT2440 has shown an ability to tolerate repeated glucose limitation periods of 2.6 min in a scale-down system. Unlike *E. coli*, the strain could retain its energy level under transient glucose limitation by storing carbon internally during excess glucose availability [34]. Furthermore, *P. putida* KT2440 is able to quickly recover from the effects of repeated dual glucose and oxygen starvation of 2.6 min. In addition, the strain showed no reduction in the final biomass concentration when repeatedly exposed to short 2 or 4 min interruptions of the oxygen supply [30]. In contrast, continuously reduced agitation in batch cultivations of *P. putida* KT2440 had an adverse effect on biomass growth, reducing the final biomass concentration by at least 24.9% [36].

Utilization of alternative feedstocks

Valorization of lignocellulosic biomass derived substrates, other than glucose, has been of high interest in recent years as a driver of cost reduction and increased sustainability of production processes. Especially the lignin fraction has been of interest as it is difficult to utilize for most microorganisms [37]. Nevertheless, *P. putida* has been shown to naturally utilize the aromatic compounds of the lignin fraction and has been used to convert these into more valuable aromatic bio-chemicals [15, 37]. However, the natural substrate range of *P. putida* consists mainly of organic acids and aromatic compounds and is limited to a few carbohydrates such as glucose and fructose, limiting the utilization of the cellulose and hemicellulose fractions [38]. Thus, the bacterium has been genetically engineered to utilize various other carbon sources related to different lignocellulosic biomass fractions.

This includes the disaccharide cellobiose of the cellulose fraction and monosaccharides D-xylose, L-arabinose and D-galactose of the hemicellulose fraction, which it was able to co-utilize along with aromatic compounds [38–40].

Genome Streamlining of *P. putida* KT2440

To further promote *P. putida* and the KT2440 strain as a microbial platform strain, genetic engineering has been carried out to streamline the strain, ridding it of futile genetic material. Generally, two different approaches have been applied to streamline the genome of *P. putida* KT2440, one applying random deletions reducing the genome with as much as ~7.4% and a rational engineering approach initially reducing the genome by ~4.3% [10, 41]. The latter approach yielded the genome reduced strains EM383 and SEM10 [10, 13].

Table 2.1: Examples of genome reduced strains developed by either random or targeted deletions in the *P. putida* KT2440 genome. Adapted from Weimer et al. (2020) [42].

Strain	Reduction	Characteristics	Reference
407.3Δ ₂	~7.4%	Random double deletion in the KT2440 genome. Showed similar or better growth in LB.	Leprince et al. (2012) [41]
EM42	~4.3%	Rational deletion of a broad scope of DNA in the KT2440 genome. Improved growth and energy and redox balances.	Martínez-García et al. (2014) [10]
EM383	~4.3%	Derived from EM42 but with an additional deletion of RecA.	Martínez-García et al. (2014) [10]
SEM10	~4.8%	Derived from EM42 by rational deletions focused on easing genetic engineering and enhancing biosafety. No improvement in growth.	Volke et al. (2020) [13]
EM371	~4.7%	Rational deletions of the KT2440 genome. The deletions focused on genes associated with surface-bound proteins. Platform strain for community engineering.	Martínez-García et al. (2020) [43]
KTU-U13	~4.1%	Deletion of GC rich genomic islands. No improvement in growth but improvement in plasmid stability.	Liang et al. (2020) [44]

The streamlining approaches presented in Table 2.1 have produced *P. putida* strains with reduced genomes and a range of improved phenotypic characteristics. A rational engineering approach is preferred as it is a solid foundation for further development for specific applications. The EM383 strain was constructed by targeting and deleting a broad set of

genes with different purposes. Martínez-García et al. (2014) first targeted prophage DNA comprising ~2.6% of the genome. Prophage DNA is considered parasitic and could potentially cause stochastic cell death if induced [10]. Furthermore, two sets of mobile elements were deleted as they may counter-select recombinant genes. The *Tn4621* transposon was of particular interest as it has been shown to be active during glucose starvation. Genes linked to the degradation of incoming DNA were also deleted to facilitate genetic engineering. Lastly, the complete flagellar operon was deleted to divert the ATP and redox power to growth or product synthesis [10]. These deletions were chosen to yield a strain with a lower metabolic burden and an increased genetic stability and susceptibility to genetic engineering [10]. EM383 showed improved growth, viability and genetic stability, all key features in industrial biotechnology [45].

Further development of EM42 was accomplished by Volke et al. (2020), focusing on the susceptibility towards genetic engineering [13]. The resulting SEM10 strain had β -lactamase-like genes deleted to decrease *P. putida* KT2440's natural resistance to β -lactam antibiotics. Furthermore, genes interfering with fluorescent selection techniques were removed to facilitate colony selection [13]. The second round of streamlining focused more on the genetic engineering aspects, but in combination with the genomic deletions of EM383, SEM10 has the potential to be a valuable *P. putida* platform strain. The genome reduced strains' applications for biotechnological processes are still few but are showing good promise. For example, a study showed increased heterologous gene expression in the genome reduced strain EM383 resulting in up to 40% higher recombinant protein yield [45]. Other laboratory studies have utilized EM42 as the platform strain for the biosynthetic production of cis,cis-muconic acid, propionic acid and polyhydroxyalkanoates (PHA), proving their applicability as platform strain [15, 46, 47].

Highlights of *P. putida* biotechnological applications

The versatility and robustness of *P. putida* have, not surprisingly, led to its use in a broad range of biotechnological applications. One heavily explored application is the production of biopolymers, especially PHAs [16, 48]. PHA comprises a large group of partially crystalline polymers characterized by their biodegradability and is considered a promising

candidate to replace many petroleum-derived plastics [49]. *P. putida* naturally accumulates PHA as a carbon storage under nutrient limitation of, for example, N or P [50]. As plastics are considered a low-value product, emphasis has been on reducing costs by, for example, using low-cost substrates for biomass accumulation and fatty acids for PHA accumulation [51].

The organic acid *cis-cis*-muconic acid is a precursor for synthetic production of, for example, terephthalic acid, which itself is a precursor for different plastics [52]. It can be produced by the degradation of aromatic compounds to the toxic intermediate catechol and then by ring-cleavage to *cis-cis*-muconic acid. As aromatic compounds are highly toxic to microorganisms, only a few species are applicable as production hosts for this process [15]. *P. putida* is a prime production candidate due to its large repertoire of tools to counteract the stresses imposed by aromatic substrates and toxic intermediates [15, 29]. The *P. putida* strain KT2440 has been genetically upgraded to produce *cis-cis*-muconic acid titers as high as 64.2 g·L⁻¹ from catechol in a 1 L bioreactor [52]. Furthermore, utilization of the *P. putida* genome reduced strain EM42, resulted in an even higher final *cis-cis*-muconic acid titer of 74 g·L⁻¹ [15].

Biosurfactants, such as rhamnolipids, have emerged as attractive alternatives to chemically derived surfactants due to their biodegradability and low toxicity. Surfactants find application in, among others, food and cosmetic products due to their emulsifying and antimicrobial properties [53]. The pathogen *Pseudomonas aeruginosa* is considered the best characterized rhamnolipid-producing bacterial species. However, to avoid complications related to the pathogenicity of *P. aeruginosa*, the close relative, *P. putida*, has received increased consideration as a production host for rhamnolipid production [18, 53]. Furthermore, the ability of *P. putida* KT2440 to endure temporal oxygen starvation has also been shown to be transferable to the production of rhamnolipids, as the product yields did not diminish when the cultivation was subjected to DO oscillations [30].

References

- [1] Nakazawa, T. "Travels of a *Pseudomonas*, from Japan around the world". In: *Environmental Microbiology* 4 (12 2002), pp. 782–786. DOI: 10.1046/j.1462-2920.2002.00310.x.
- [2] Bagdasarian, M. M., Lurz, R., Riickert, B., Frey, J., and Timmis, K. N. "Specific-purpose plasmid cloning vectors II. Broad host range, high copy number, RSF1010-derived gene cloning in". In: *Gene* 16 (1981), pp. 237–247.
- [3] Kampers, L. F., Volkers, R. J., and Santos, V. A. M. dos. "Pseudomonas putida KT2440 is HV1 certified, not GRAS". In: *Microbial Biotechnology* (635536 2019), pp. 10–13. DOI: 10.1111/1751-7915.13443.
- [4] Timmis, K. N. "Pseudomonas putida : a cosmopolitan opportunist par excellence". In: *Environ. Microbiol.* 4 (12 2002), pp. 779–781.
- [5] Ebert, B. E., Kurth, F., Grund, M., Blank, L. M., and Schmid, A. "Response of *Pseudomonas putida* KT2440 to increased NADH and ATP demand". In: *Applied and Environmental Microbiology* 77 (18 2011), pp. 6597–6605. DOI: 10.1128/AEM.05588-11.
- [6] Chavarría, M., Nikel, P. I., Pérez-Pantoja, D., and Lorenzo, V. D. "The Entner-Doudoroff pathway empowers *Pseudomonas putida*KT2440 with a high tolerance to oxidative stress". In: *Environmental Microbiology* 15 (6 2013), pp. 1772–1785. DOI: 10.1111/1462-2920.12069.
- [7] Nelson, K. E., Weinl, C., Paulsen, I. T., Dodson, R. J., Hilbert, H., Santos, V. A. M. dos, Fouts, D. E., Gill, S. R., Pop, M., Holmes, M., Brinkac, L., Beanan, M., De-Boy, R. T., Daugherty, S., Kolonay, J., Madupu, R., Nelson, W., White, O., Peterson, J., Khouri, H., Hance, I., Lee, P. C., Holtzapple, E., Scanlan, D., Tran, K., Moazzez, A., Utterback, T., Rizzo, M., Lee, K., Kosack, D., Moestl, D., Wedler, H., Lauber, J., Stjepandic, D., Hoheisel, J., Straetz, M., Heim, S., Kiewitz, C., Eisen, J., Timmis, K. N., Dusterhöft, A., Tümmler, B., and Fraser, C. M. "Complete genome sequence and comparative analysis of the metabolically versatile *Pseudomonas*

- putida KT2440". In: *Environmental Microbiology* 4 (12 2002), pp. 799–808. DOI: 10.1046/j.1462-2920.2002.00366.x.
- [8] Nogales, J., Palsson, B., and Thiele, I. "A genome-scale metabolic reconstruction of *Pseudomonas putida* KT2440: iJN746 as a cell factory". In: *BMC Systems Biology* 2 (2008), pp. 1–20. DOI: 10.1186/1752-0509-2-79.
- [9] Puchałka, J., Oberhardt, M. A., Godinho, M., Bielecka, A., Regenhardt, D., Timmis, K. N., Papin, J. A., and Santos, V. A. M. D. "Genome-scale reconstruction and analysis of the *Pseudomonas putida* KT2440 metabolic network facilitates applications in biotechnology". In: *PLoS Computational Biology* 4 (10 2008). DOI: 10.1371/journal.pcbi.1000210.
- [10] Martínez-García, E., Nikel, P. I., Aparicio, T., and Lorenzo, V. de. "Pseudomonas 2.0: Genetic upgrading of *P. putida* KT2440 as an enhanced host for heterologous gene expression". In: *Microbial Cell Factories* 13 (1 2014), pp. 1–15. DOI: 10.1186/s12934-014-0159-3.
- [11] Martínez-García, E. and Lorenzo, V. de. "Molecular tools and emerging strategies for deep genetic/genomic refactoring of *Pseudomonas*". In: *Current Opinion in Biotechnology* 47 (2017), pp. 120–132. DOI: 10.1016/j.copbio.2017.06.013.
- [12] Aparicio, T., Lorenzo, V. de, and Martínez-García, E. "CRISPR/Cas9-Based Counterselection Boosts Recombineering Efficiency in *Pseudomonas putida*". In: *Biotechnology Journal* 13 (5 2018). DOI: 10.1002/biot.201700161.
- [13] Volke, D. C., Friis, L., Wirth, N. T., Turlin, J., and Nikel, P. I. "Synthetic control of plasmid replication enables target- and self-curing of vectors and expedites genome engineering of *Pseudomonas putida*". In: *Metabolic Engineering Communications* 10 (January 2020), e00126. DOI: 10.1016/j.mec.2020.e00126.
- [14] Calero, P. and Nikel, P. I. "Chasing bacterial chassis for metabolic engineering: a perspective review from classical to non-traditional microorganisms". In: *Microbial Biotechnology* 12 (1 2019), pp. 98–124. DOI: 10.1111/1751-7915.13292.
- [15] Kohlstedt, M., Weimer, A., Weiland, F., Stolzenberger, J., Selzer, M., Sanz, M., Kramps, L., and Wittmann, C. "Biobased PET from lignin using an engineered *cis*,

- cis-muconate-producing *Pseudomonas putida* strain with superior robustness, energy and redox properties". In: *Metabolic Engineering* 72 (2022), pp. 337–352. DOI: 10.1016/j.ymben.2022.05.001.
- [16] Poblete-Castro, I., Rodriguez, A. L., Lam, C. M. C., and Kessler, W. "Improved production of medium-chain-length polyhydroxyalkanoates in glucose-based fed-batch cultivations of metabolically engineered *Pseudomonas putida* strains". In: *Journal of Microbiology and Biotechnology* 24 (1 2014). Look at cites, pp. 59–69. DOI: 10.4014/jmb.1308.08052.
- [17] Patil, M. D., Shinde, K. D., Patel, G., Chisti, Y., and Banerjee, U. C. "Use of response surface method for maximizing the production of arginine deiminase by *Pseudomonas putida*". In: *Biotechnology Reports* 10 (2016), pp. 29–37. DOI: 10.1016/j.btre.2016.03.002.
- [18] Tiso, T., Ihling, N., Kubicki, S., Biselli, A., Schonhoff, A., Bator, I., Thies, S., Kar-mainski, T., Kruth, S., Willenbrink, A. L., Loeschcke, A., Zapp, P., Jupke, A., Jaeger, K. E., Büchs, J., and Blank, L. M. "Integration of Genetic and Process Engineering for Optimized Rhamnolipid Production Using *Pseudomonas putida*". In: *Frontiers in Bioengineering and Biotechnology* 8 (2020). DOI: 10.3389/fbioe.2020.00976.
- [19] Lessie, T. G. and Phibbs, P. V. "Alternative Pathways of Carbohydrate Utilization in Pseudomonads". In: *Annual Reviews of Microbiology* 38 (1984), pp. 359–387. DOI: 10.1146/annurev.mi.38.100184.002043.
- [20] Castillo, T. D., Ramos, J. L., Rodríguez-Herva, J. J., Fuhrer, T., Sauer, U., and Duque, E. "Convergent peripheral pathways catalyze initial glucose catabolism in *Pseudomonas putida*: Genomic and flux analysis". In: *Journal of Bacteriology* 189 (14 2007), pp. 5142–5152. DOI: 10.1128/JB.00203-07.
- [21] Nikel, P. I., Chavarría, M., Fuhrer, T., Sauer, U., and Lorenzo, V. de. "*Pseudomonas putida* KT2440 Strain Metabolizes Glucose through a Cycle Formed by Enzymes of the Entner-Doudoroff, Embden-Meyerhof-Parnas, and Pentose Phosphate Pathways". In: *Journal of Biological Chemistry* 290 (43 2015), pp. 25920–25932. DOI: 10.1074/jbc.M115.687749.

- [22] Nikel, P. I., Fuhrer, T., Chavarría, M., Sánchez-Pascuala, A., Sauer, U., and Lorenzo, V. de. "Reconfiguration of metabolic fluxes in *Pseudomonas putida* as a response to sub-lethal oxidative stress". In: *ISME Journal* 15 (6 2021), pp. 1751–1766. DOI: 10.1038/s41396-020-00884-9.
- [23] Peng, J., Miao, L., Chen, X., and Liu, P. "Comparative transcriptome analysis of *Pseudomonas putida* KT2440 revealed its response mechanisms to elevated levels of zinc stress". In: *Frontiers in Microbiology* 9 (JUL July 2018). DOI: 10.3389/fmicb.2018.01669.
- [24] Manara, A., DalCorso, G., Baliardini, C., Farinati, S., Cecconi, D., and Furini, A. "Pseudomonas putida Response to Cadmium: Changes in Membrane and Cytosolic Proteomes". In: *Journal of Proteome Research* 11 (8 Aug. 2012), pp. 4169–4179. DOI: 10.1021/pr300281f.
- [25] Blank, L. M., Ionidis, G., Ebert, B. E., Bühler, B., and Schmid, A. "Metabolic response of *Pseudomonas putida* during redox biocatalysis in the presence of a second octanol phase". In: *FEBS Journal* 275 (20 Oct. 2008), pp. 5173–5190. DOI: 10.1111/j.1742-4658.2008.06648.x.
- [26] Nikel, P. I., Martínez-García, E., and Lorenzo, V. D. "Biotechnological domestication of pseudomonads using synthetic biology". In: *Nature Reviews Microbiology* 12 (5 2014), pp. 368–379. DOI: 10.1038/nrmicro3253.
- [27] Ramos, J. L., Duque, E., Mari, M., Huertas, M.-J., Hai'dour, A., and Hai'dour, H. *Isolation and Expansion of the Catabolic Potential of a Pseudomonas putida Strain Able To Grow in the Presence of High Concentrations of Aromatic Hydrocarbons*. 1995, pp. 3911–3916.
- [28] García-Franco, A., Godoy, P., Duque, E., and Ramos, J. L. "Insights into the susceptibility of *Pseudomonas putida* to industrially relevant aromatic hydrocarbons that it can synthesize from sugars". In: *Microbial Cell Factories* 22 (1 Dec. 2023). DOI: 10.1186/s12934-023-02028-y.
- [29] Ramos, J. L., Cuenca, M. S., Molina-Santiago, C., Segura, A., Duque, E., Gómez-García, M. R., Udaondo, Z., and Roca, A. "Mechanisms of solvent resistance medi-

- ated by interplay of cellular factors in *Pseudomonas putida*". In: *FEMS Microbiology Reviews* 39 (4 July 2015), pp. 555–566. DOI: 10.1093/femsre/fuv006.
- [30] Demling, P., Ankenbauer, A., Klein, B., Noack, S., Tiso, T., Takors, R., and Blank, L. M. "Pseudomonas putida KT2440 endures temporary oxygen limitations". In: *Biotechnology and Bioengineering* 118 (12 2021), pp. 4735–4750. DOI: 10.1002/bit.27938.
- [31] Heerema, L., Wierckx, N., Roelands, M., Hanemaaijer, J. H., Goetheer, E., Verdoes, D., and Keurentjes, J. "In situ phenol removal from fed-batch fermentations of solvent tolerant *Pseudomonas putida* S12 by pertraction". In: *Biochemical Engineering Journal* 53 (3 Feb. 2011), pp. 245–252. DOI: 10.1016/j.bej.2010.11.002.
- [32] Nadal-Rey, G., McClure, D. D., Kavanagh, J. M., Cassells, B., Cornelissen, S., Fletcher, D. F., and Gernaey, K. V. "Development of dynamic compartment models for industrial aerobic fed-batch fermentation processes". In: *Chemical Engineering Journal* 420 (2021). DOI: 10.1016/j.cej.2021.130402.
- [33] Haringa, C., Tang, W., Deshmukh, A. T., Xia, J., Reuss, M., Heijnen, J. J., Mudde, R. F., and Noorman, H. J. "Euler-Lagrange computational fluid dynamics for (bio)reactor scale down: An analysis of organism lifelines". In: *Engineering in Life Sciences* 16 (7 2016), pp. 652–663. DOI: 10.1002/elsc.201600061.
- [34] Ankenbauer, A., Schäfer, R. A., Viegas, S. C., Pobre, V., Voß, B., Arraiano, C. M., and Takors, R. "Pseudomonas putida KT2440 is naturally endowed to withstand industrial-scale stress conditions". In: *Microbial Biotechnology* 13 (4 2020), pp. 1145–1161. DOI: 10.1111/1751-7915.13571.
- [35] Kuschel, M., Siebler, F., and Takors, R. "Lagrangian Trajectories to Predict the Formation of Population Heterogeneity in Large-Scale Bioreactors". In: *Bioengineering* 4 (4 2017), p. 27. DOI: 10.3390/bioengineering4020027.
- [36] Rodriguez, A., Escobar, S., Gomez, E., Santos, V. E., and Garcia-Ochoa, F. "Behavior of several pseudomonas putida strains growth under different agitation and oxygen supply conditions". In: *Biotechnology Progress* 34 (4 2018), pp. 900–909. DOI: 10.1002/btpr.2634.

- [37] Bugg, T. D., Williamson, J. J., and Alberti, F. "Microbial hosts for metabolic engineering of lignin bioconversion to renewable chemicals". In: *Renewable and Sustainable Energy Reviews* 152 (Dec. 2021). DOI: 10.1016/j.rser.2021.111674.
- [38] Dvořák, P. and Lorenzo, V. de. "Refactoring the upper sugar metabolism of *Pseudomonas putida* for co-utilization of cellobiose, xylose, and glucose". In: *Metabolic Engineering* 48 (July 2018), pp. 94–108. DOI: 10.1016/j.ymben.2018.05.019.
- [39] Elmore, J. R., Dexter, G. N., Salvachúa, D., O'Brien, M., Klingeman, D. M., Gorday, K., Michener, J. K., Peterson, D. J., Beckham, G. T., and Guss, A. M. "Engineered *Pseudomonas putida* simultaneously catabolizes five major components of corn stover lignocellulose: Glucose, xylose, arabinose, p-coumaric acid, and acetic acid". In: *Metabolic Engineering* 62 (Nov. 2020), pp. 62–71. DOI: 10.1016/j.ymben.2020.08.001.
- [40] Peabody, G. L., Elmore, J. R., Martinez-Baird, J., and Guss, A. M. "Engineered *Pseudomonas putida* KT2440 co-utilizes galactose and glucose". In: *Biotechnology for Biofuels* 12 (1 Dec. 2019). DOI: 10.1186/s13068-019-1627-0.
- [41] Leprince, A., Lorenzo, V. de, Völler, P., Passel, M. W. van, and Santos, V. A. M. dos. "Random and cyclical deletion of large DNA segments in the genome of *Pseudomonas putida*". In: *Environmental Microbiology* 14 (6 2012), pp. 1444–1453. DOI: 10.1111/j.1462-2920.2012.02730.x.
- [42] Weimer, A., Kohlstedt, M., Volke, D. C., Nickel, P. I., and Wittmann, C. "Industrial biotechnology of *Pseudomonas putida*: advances and prospects". In: *Applied Microbiology and Biotechnology* 104 (18 2020), pp. 7745–7766. DOI: 10.1007/s00253-020-10811-9.
- [43] Martínez-García, E., Fraile, S., Espeso, D. R., Vecchiotti, D., Bertoni, G., and Lorenzo, V. D. "Naked Bacterium: Emerging Properties of a Surfome-Streamlined *Pseudomonas putida* Strain". In: *ACS Synthetic Biology* 9 (9 2020), pp. 2477–2492. DOI: 10.1021/acssynbio.0c00272.
- [44] Liang, P., Zhang, Y., Xu, B., Zhao, Y., Liu, X., Gao, W., Ma, T., Yang, C., Wang, S., and Liu, R. "Deletion of genomic islands in the *Pseudomonas putida* KT2440

- genome can create an optimal chassis for synthetic biology applications”. In: *Microbial Cell Factories* 19 (1 2020). DOI: 10.1186/s12934-020-01329-w.
- [45] Lieder, S., Nikel, P. I., Lorenzo, V. de, and Takors, R. “Genome reduction boosts heterologous gene expression in *Pseudomonas putida*”. In: *Microbial Cell Factories* 14 (1 2015), pp. 1–14. DOI: 10.1186/s12934-015-0207-7.
- [46] Tiwari, R., Sathesh-Prabu, C., and Lee, S. K. “Bioproduction of propionic acid using levulinic acid by engineered *Pseudomonas putida*”. In: *Frontiers in Bioengineering and Biotechnology* 10 (2022). DOI: 10.3389/fbioe.2022.939248.
- [47] Cha, D., Ha, H. S., and Lee, S. K. “Metabolic engineering of *Pseudomonas putida* for the production of various types of short-chain-length polyhydroxyalkanoates from levulinic acid”. In: *Bioresource Technology* 309 (2020). DOI: 10.1016/j.biortech.2020.123332.
- [48] Follonier, S., Henes, B., Panke, S., and Zinn, M. “Putting cells under pressure: A simple and efficient way to enhance the productivity of medium-chain-length polyhydroxyalkanoate in processes with *Pseudomonas putida* KT2440”. In: *Biotechnology and Bioengineering* 109 (2 2012), pp. 451–461. DOI: 10.1002/bit.23312.
- [49] Khanna, S. and Srivastava, A. K. “Recent advances in microbial polyhydroxyalkanoates”. In: *Process Biochemistry* 40 (2 2005), pp. 607–619. DOI: 10.1016/j.procbio.2004.01.053.
- [50] Poblete-Castro, I., Escapa, I. F., Jäger, C., Puchalka, J., Ming, C., Lam, C., Schomburg, D., Prieto, M. A., Martins, V. A., and Santos, D. “The metabolic response of *P. putida* KT2442 producing high levels of polyhydroxyalkanoate under single-and multiple-nutrient-limited growth: Highlights from a multi-level omics approach”. In: *Microbial Cell Factories* 11 (1 2012).
- [51] Follonier, S., Riesen, R., and Zinn, M. “Pilot-scale production of functionalized mcl-PHA from grape pomace supplemented with fatty acids”. In: *Chemical and Biochemical Engineering Quarterly* 29 (2 2015), pp. 113–121. DOI: 10.15255/CABEQ.2014.2251.

- [52] Kohlstedt, M., Starck, S., Barton, N., Stolzenberger, J., Selzer, M., Mehlmann, K., Schneider, R., Pleissner, D., Rinkel, J., Dickschat, J. S., Venus, J., Duuren, J. B. van, and Wittmann, C. "From lignin to nylon: Cascaded chemical and biochemical conversion using metabolically engineered *Pseudomonas putida*". In: *Metabolic Engineering* 47 (May 2018), pp. 279–293. DOI: 10.1016/j.ymben.2018.03.003.
- [53] Tiso, T., Thies, S., Müller, M., Tsvetanova, L., Carraresi, L., Bröring, S., Jaeger, K.-E., and Blank, L. M. "Rhamnolipids: Production, Performance, and Application". In: Springer International Publishing, 2017, pp. 587–622. DOI: 10.1007/978-3-319-50436-0_388.

3 Genome reduced *Pseudomonas putida* SEM10 strain tolerates oxygen depletion

Abstract

Application of the obligate aerobe *Pseudomonas putida* in industrial scale production requires a good understanding of the effect of changing oxygen availability due to the dissolved oxygen (DO) gradients apparent at such scale. To that end, the *P. putida* wild type KT2440 and genome reduced SEM10 strains were subjected to different oxygen partial pressures (p_{O_2}) in the aeration gas, to evaluate the effect of low oxygen availability on growth characteristics in batch mode. During exponential growth at low p_{O_2} (0.0525 atm), both strains observed an 8-10 % increase in biomass yield on glucose ($Y_{X/S}$) compared to high p_{O_2} (0.21 atm). However, the increased carbon efficiency diminished as dissolved oxygen became limiting, reducing the overall $Y_{X/S}$. At the end of the cultivation, KT2440 achieved an overall $Y_{X/S}$ of $0.352 \pm 0.027 \text{ g} \cdot \text{g}^{-1}$, similar to the $Y_{X/S}$ of $0.383 \pm 0.016 \text{ g} \cdot \text{g}^{-1}$ at high p_{O_2} . Likewise, SEM10 achieved a similar overall $Y_{X/S}$ at both high and low p_{O_2} of $0.432 \pm 0.015 \text{ g} \cdot \text{g}^{-1}$ and $0.434 \pm 0.008 \text{ g} \cdot \text{g}^{-1}$, respectively. Overall, the genome reduced SEM10 strain retained its superior growth characteristics, compared to the wild type KT2440, during growth at both high and low p_{O_2} with DO limitation. These findings indicated that the genome reduction was beneficial during growth at low oxygen availability, highlighting the advantages of utilizing the investigated genome reduced strain.

3.1 Introduction

The obligate aerobic soil bacterium *Pseudomonas putida* has emerged as an alternative host for biochemical production over the past decades [1, 2]. The bacterium harbors a remarkable versatile metabolism that allows it to adapt readily to a range of environmental demands [3]. Accordingly, the versatile metabolism of *P. putida* has been the basis for the development of the species for biochemical production of a wide scope of products,

ranging from biosurfactants to biopolymers and even aromatics [4–6]. Development has not been limited to product-specific research as the *P. putida* KT2440 strain has been subject to genome streamlining to produce more carbon-efficient platform strains. The wild type *P. putida* KT2440 had its genome reduced by ~4.3%, resulting in the EM383 strain, which was further reduced by ~0.5% to yield the SEM10 strain [7, 8]. For example, transposons and antibiotic resistance genes were deleted to produce strains with higher genetic stability and more susceptible to genetic engineering. In addition, a considerable amount of prophage genes and the flagellar operon were deleted to reduce the metabolic burden of the genome reduced strain [7, 8]. As a result, EM383 showed improved growth characteristics such as higher maximum specific growth rate, higher biomass yield and higher protein yields in bioreactor studies [7, 9]. Furthermore, the SEM10 strain showed similar growth profiles in shake flask cultivations compared to its predecessor [7, 8].

Cultivating microorganisms in large-scale industrial bioreactors can be challenging due to the mass transfer limitations observed at that scale. The mass transfer limitations often result in gradients of, for example, substrate, dissolved oxygen (DO) or pH during cultivation [10–12]. Such gradients expose the microorganisms to ever-changing nutrient limitations such as high and low DO concentrations [10, 12]. Simulated glucose gradients by computational fluid dynamics have been shown to adversely affect the growth and production of microorganisms, such as *P. putida* KT2440 and *Penicillium chrysogenum* [13, 14]. Similarly, *P. putida* KT2440 was exposed to glucose and oxygen starvation in scale-down systems, demonstrating a remarkable ability to endure temporal nutrient starvation [15, 16]. However, other studies showed that changes in oxygen availability affected biomass accumulation during growth on glycerol [17]. In addition, the different steps of periplasmic glucose conversion in *P. putida* mt-2 have different oxygen demands [17–19].

This study aimed to elucidate if continued low oxygen availability affects *P. putida* KT2440 and SEM10 growth glucose and if the genome reduced strain maintained its advantageous growth characteristics at low oxygen availability. Furthermore, the wild type

KT2440 and genome reduced SEM10 strains were compared to evaluate the applicability of SEM10 as a *P. putida* platform strain. To this end, *P. putida* KT2440 and SEM10 were cultivated in batch mode at high and low oxygen transfer rates to elucidate the dynamic behavior of *P. putida* growth at low oxygen availability.

3.2 Materials and Methods

Bacterial Strains and Medium

Bacterial strains *Pseudomonas putida* KT2440 and SEM10 were used in this study and stored at -80°C in 50 % (w/w) glycerol. Lysogeny broth (LB) agar medium contained per liter: 10 g tryptone, 5 g yeast extract, 10 g NaCl and 20 g agar. The defined basis medium contained per liter: 3.88 g K₂HPO₄, 2.12 g NaH₂PO₄ · 2H₂O and 10 mL trace element solution. The trace element solution contained per liter: 1 g EDTA, 10 g MgCl₂ · 6H₂O, 0.2 g ZnSO₄ · 7H₂O, 0.1 g CaCl₂ · 2H₂O, 0.5 g FeSO₄ · 7H₂O, 0.02 g Na₂MoO₄ · 2H₂O, 0.02 g CuSO₄ · 5H₂O, 0.04 g CoCl₂ · 6H₂O and 0.122 g MnCl₂ · 4H₂O. Shaken cultures were supplemented with 4 g·L⁻¹ and 2 g·L⁻¹ (NH₄)₂SO₄ and bioreactor cultivations with 10 g·L⁻¹ glucose and 5 g·L⁻¹ (NH₄)₂SO₄. All chemicals were purchased from Merck (USA).

Shake flask cultures

Precultures were prepared in three steps: First, glycerol stocks were activated by streaking on LB agar plates (Sarsted, Germany) and incubating at 30°C for 18 h. Second, a liquid preculture, of 5 mL basis medium in a 14 mL cultivation tube (Falcon, Corning, Mexico), was inoculated with 3 colonies from a fresh LB agar plate and incubated at 30°C and 180 rpm for 8 h in a rotary shaker (Ecotron, Infors HT, Switzerland). Third, a final liquid preculture was inoculated to an initial cell dry weight (CDW) concentration of 4.59 mg·L⁻¹ in 500 mL baffled shake flasks (DWK Life Sciences, United Kingdom) containing 50 mL basis medium and incubated at 30°C and 180 rpm for 18 h in a rotary shaker (Ecotron, Infors HT, Switzerland).

Shake flask cultivations were performed with 200 mL basis medium in 2000 mL baffled shake flasks (KAVALIERGLASS, Czech Republic). The cultures were inoculated to an initial CDW concentration of 45.9 mg·L⁻¹ and incubated at 30°C and 180 rpm in a rotary

shaker (Ecotron, Infors HT, Switzerland).

Biolector cultivations

A Biolector II Pro system (m2p-labs, Germany) was used as the platform for Biolector cultivations. BOH-1 type 48-well FlowerPlate® (m2p-labs, Germany) with fluorescent optodes for online measurements of dissolved oxygen (DO) and pH was used as the cultivation vessel. Biomass was measured as the intensity of backscattered light at 600 nm, DO was measured as the fluorescence at excitation/emission of 520/600 nm. Cultivation conditions for all experiments were: 30°C, 800 rpm, humidity control at 85% relative humidity, 1 mL total cultivation volume and 1 min cycle time, initial CDW concentration of 45.9 mg·L⁻¹. All Biolector cultivations were performed with 6 replicates.

Bioreactor cultivations

Bioreactor batch cultivations were performed in a 2 L working volume EZ-control bioreactor (Gefco, Sweden). The bioreactor was inoculated with a 2% (v/v) shake flask preculture. Agitation and temperature were maintained at 1000 rpm and 30°C, respectively, throughout the cultivation. Aeration was fixed at 2 L_n·min⁻¹, but the gas composition was varied to adjust the oxygen partial pressure. The partial pressure was kept constant throughout the cultivation at either 0.21 atm or 0.0525 atm. S50 mass flow controllers (Sierra Instruments, USA) controlled individual gas flow of air and N₂. The pH was controlled by the addition of 2 M NaOH or 2 M HCl. Antifoam agent Antifoam 204 (Sigma Aldrich, USA) was added as required aseptically with a syringe. Off-gas composition of O₂ and CO₂ was measured online by BlueInOne Cell (BlueSens, Germany). The off-gas composition of KT2440 cultivations was measured every 16 min and every minute for SEM10 cultivations. The KT2440 off-gas data were interpolated using a MATLAB 2019b shape-preserving piecewise cubic interpolation function to obtain data at the sampling points.

Offline Analytics

Samples for high pressure liquid chromatography (HPLC) analysis were filtered through a 0.2 µm cellulose acetate syringe filter (Phenomenex, USA). The filtered samples were stored at - 18°C prior to analysis. Glucose, gluconate and 2-ketogluconate concentrations

were measured by HPLC. Analysis was performed in an Ultimate 3000 (Thermo Scientific, USA) equipped with an Aminex HPX-87H ion exchange column (Bio-Rad, USA). Operation settings were 30°C column temperature, 5 mM H₂SO₄ mobile phase, 0.6 mL·min⁻¹ flow rate, detection in the refractive index and ultraviolet (UV) channel at 210 nm. Glucose and gluconate co-elute, but their concentrations were correlated by their differential contribution in the refractive index and UV channel.

Total biomass was analyzed as cell dry weight (CDW). An appropriately diluted sample was filtered through a 0.2 µm polyethersulfone membrane filter (Sartorius Stedim Biotech, Germany) and the filter was flushed twice with 5 mL deionized water. The filter was then dried in a microwave oven for 20 min at 180 W and cooled for 48 h in a desiccator. The biomass content of shake flask cultivations was estimated by optical density measurements at 600 nm (OD₆₀₀) using a UV-1800 UV-spectrophotometer (Shimadzu, Japan). The optical density was correlated to CDW as follows:

$$CDW(g \cdot L^{-1}) = 0.459 \cdot OD_{600} \quad (3.1)$$

Statistical Analysis

Shake flask experiments were performed with 3 replicates, Biolector experiments with 6 replicates and bioreactor experiments with 2 replicates. Significant differences between parameters were evaluated with either two-tailed t-test or analysis of variance (ANOVA), considering p-value < 0.05 as significant.

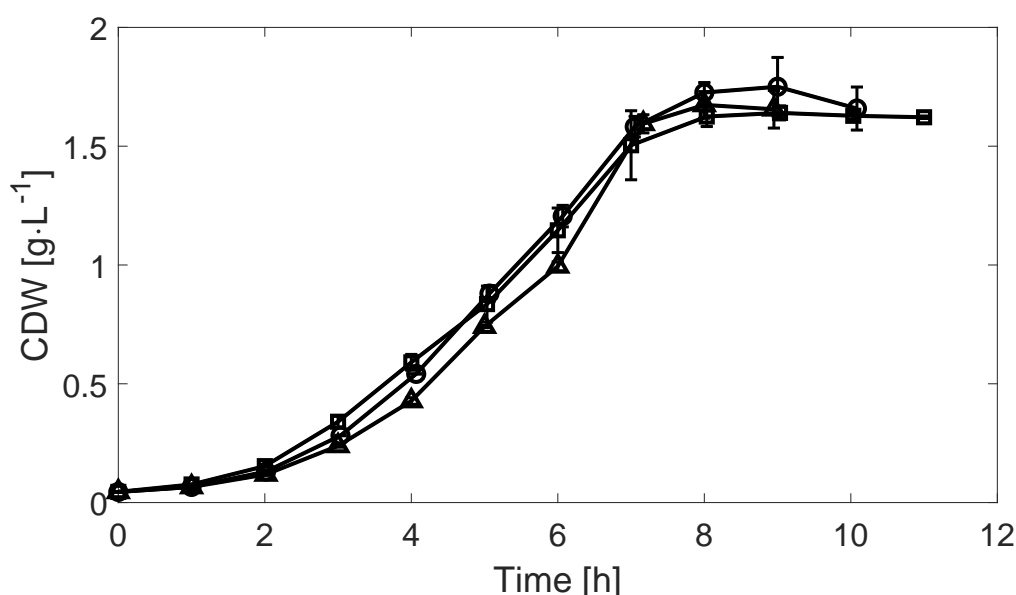
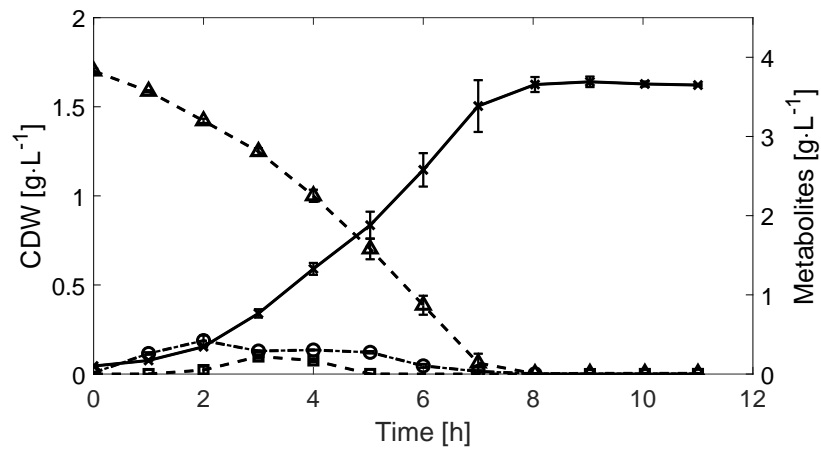


Figure 3.1: Shake flask cultivations of *P. putida* KT2440 at various agitation speeds. Biomass accumulation illustrated as optical density OD₆₀₀. 80 rpm (□), 180 rpm (○) and 280 rpm (△).

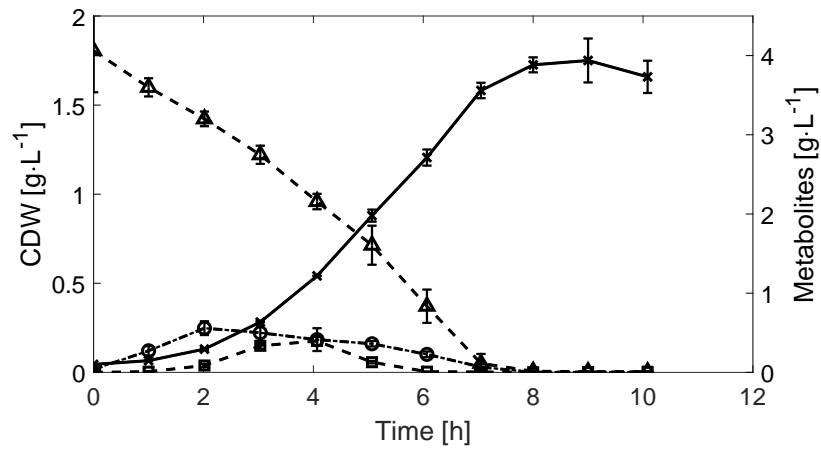
3.3 Results and discussion

Effect of oxygen supply on *P. putida* KT2440 in shaken cultures

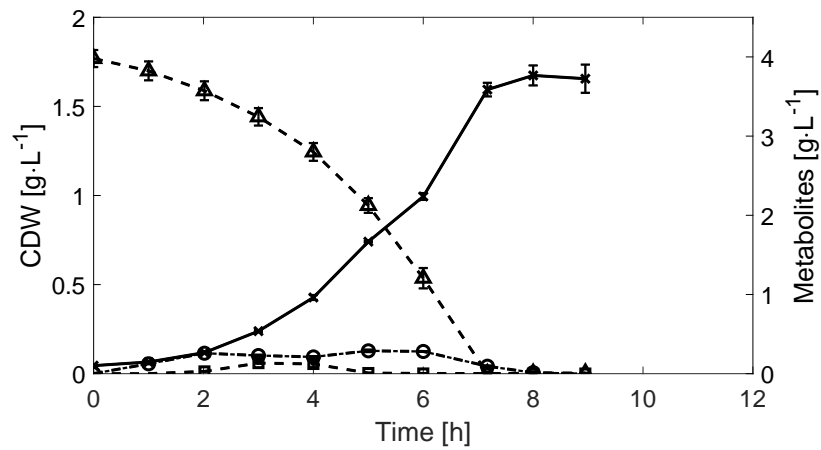
The supply of oxygen is a crucial aspect of bioprocesses as the lack of oxygen can lead to undesired behavior of the microorganism. Low DO concentrations have been shown to reduce the biomass yield and change glucose conversion patterns in the periplasm of *P. putida* BM014 and must thus be evaluated [18]. To this end, the *P. putida* wild type strain KT2440 was cultivated in shake flasks at three different agitation speeds to evaluate the effect of different oxygen transfer rates. The growth profiles obtained at 80, 180 and 280 rpm are illustrated in Figure 3.1. Changing agitation in the applied interval did not incur any apparent effect on the biomass accumulation profiles. However, the calculated maximum specific growth rates (μ_{\max}) were significantly different (ANOVA, $p < 0.05$) as presented in Table 3.1. The lowest μ_{\max} , $0.614 \pm 0.004 \text{ h}^{-1}$, was observed at the highest agitation speed and the highest, $0.694 \pm 0.005 \text{ h}^{-1}$, at 180 rpm, whereas an intermediate μ_{\max} , $0.664 \pm 0.017 \text{ h}^{-1}$, was observed at the lowest agitation speed. *P. putida* KT2440 appeared to be susceptible to both insufficient and excess agitation. A different *P. putida* strain, KTH2, has been shown to endure hydrodynamic stress at high agitation speeds



(a)



(b)



(c)

Figure 3.2: Biomass and metabolite profiles of *P. putida* KT2440 shake flask cultivations at various agitation speeds: (a) 80 rpm, (b) 180 rpm and (c) 280 rpm. Cell dry weight (CDW) (X), glucose (Δ), gluconate (O) and 2-ketogluconate (□).

Table 3.1: Parameters of *P. putida* KT2440 shake flask cultivations at various agitation speeds.

Agitation (rpm)	$\mu_{\max,1}$ (h^{-1})	CDW_{\max} ($\text{g}\cdot\text{L}^{-1}$)
80	0.664 ± 0.017	1.66 ± 0.02
180	0.694 ± 0.005	1.77 ± 0.11
280	0.614 ± 0.004	1.70 ± 0.06

but reduce the growth on glycerol at insufficient oxygen supply [17, 20]. This indicates that the growth rate reduction at 80 rpm results from a lower oxygen supply. Whereas the decrease in growth rate at 280 rpm could result from increased oxygen supply as glucose would, to a greater extent, be converted to gluconate, as can be observed in Figure 3.2. Oxygen availability and demand have previously been shown to affect the conversion of glucose and the growth rate in *P. putida* [18, 19].

Shake flask cultures are limited by the information they provide, in this case, specifically the DO concentration. To gain insights into this aspect, the KT2440 and SEM10 strains were cultivated in Biolector II Pro, where both biomass and DO were measured continuously. An added benefit of the Biolector system is the ability to control the partial pressure of oxygen (pO_2) in the cultivation chamber as a method of varying the maximum oxygen transfer rate. This method was chosen because the removal of the flagellar, as in SEM10, has caused increased sedimentation, as reported for other *P. putida* strains without flagellar [7]. The pO_2 was controlled at 0.21 atm, corresponding to ambient conditions, and 0.105 atm during the Biolector cultivations. The KT2440 growth profiles presented in Figure 3.3 (a) showed similar growth profiles between the applied pO_2 levels. This was in contrast to the maximum specific growth rates (μ_{\max}) of $0.842\pm0.016 \text{ h}^{-1}$ and $0.802\pm0.041 \text{ h}^{-1}$ for a pO_2 0.21 atm and a pO_2 0.105 atm, respectively. SEM10 was growing more slowly, as visible from both the biomass and DO profiles. However, the initial μ_{\max} was slightly higher under ambient conditions compared to KT2440. The μ_{\max} of SEM10 was $0.870\pm0.040 \text{ h}^{-1}$ and $0.782\pm0.030 \text{ h}^{-1}$ for a pO_2 of 0.21 atm and a pO_2 of 0.105 atm, respectively. The μ_{\max} was calculated during exponential growth before the cultures reached 100 backscatter A.U. to mitigate the influence of apparent sedimenta-

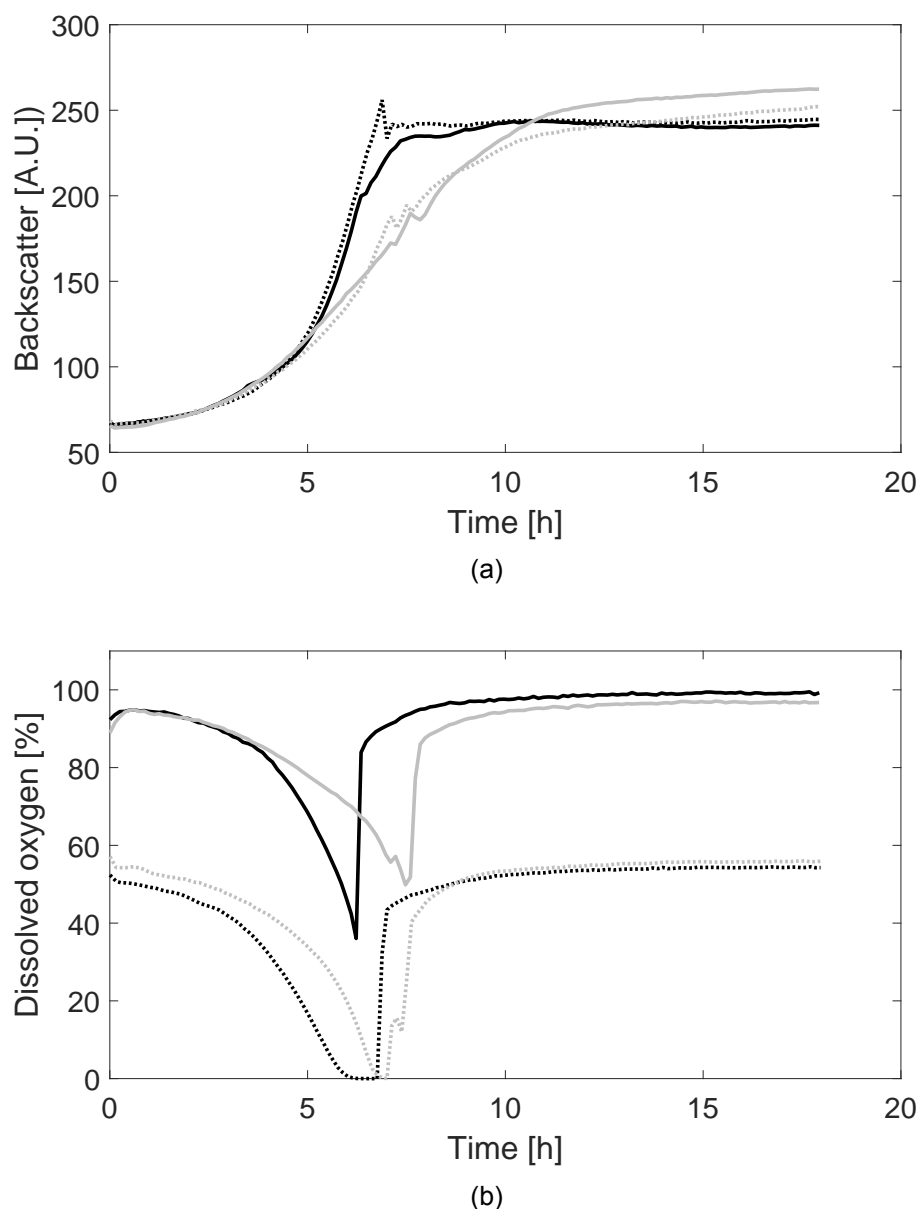


Figure 3.3: Biolector cultivation of *P. putida* KT2440 (black) and SEM10 (light grey) at an oxygen partial pressure of 0.21 atm (-) and 0.105 atm (··). (a): Biomass profiles as backscatter. (b): DO profiles.

tion on SEM10 growth. Only the pO_2 was a significant factor (ANOVA, $p < 0.05$) affecting the μ_{max} whereas strain type, surprisingly, did not have a significant impact (ANOVA, $p > 0.05$). The time points of glucose depletion (noted as the increase in DO) were similar between the tested pO_2 but different between the strains. The latter may be attributed to the possible sedimentation. The compromised growth of SEM10 in the Biolector made the comparison of the two strains impossible. Nevertheless, results indicated that reduction

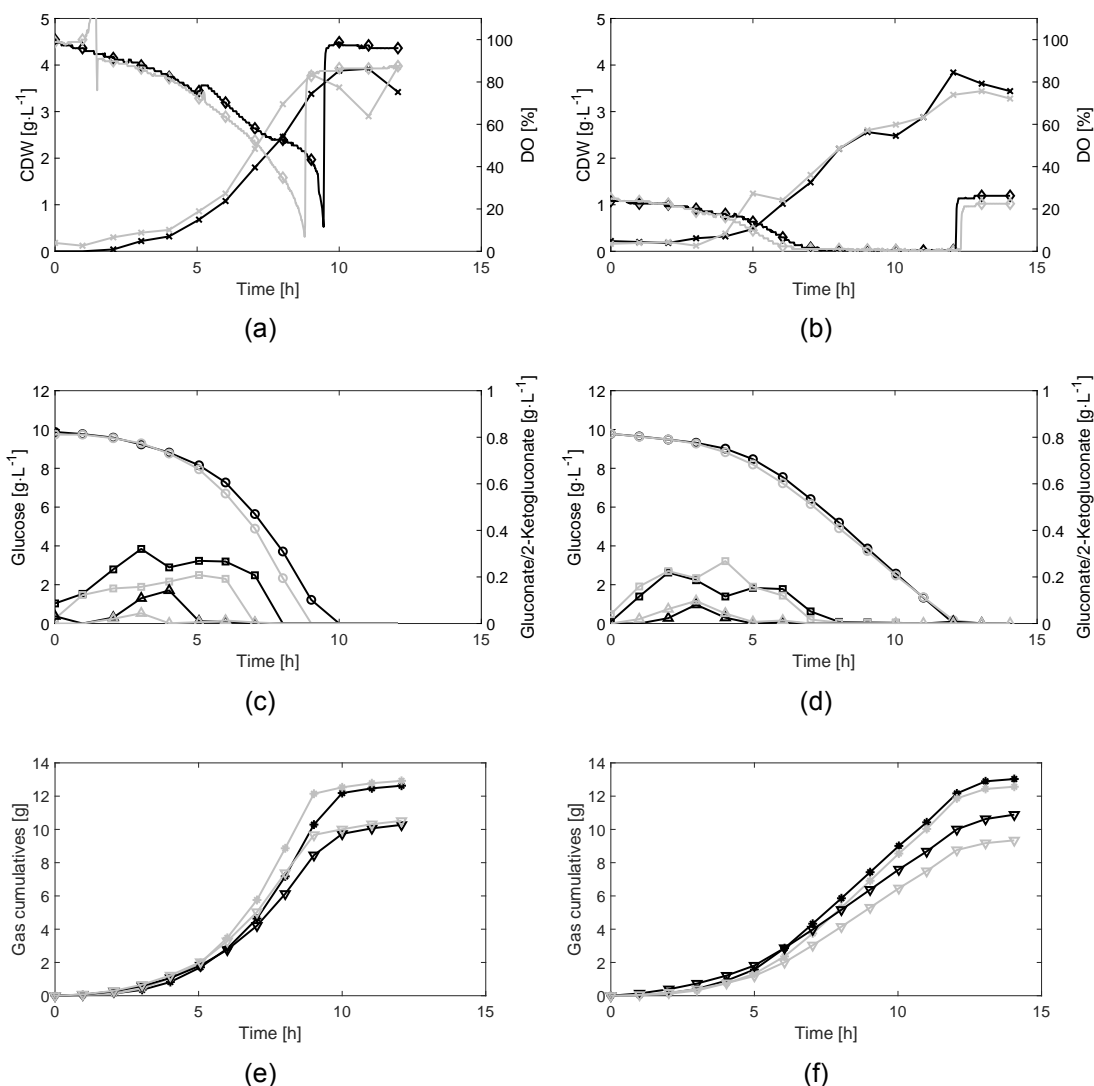


Figure 3.4: Batch cultivation of *P. putida* KT2440 at an oxygen partial pressure of 0.21 atm ((a), (c) and (e)) and 0.0525 atm ((b), (d) and (f)). (a) and (b): CDW concentration ($\text{g}\cdot\text{L}^{-1}$, X), DO concentration (%), \diamond). (c) and (d): CDW concentration ($\text{g}\cdot\text{L}^{-1}$, X), glucose concentration ($\text{g}\cdot\text{L}^{-1}$, O), gluconate concentration ($\text{g}\cdot\text{L}^{-1}$, \square) and 2-ketogluconate concentration ($\text{g}\cdot\text{L}^{-1}$, \triangle). (e) and (f): consumed O_2 (g, *) and produced CO_2 (g, ∇). Black and light grey colors denote different replicates.

of pO_2 could affect *P. putida* growth.

Cultivation of *P. putida* KT2440 and SEM10 strains at high and low pO_2 in a bioreactor

To avoid possible sedimentation of SEM10, further reduce the pO_2 and include off-gas data, the bacterial strains were cultivated in batch mode using a bioreactor. The pO_2 was kept constant throughout the cultivations at either 0.21 atm (high) or 0.0525 atm (low). Adjusting pO_2 rather than agitation ensured that SEM10 would not sediment and a low

Table 3.2: Cultivation parameters at different pO₂ for *P. putida* KT2440 and SEM10 bioreactor batch cultivations. Maximum specific growth rates and yields were calculated during exponential growth.

Strain	pO ₂ (atm)	μ_{\max} (h ⁻¹)	$Y_{X/S}$ (g·g ⁻¹)	Y_{X/O_2} (g·g ⁻¹)	Y_{X/CO_2} (g·g ⁻¹)
KT2440	0.21	0.596±0.007	0.413±0.011	0.835±0.009	0.681±0.017
KT2440	0.0525	0.551±0.013	0.454±0.017	0.931±0.126	0.737±0.054
SEM10	0.21	0.637±0.004	0.454±0.023	0.978±0.063	0.771±0.004
SEM10	0.0525	0.649±0.027	0.492±0.016	1.163±0.018	0.886±0.008

DO concentration would be present already at the start of the cultivation. Figure 3.4 illustrates the growth profiles of *P. putida* KT2440 at a pO₂ of 0.21 atm and 0.0525 atm and Table 3.2 details growth parameters obtained in the exponential growth phase. KT2440 grew as anticipated at high pO₂ (0.21 atm), with a μ_{\max} of 0.596±0.007 h⁻¹ and a biomass yield on glucose ($Y_{X/S}$) of 0.413±0.011 g CDW · (g glucose)⁻¹, which reached glucose depletion at approximately 9-10 h. Production and consumption of both gluconate and 2-ketogluconate occurred simultaneously and prior to glucose depletion as presented in Figure 3.4 (c). O₂ consumption and CO₂ production followed similar trends and accumulated to the same extent. KT2440 cultivations at a lower pO₂ (0.0525 atm) grew 7.6% more slowly (μ_{\max} = 0.551±0.013 h⁻¹) and seemingly reached a 9.9% higher $Y_{X/S}$ (0.454±0.017 g·g⁻¹) during exponential growth, compared to high pO₂. In addition, the cultivations at low pO₂ reached DO depletion after approximately 7 h, further reducing growth as visible from the CDW concentration profiles in Figure 3.4 (b). During exponential growth, KT2440 utilized O₂ more efficiently at low than at high pO₂ achieving a biomass yield on O₂ (Y_{X/O_2} g CDW · (g O₂)⁻¹) of 0.931±0.126 and 0.835±0.009, respectively.

The yields calculated in the exponential phase (Table 3.2) indicate that the KT2440 utilizes glucose for growth more efficiently at low pO₂ compared to high pO₂, though none are significantly different (t-test, $p > 0.05$). This is in contrast to the lower final biomass concentration observed for *P. putida* KT2440 growth on glutamic acid and glycerol at reduced maximum oxygen transfer rate (OTR_{max}) [17, 20]. Furthermore, it contrasts the lower $Y_{X/S}$ reported for *P. putida* BM014 growth on glucose at different DO levels [18]. Considering these contrasts and that the exponential growth phase only covers the non-DO limited

Table 3.3: Cultivation parameters at different pO₂ for *P. putida* KT2440 and SEM10 bioreactor batch cultivations. The yields and CDW concentrations were obtained at the time point of maximum CDW accumulation.

Strain	pO ₂ (atm)	CDW _{max} (g·L ⁻¹)	Y _{X/S, max} (g·g ⁻¹)	Y _{X/O₂, max} (g·g ⁻¹)	Y _{X/CO₂, max} (g·g ⁻¹)
KT2440	0.21	3.94±0.03	0.383±0.016	0.775±0.037	0.618±0.031
KT2440	0.0525	3.64±0.28	0.352±0.027	0.727±0.005	0.567±0.039
SEM10	0.21	4.40±0.00	0.432±0.015	0.947±0.113	0.738±0.059
SEM10	0.0525	4.56±0.23	0.434±0.008	0.985±0.003	0.737±0.058

period, yields obtained at the point of maximum CDW accumulation would better represent the entire cultivation period than yields obtained during exponential growth. Table 3.3 showed a similar maximum CDW concentration of 3.64±0.28 g·L⁻¹ and 3.94±0.03 g·L⁻¹ at low and high pO₂, respectively.

Figure 3.4 (d) showed an absence of gluconate and 2-ketogluconate after DO depletion during growth at low pO₂. This indicated that glucose was phosphorylated rather than converted through the oxidative pathway in the periplasm. The absence of gluconate and 2-ketogluconate is in agreement with the reported lack of these metabolites during oxygen limited growth of *P. putida* BM014 [18]. However, Choi et al. (1998) also reported a lower biomass concentration at oxygen limited growth, which is not the case in this study [18]. This indicates that *P. putida* KT2440 shifts from conversion of glucose through the oxidative pathway to phosphorylation during oxygen limitation and is able to retain similar biomass yields.

At high pO₂, the genome reduced SEM10 strain grew slightly faster ($\mu_{max} = 0.637 \pm 0.004$ h⁻¹) and achieved a 9.9% higher Y_{X/S} (0.454±0.017 g·g⁻¹) compared to KT2440 during exponential growth (see Table 3.2). In the same line, Y_{X/O₂} and Y_{X/CO₂} of exponential growth were 17.1% and 13.1% higher, respectively, compared to KT2440. Otherwise, SEM10 growth at high pO₂ showed the same trends as KT2440. SEM10 cultivations at low pO₂ showed similar trends in growth profiles (see Figure 3.4 and Figure 3.5), and parameters (see Table 3.2), compared to KT2440. The improved growth characteristics of SEM10 over KT2440 were in good agreement with other studies comparing KT2440 and predecessors of the SEM10 strain under non-DO limited conditions [7–9].

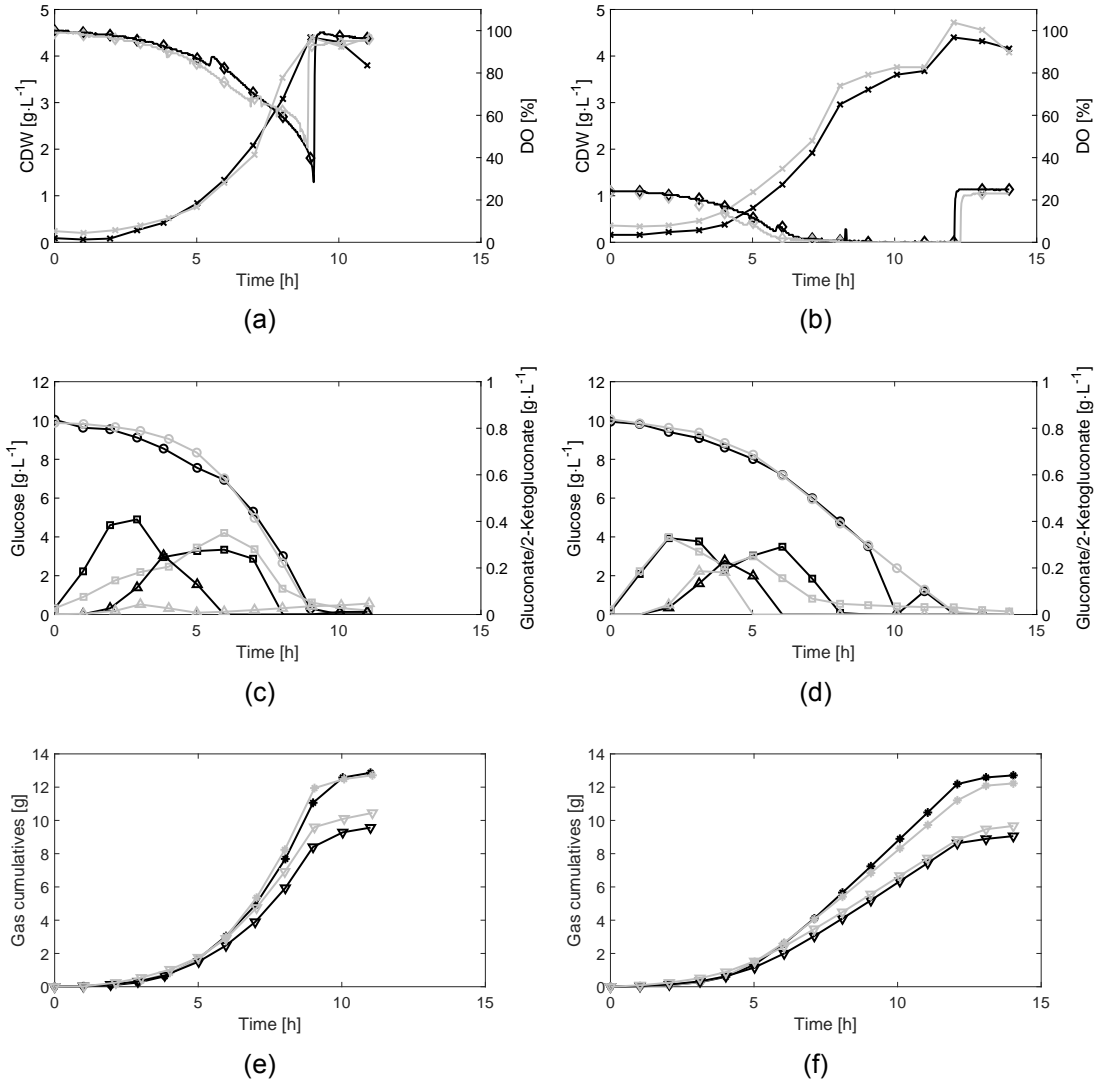


Figure 3.5: Batch cultivation of *P. putida* SEM10 at a pO_2 of 0.21 atm ((a), (c) and (e)) and 0.0525 atm ((b), (d) and (f)). (a) and (b): CDW concentration ($g \cdot L^{-1}$, X), DO concentration (%), (\diamond). (c) and (d): CDW concentration ($g \cdot L^{-1}$, X), glucose concentration ($g \cdot L^{-1}$, O), gluconate concentration ($g \cdot L^{-1}$, \square) and 2-ketogluconate concentration ($g \cdot L^{-1}$, \triangle). (e) and (f): consumed O_2 (g, $*$) and produced CO_2 (g, ∇). Black and light grey colors denote different replicates. Online logging of DO was not turned on for the first 4 h of cultivation of (b) light grey replicate.

Similar to KT2440, SEM10 experienced higher yields in the exponential phase at low pO_2 compared to high pO_2 . Furthermore, the maximum CDW accumulation and yields calculated at that time point (Table 3.3) were similar to those at high pO_2 . This might indicate that SEM10 retains its favorable growth characteristics, despite a longer overall cultivation time at lower pO_2 . Low DO concentrations have been suggested elsewhere to reduce the activity of the respiratory chain of *P. putida* KT2440, thereby compromising the activity of

the ATP synthase [2, 16]. The streamlined genome of SEM10, which spends less ATP on futile cellular processes, would thereby be able to allocate a scarce ATP supply more efficiently than KT2440. This was apparent from the lower $Y_{X/O_2, \max}$ of KT2440 ($0.727 \pm 0.005 \text{ g CDW} \cdot (\text{g O}_2)^{-1}$) compared to SEM10 ($0.985 \pm 0.003 \text{ g CDW} \cdot (\text{g O}_2)^{-1}$) indicating that less oxygen was required for, for example, ATP generation (see Table 3.3). This notion was further supported by the lower ATP maintenance requirement of the SEM10 predecessor EM383 compared to KT2440 during non-DO limited growth [9].

Comparison of KT2440 and SEM10 across the tested pO_2 showed that during exponential growth, there was a significant difference at both the level of pO_2 and the choice of strain (ANOVA two-factor, $p < 0.05$). However, when inspecting the overall yields and CDW concentrations of Table 3.3, significant differences were only found on the strain level (ANOVA two-factor, $p < 0.05$) but not for the pO_2 (ANOVA two-factor, $p > 0.05$). This indicated that the DO concentration was critical during exponential growth and as a determinant of cultivation time. In contrast, the pO_2 was insignificant for the overall performance of *P. putida* KT2440 and SEM10 cultivations at high and low pO_2 . Furthermore, this suggested SEM10 to be the superior strain when faced with optimal and suboptimal oxygen supplies.

3.4 Conclusions

Different agitation speeds of *P. putida* KT2440 shake flask cultivations did not yield apparent variation in the growth profiles. However, the maximum specific growth rate significantly differed between the applied agitation speeds. At the intermediate agitation, KT2440 observed the highest μ_{\max} of $0.694 \pm 0.005 \text{ h}^{-1}$, suggesting that both excess and insufficient agitation are detrimental to growth. Reduction of the pO_2 of the Biolector system cultivation chamber showed a small insignificant increase in cultivation time for *P. putida* KT2440 and SEM10 strains. In addition, SEM10 showed a growth deficiency in the Biolector system attributed to the lack of flagellar. As such, it was suggested that the Biolector system was unsuitable for investigating the effect of reduced oxygen availability on SEM10.

Cultivation of KT2440 and SEM10 in a bioreactor allowed for an appropriate comparison of the strains and investigation of low pO_2 . Growth at ambient pO_2 showed the anticipated advantageous growth characteristics of the genome reduced SEM10 strain compared to the wild type KT2440. Interestingly, both strains of the obligate aerobic bacterium showed improved growth yields during exponential growth at a pO_2 of 0.0525 atm compared to growth at a pO_2 of 0.21 atm. However, subsequent DO limitation reduced the overall yields of both strains and prolonged the cultivation. Overall, neither KT2440 nor SEM10 showed significantly different growth characteristics between high and low pO_2 . Although the genome reduced SEM10 strain still showed significantly higher biomass yields overall, independent of the pO_2 . These findings might indicate that the reduced futile ATP spending of SEM10 was beneficial during DO limited growth, further highlighting the advantages of utilizing the investigated genome reduced strain.

The significant difference between both the partial pressure of oxygen and the strains during exponential growth suggested that the applied oxygen supply strategy is important for the performance of a *P. putida* cultivation. Furthermore, deeper investigation of the dynamics of glucose metabolism through the periplasmic pathway as a consequence of DO concentration should be investigated further to elucidate and aid proper cultivation strategies and maturation of *P. putida* for industrial application.

References

- [1] Poblete-Castro, I., Acuña, J. M. B.-d., Nikel, P. I., Kohlstedt, M., and Wittmann, C. "Host Organism: *Pseudomonas putida*". In: Wiley-VCH Verlag GmbH & Co. KGaA, 2016, pp. 299–326. DOI: 10.1002/9783527807796.ch8.
- [2] Nikel, P. I. and Lorenzo, V. de. "Engineering an anaerobic metabolic regime in *Pseudomonas putida* KT2440 for the anoxic biodegradation of 1,3-dichloroprop-1-ene". In: *Metabolic Engineering* 15 (1 2013). AEC ATP/ADP, pp. 98–112. DOI: 10.1016/j.ymben.2012.09.006.
- [3] Nikel, P. I., Chavarría, M., Fuhrer, T., Sauer, U., and Lorenzo, V. de. "*Pseudomonas putida* KT2440 Strain Metabolizes Glucose through a Cycle Formed by Enzymes

- of the Entner-Doudoroff, Embden-Meyerhof-Parnas, and Pentose Phosphate Pathways". In: *Journal of Biological Chemistry* 290 (43 2015), pp. 25920–25932. DOI: 10.1074/jbc.M115.687749.
- [4] Tiso, T., Ihling, N., Kubicki, S., Biselli, A., Schonhoff, A., Bator, I., Thies, S., Karmainski, T., Kruth, S., Willenbrink, A. L., Loeschcke, A., Zapp, P., Jupke, A., Jaeger, K. E., Büchs, J., and Blank, L. M. "Integration of Genetic and Process Engineering for Optimized Rhamnolipid Production Using *Pseudomonas putida*". In: *Frontiers in Bioengineering and Biotechnology* 8 (2020). DOI: 10.3389/fbioe.2020.00976.
- [5] Poblete-Castro, I., Rodriguez, A. L., Lam, C. M. C., and Kessler, W. "Improved production of medium-chain-length polyhydroxyalkanoates in glucose-based fed-batch cultivations of metabolically engineered *Pseudomonas putida* strains". In: *Journal of Microbiology and Biotechnology* 24 (1 2014). Look at cites, pp. 59–69. DOI: 10.4014/jmb.1308.08052.
- [6] Hudcova, T., Halecky, M., Kozliak, E., Stiborova, M., and Paca, J. "Aerobic degradation of 2,4-dinitrotoluene by individual bacterial strains and defined mixed population in submerged cultures". In: *Journal of Hazardous Materials* 192 (2 2011), pp. 605–613. DOI: 10.1016/j.jhazmat.2011.05.061.
- [7] Martínez-García, E., Nikel, P. I., Aparicio, T., and Lorenzo, V. de. "Pseudomonas 2.0: Genetic upgrading of *P. putida* KT2440 as an enhanced host for heterologous gene expression". In: *Microbial Cell Factories* 13 (1 2014), pp. 1–15. DOI: 10.1186/s12934-014-0159-3.
- [8] Volke, D. C., Friis, L., Wirth, N. T., Turlin, J., and Nikel, P. I. "Synthetic control of plasmid replication enables target- and self-curing of vectors and expedites genome engineering of *Pseudomonas putida*". In: *Metabolic Engineering Communications* 10 (January 2020), e00126. DOI: 10.1016/j.mec.2020.e00126.
- [9] Lieder, S., Nikel, P. I., Lorenzo, V. de, and Takors, R. "Genome reduction boosts heterologous gene expression in *Pseudomonas putida*". In: *Microbial Cell Factories* 14 (1 2015), pp. 1–14. DOI: 10.1186/s12934-015-0207-7.

- [10] Kuschel, M. and Takors, R. "Simulated oxygen and glucose gradients as a prerequisite for predicting industrial scale performance a priori". In: *Biotechnology and Bioengineering* 117 (9 2020), pp. 2760–2770. DOI: 10.1002/bit.27457.
- [11] Spann, R., Glibstrup, J., Pellicer-Alborch, K., Junne, S., Neubauer, P., Roca, C., Kold, D., Lantz, A. E., Sin, G., Gernaey, K. V., and Krühne, U. "CFD predicted pH gradients in lactic acid bacteria cultivations". In: *Biotechnology and Bioengineering* 116 (4 2019), pp. 769–780. DOI: 10.1002/bit.26868.
- [12] Nadal-Rey, G., McClure, D. D., Kavanagh, J. M., Cassells, B., Cornelissen, S., Fletcher, D. F., and Gernaey, K. V. "Development of dynamic compartment models for industrial aerobic fed-batch fermentation processes". In: *Chemical Engineering Journal* 420 (2021). DOI: 10.1016/j.cej.2021.130402.
- [13] Kuschel, M., Siebler, F., and Takors, R. "Lagrangian Trajectories to Predict the Formation of Population Heterogeneity in Large-Scale Bioreactors". In: *Bioengineering* 4 (4 2017), p. 27. DOI: 10.3390/bioengineering4020027.
- [14] Haringa, C., Tang, W., Wang, G., Deshmukh, A. T., Winden, W. A. van, Chu, J., Gulik, W. M. van, Heijnen, J. J., Mudde, R. F., and Noorman, H. J. "Computational fluid dynamics simulation of an industrial *P. chrysogenum* fermentation with a coupled 9-pool metabolic model: Towards rational scale-down and design optimization". In: *Chemical Engineering Science* 175 (2018), pp. 12–24. DOI: 10.1016/j.ces.2017.09.020.
- [15] Ankenbauer, A., Schäfer, R. A., Viegas, S. C., Pobre, V., Voß, B., Arraiano, C. M., and Takors, R. "Pseudomonas putida KT2440 is naturally endowed to withstand industrial-scale stress conditions". In: *Microbial Biotechnology* 13 (4 2020), pp. 1145–1161. DOI: 10.1111/1751-7915.13571.
- [16] Demling, P., Ankenbauer, A., Klein, B., Noack, S., Tiso, T., Takors, R., and Blank, L. M. "Pseudomonas putida KT2440 endures temporary oxygen limitations". In: *Biotechnology and Bioengineering* 118 (12 2021), pp. 4735–4750. DOI: 10.1002/bit.27938.

- [17] Rodriguez, A., Escobar, S., Gomez, E., Santos, V. E., and Garcia-Ochoa, F. "Behavior of several pseudomonas putida strains growth under different agitation and oxygen supply conditions". In: *Biotechnology Progress* 34 (4 2018), pp. 900–909. DOI: 10.1002/btpr.2634.
- [18] Choi, W. J., Lee, E. Y., and Choi, C. Y. "Effect of dissolved oxygen concentration on the metabolism of glucose in Pseudomonas putida BM014". In: *Biotechnology and Bioprocess Engineering* 3 (2 1998), pp. 109–111. DOI: 10.1007/BF02932512.
- [19] Tlemçani, L. L., Corroler, D., Barillier, D., and Mosrati, R. "Physiological states and energetic adaptation during growth of Pseudomonas putida mt-2 on glucose". In: *Archives of Microbiology* 190 (2 2008), pp. 141–150. DOI: 10.1007/s00203-008-0380-8.
- [20] Escobar, S., Rodriguez, A., Gomez, E., Alcon, A., Santos, V. E., and Garcia-Ochoa, F. "Influence of oxygen transfer on Pseudomonas putida effects on growth rate and biodesulfurization capacity". In: *Bioprocess and Biosystems Engineering* 39 (4 2016), pp. 545–554. DOI: 10.1007/s00449-016-1536-6.

4 Medium Design for *Pseudomonas putida* fed-batch cultivation

Abstract

Due to its versatile metabolism and natural tolerance to environmental stress research on *Pseudomonas putida* as a production platform for biochemicals has been ever-increasing over the past years. However, only little information is available on the effect of nutritional compounds used in *P. putida* KT2440 cultivation media. Here we investigate the potential inhibitory effects of common medium components used for the cultivation of the wild type (KT2440) and the genome reduced strain (SEM10). Ammonium salts, phosphate buffer, glucose and acidic pH showed pronounced inhibitory growth effects. Both ammonium sulfate and ammonium chloride showed inhibition above 0.121 M nitrogen, phosphate buffer above 0.108 M phosphorous and glucose showed uninhibited growth up to 25 g·L⁻¹. Growth on glucose was significantly inhibited at pH below 6.8, whereas no inhibition was observed by increasing the pH. Both strains observed similar inhibitory trends across the tested conditions. In summary, the results showed that the inhibitory effects of the tested conditions can be avoided by utilizing an appropriately designed fed-batch cultivation rather than batch cultivation.

4.1 Introduction

The application of microorganisms for the production of commodity and fine chemicals has been an ever-increasing research topic over the past decades [1, 2]. The most successful applications have been attributed to the use of model microorganisms like *Escherichia coli* and *Saccharomyces cerevisiae*, although more research on non-traditional microorganism has gained traction in the past years [3, 4]. One such microorganism is the soil bacterium *Pseudomonas putida*, where research has been conducted to produce a genome reduced platform strain for biotechnological production [5, 6]. It is capable of adapting to physicochemical changes in the environment and enjoys a versatile metabolism that

enables it to survive oxidative stress [7–9]. Due to its naturally versatile metabolism, *P. putida* has been applied in several cases to, among others, convert aromatics, produce polyhydroxyalkanoates and biosurfactants [3, 10–13]. In addition to the naturally endowed advantages, it is also certified as host-vector safety level 1 by the U.S. Food and Drug Administration, enabling the safe application of *P. putida* KT2440 [14].

The majority of research has focused on the physiology associated with its particular metabolism and product-specific applications. However, little research has focused on the nutritional requirements of *P. putida*, likewise, the research available is scattered, limited in scope and often application specific. Media for cultivation in literature are diverse, with no particular consensus on the concentrations required. This study aims to develop a defined medium suitable for both batch and fed-batch cultivations based on a thorough analysis of the nutritional requirements. This includes the evaluation of inhibitory effects on the growth of the wild type strain (KT2440) compared to the genome reduced strain (SEM10). The compounds of the medium were tested at a range of concentrations to evaluate the inhibitory effects on the growth of *P. putida* KT2440 and the genome reduced strain SEM10 [6].

4.2 Materials and Methods

Bacterial Strains, Medium and Preculture Conditions

Bacterial strains of *Pseudomonas putida*, KT2440 and SEM10 were used in this study and stored at -80°C in 50 % (w/w) glycerol. Lysogeny broth agar medium contained per liter: 10 g tryptone, 5 g yeast extract, 10 g NaCl and 20 g agar. The defined basis medium contained per liter: 3.88 g K_2HPO_4 , 2.12 g $\text{NaH}_2\text{PO}_4 \cdot 2\text{H}_2\text{O}$, 2 g $(\text{NH}_4)_2\text{SO}_4$ and 1 mL trace element solution (TE). The trace element solution contained per liter: 10g EDTA, 100 g $\text{MgCl}_2 \cdot 6\text{H}_2\text{O}$, 2 g $\text{ZnSO}_4 \cdot 7\text{H}_2\text{O}$, 1 g $\text{CaCl}_2 \cdot 2\text{H}_2\text{O}$, 5 g $\text{FeSO}_4 \cdot 7\text{H}_2\text{O}$, 0.2 g $\text{Na}_2\text{MoO}_4 \cdot 2\text{H}_2\text{O}$, 0.2 g $\text{CuSO}_4 \cdot 5\text{H}_2\text{O}$, 0.4 g $\text{CoCl}_2 \cdot 6\text{H}_2\text{O}$ and 1.22 g $\text{MnCl}_2 \cdot 4\text{H}_2\text{O}$. Unless otherwise noted, all cultures were supplemented with $4 \text{ g} \cdot \text{L}^{-1}$ glucose. All chemicals were purchased from Merck, U.S.A. Precultures were prepared in three steps: First, glycerol stocks were activated by streaking on LB agar plates and incubating at 30°C

for 18 h. Second, 14 mL cultivation tube filled with 5 mL of basis medium, was inoculated with 3 colonies from a fresh LB agar plate and incubated at 30°C and 180 rpm for 8 h in a rotary shaker. Third, a liquid preculture was inoculated to an initial cell dry weight concentration of 4.59 mg·L⁻¹ in 500 mL baffled shake flasks (DWK Life Sciences, United Kingdom) containing 50 mL basis medium and incubated at 30°C and 180 rpm for 18 h in a rotary shaker. An Ecotron incubation shaker (Infors HT, Switzerland) was used for all preculture incubations.

Biolector cultivations

All cultivations were performed in a Biolector II Pro system (m2p-labs, Germany). BOH-1 type 48-well FlowerPlate® (m2p-labs, Germany) with fluorescent optodes for online measurements of dissolved oxygen (DO) and pH was used as the cultivation plate. Biomass was measured as the intensity of backscattered (arbitrary units (a.u.)) light at 600 nm, DO (%) was measured as the fluorescence at excitation/emission of 520/600 nm and the pH was measured as the fluorescence at excitation/emission of 470/525 nm. Cultivation conditions for all experiments were: 30°C, 800 rpm, humidity control at 85% relative humidity, 1 mL total well volume, 2.5% (v/v) inoculum and 1 min cycle time. The base medium was adjusted according to Table 4.1 and the pH was adjusted to 7.0 with 4 M NaOH. A phosphate buffer of K₂HPO₄ and NaH₂PO₄ · 2H₂O controlled the pH of the medium. Different buffer compositions enabled pH control in the range of 5.8 to 8.0 pH. The composition of the phosphate buffer was prepared according to G. Gomori (1955), except that Na₂HPO₄ was exchanged by K₂HPO₄ [15]. The pH of the pH and Glc media (Table 4.1) were not adjusted. All Biolector cultivations were performed in triplicates.

***P. putida* Fed-batch Medium Design**

The designed media were based on the literature yields and elemental composition of *P. putida* KT2440 as well as a general elemental composition of bacteria. A target biomass concentration of 55 g·L⁻¹ was based on an experimental window of 72 h and the feasible operational fed-batch bioreactor volume of 1.3 L to 2.0 L. Precipitation experiments of the designed media were performed by filling a 50 mL centrifuge tube with 50 mL of medium and incubating at room temperature for 16 h prior to visual inspection.

Table 4.1: Media composition ranges (media abbreviations in brackets): Phosphate buffer (PB), trace elements (TEm), ammonium sulfate (NS), ammonium chloride (NCl), sodium chloride (Clm), glucose (Glc) and pH (pHm).

Med. name	Phosphate (mM P)	TE (mL·L ⁻¹)	(NH ₃) ₂ SO ₄ (M nitrogen)	NH ₄ Cl (M Nitrogen)	NaCl (M Cl)	Glucose (g·L ⁻¹)	pH -
PB	36-179	1	0.03	0	0	4	7.0
TEm	36	1-40	0.03	0	0	4	7.0
NS	36	1	0.03-2.2	0	0	4	7.0
NCl	36	1	0.03	0.03-2.2	0	4	7.0
Clm	36	1	0.03	0	0.03-2.2	4	7.0
Glc	36	1	0.03	0	0	4-300	7.0
pHm	36	1	0.03	0	0	4	5.8-8.0

Supersaturation and possible precipitation were estimated with PHREEQC version 3.7.3 according to Parkhurst and Apello (2013) [16, 17]. For each medium design, an aqueous solution with all elemental species was created and the species distribution was calculated with the PHREEQC database 'minteq' as thermodynamic input. The saturation indices (SI) of minerals were calculated according to eq. (4.1), where *IAP* is the ion activity product and *K* is the solubility constant.

$$SI = \log(IAP/K) \quad (4.1)$$

4.3 Results and Discussion

Development of fed-batch medium for *P. putida* bioreactor cultivation

Media applied for cultivations of *P. putida* are abundant and vary vastly in both the composition and the applied cultivation vessel. In Table 4.2 a set of media applied in literature for bioreactor cultivations of *P. putida*, as well as the minimal medium applied in this study, are presented. The elemental composition varies considerably between the studies presented and if the sources of each element are considered, the variation is even greater. A reasonable argument for the variation is the span of biomass produced in each study, ranging from 6.15 g to 333.2 g. Table 4.3 shows the biomass normalized elemental composition of the media presented in Table 4.2, again showing great variation in the composition. Such variation in media composition complicates process and media de-

Table 4.2: Elemental mole composition of *P. putida* media applied in literature and this study, with glucose as carbon source.

Source	This study	Sun et al. 2006[18]	Tlemçani et al. 2008[19]	Lieder et al. 2016[20]	Follonier et al. 2012[21]	Poblete-Castro et al. 2014[12]
Type	Batch	Fed-batch	Batch	Batch	Chemostat	Fed-batch
Biomass (g)	7.68	64.6	16.4	6.15	136.8	333.2
N	151.355	56.909	90.813	49.947	678.674	284.547
P	71.717	77.526	108.766	22.045	209.426	279.174
S	75.729	31.450	49.540	27.478	387.453	144.534
K	89.103	23.808	58.786	22.045	209.426	88.180
Na	27.168	107.445	100.473	0.743	21.777	416.213
Mg	0.984	2.597	4.057	2.434	38.544	1.947
Cl	2.026	0.341	1.891	1.345	8.186	34.223
Ca	0.014	0.163	0.680	0.408	1.939	0.216
Fe	0.036	0.288	0.065	0.054	9.568	0.173
Zn	0.014	0.061	0.001	0.010	0.003	0.056
Mo	0.002	0.005	0.000	0.000	0.039	-
Cu	0.002	0.032	0.002	0.006	1.115	0.011
Co	0.003	0.007	0.004	-	0.080	0.019
Mn	0.012	0.018	0.012	0.008	0.960	0.055
B	-	0.039	0.016	0.007	-	0.010
Ni	-	0.001	0.000	0.000	-	-

velopment, a crucial step towards maturing *P. putida* as a biotechnological production host.

As evident from Table 4.3, a cultivation medium requires a range of elements from various sources, which can be complicated to combine in adequate proportions. The requirement of C, N, P and Mg were obtained from Sun et al. (2006) on the basis of the measured yield coefficients $Y_{x/s} = 0.41 \text{ g} \cdot \text{g}^{-1}$, $Y_{x/\text{NH}_4} = 5.44 \text{ g} \cdot \text{g}^{-1}$, $Y_{x/\text{PO}_4} = 13.7 \text{ g} \cdot \text{g}^{-1}$ and $Y_{x/\text{Mg}} = 236 \text{ g} \cdot \text{g}^{-1}$. The *P. putida* elemental composition $\text{CH}_{1.52}\text{O}_{0.41}\text{N}_{0.27}\text{P}_{0.02}\text{S}_{0.054}$ estimated by van Dureen et al. (2013) based on a genome-scale metabolic model provided the S requirement [22]. General bacterial requirements of K, Na, Ca, Mg, Cl, Fe, Zn, Mo, Cu, Co and Mn were obtained from the typical composition presented by Plugge (2005) as these were not available for *P. putida* [23]. Minor nutrients Zn, Mo, Cu, Co and Mn were not presented by Plugge 2005 and were instead considered as an equal distribution of 'others' [23]. The requirement for H and O was not considered as they were expected to be added adequately through other compounds and continuous aeration. Elements B and Ni were not considered as well as they were not a consistent component of media applied in literature. Lastly, the C requirement will not be discussed as the supplied carbon is

Table 4.3: Biomass normalized elemental composition (mole element · (g biomass)⁻¹) of *P. putida* media applied in literature for bioreactor cultivations in addition to the media applied in this study.

Source	This study	Sun et al. 2006[18]	Tlemçani et al. 2008[19]	Lieder et al. 2016[20]	Follonier et al. 2012[21]	Poblete-Castro et al. 2014[12]
Type	Batch	Fed-batch	Batch	Batch	Chemostat	Fed-batch
C-source	Glucose	Glucose	Glucose	Glucose	Octanoate	Glucose
Biomass (g)	7.68	64.6	16.4	6.15	136.8	333.2
N	19.71	0.88	5.54	8.12	4.96	0.85
P	9.34	1.20	6.63	3.58	1.53	0.84
S	9.86	0.49	3.02	4.47	2.83	0.43
K	11.60	0.37	3.58	3.58	1.53	0.26
Na	3.54	1.66	6.13	0.12	0.16	1.25
Mg	0.13	0.04	0.25	0.40	0.28	0.01
Cl	0.26	0.01	0.12	0.22	0.06	0.10
Ca	0.00177	0.00253	0.04148	0.06636	0.01417	0.00065
Fe	0.00468	0.00445	0.00395	0.00877	0.06994	0.00052
Zn	0.00181	0.00095	0.00009	0.00170	0.00002	0.00017
Mo	0.00022	0.00008	0.00002	0.00000	0.00029	-
Cu	0.00021	0.00050	0.00014	0.00098	0.00815	0.00003
Co	0.00044	0.00010	0.00026	-	0.00058	0.00006
Mn	0.00161	0.00028	0.00072	0.00123	0.00702	0.00016

generally a more dominant determinant of the produced biomass than the other nutrients discussed.

Table 4.4 shows a tendency of relatively low amounts of N according to the requirements, which in these cases comes down to the use of NH₄OH as base for pH control. Utilizing NH₄OH allows for a combined pH control and N-source supply, limiting the volume added through a cultivation. This also complicates the comparison of the N requirements across different media. This may also hold true for both S and Mg in fed-batch cultivations as they are often added through the feed as MgSO₄. All other compounds were added initially and can therefore serve as the basis for comparison and further medium development. The major components P, S, K and Na in Table 4.4 are generally supplied in excess. Minor constituents Cl, Fe, Zn, Mo, Cu, Co and Mn are mostly supplied in insufficient amounts according to the calculated minimal requirements.

With the nutritional requirements established from a theoretical calculation and reported media, the scope of development was established. The medium was designed with the purpose of reaching 55 g·L⁻¹ biomass in a fed-batch with an initial volume of 1.3 L, a

Table 4.4: Biomass normalized elemental composition (mole element · (g biomass)⁻¹) of *P. putida* media relative to the calculated minimal nutritional requirements.

Source	this study	Sun et al. 2006[18]	Tlemçani et al. 2008[19]	Lieder et al. 2016[20]	Follonier et al. 2012[21]	Poblete-Castro et al. 2014[12]	Requirement
Type	Batch	Fed-batch	Batch	Batch	Chemostat	Fed-batch	-
Biomass (g)	7.68	64.6	16.4	6.15	136.8	333.2	1
N	1.93	0.09	0.54	0.80	0.49	0.08	1.00
P	12.15	1.56	8.63	4.66	1.99	1.09	1.00
S	45.17	2.23	13.84	20.47	12.97	1.99	1.00
K	45.36	1.44	14.01	14.01	5.99	1.03	1.00
Na	8.13	3.82	14.08	0.28	0.37	2.87	1.00
Ca	0.01	0.02	0.33	0.53	0.11	0.01	1.00
Mg	0.73	0.23	1.42	2.27	1.62	0.03	1.00
Cl	1.87	0.04	0.82	1.55	0.42	0.73	1.00
Fe	0.13	0.12	0.11	0.24	1.95	0.01	1.00
Zn	0.30	0.15	0.01	0.28	0.00	0.03	1.00
Mo	0.05	0.02	0.00	0.00	0.07	-	1.00
Cu	0.03	0.08	0.02	0.16	1.29	0.01	1.00
Co	0.06	0.02	0.04	-	0.09	0.01	1.00
Mn	0.22	0.04	0.10	0.17	0.96	0.02	1.00

final volume of 2 L and a 0.7 L feed solution. The base control via NaOH would supply additional Na, whereas glucose feed would be supplemented with MgCl₂ to supply Mg and remaining Cl and an additional feed of ammonium salt would supply the required N. Elements such as Ca, Fe, Zn, Mo, Cu, Co and Mn would be supplied by a TE solution adapted from this study. According to the calculated design, the TE would have to be significantly more concentrated than any of the media listed in Table 4.3. Therefore, the concentration of the TE was adjusted to be within the range of the media in Table 4.3. Not least, Co is labeled as a cancerous chemical and the calculated requirement would exceed the concentration limits set by the Danish Health Authorities [24].

Design 1, listed in Table 4.5, represents a case where all nutrients were present in the batch medium. Design 2 illustrates a case where all nutrients except for approximately half of the phosphate buffer are present in the batch phase. Design 3 represents the same case as Design 1, but the TE volume has been halved and additional Fe, Ca and Cu were supplemented in a TE-booster solution with additional EDTA. The Fe concentration remained unchanged, but Ca and Cu concentration was adjusted to reflect the concentration of other media more closely. Design 4 represents Design 3, except that most of the required TE elements were moved to the feed solution. Design 5 represents Design 3, except the majority of the phosphate buffer was moved to the feed.

Table 4.5: Biomass normalized elemental composition (mole element · (g biomass)⁻¹) of designed media relative to the minimal nutritional requirements calculated.

Element	Design 1	Design 2	Design 3	Design 4	Design 5
N	0.09	0.09	0.09	0.09	0.09
P	1.00	0.55	1.00	1.00	0.11
S	2.10	2.11	2.10	2.05	2.08
K	3.73	2.06	3.73	3.73	0.41
Na	0.67	0.37	0.67	0.67	0.07
Ca	0.03	0.04	0.04	0.00	0.04
Mg	0.23	0.23	0.23	0.23	0.23
Cl	0.68	0.70	0.67	0.59	0.67
Fe	0.24	0.24	0.24	0.02	0.24
Zn	0.54	0.54	0.27	0.03	0.27
Mo	0.09	0.09	0.05	0.00	0.05
Cu	0.06	0.15	0.15	0.02	0.15
Co	0.12	0.12	0.06	0.01	0.06
Mn	0.40	0.40	0.20	0.02	0.20

From Table 4.5, Design 1 and 2 can readily be discarded. The former is due to the low concentration of Cu and precipitation and the latter is due to precipitation. For both media, several possible supersaturated species were identified by calculating the saturation index (SI) of the media (Table 4.6). An inspection of Table 4.6 shows several supersaturated species (positive SI indicates supersaturation and a possibility of precipitation) for all presented media designs. All supersaturated species contain a phosphate group and a TE cation, indicating that the presence of the phosphate buffer as a driver of possible mineral precipitation. Lastly, Design 4 did not show any precipitation during the precipitation experiment (data not shown).

The negative SI of $\text{Fe}_3(\text{PO}_4)_2 \cdot 8\text{H}_2\text{O}$ in Design 3 to 5 indicate that supersaturation of this species can be avoided by adding the additional Fe in combination with EDTA to chelate the ion. Supersaturation of the remaining species in Table 4.6 could possibly be avoided by further increasing the EDTA concentration. However, a precipitation experiment of Design 1 (Figure 4.1) showed that an equimolar concentration of EDTA compared to the TE cations leads to precipitation. In addition, non-complexed EDTA has been shown to be inhibitory towards *Pseudomonas brassicacearum*, suggesting that increases in EDTA concentration should be limited [25]. Leaving two options to avoid precipitation, relocate

Table 4.6: The PHREEQ calculated saturation index of the designed media.

Mineral	Design 1	Design 2	Design 3	Design 4	Design 5
$\text{Ca}_3(\text{PO}_4)_2$	0.4	0.88	-0.02	-2.4	-1.04
$\text{Ca}_4(\text{PO}_4)_3 \cdot 3\text{H}_2\text{O}$	-0.65	-0.08	-1.2	-4.38	-2.84
CaHPO_4	0.33	0.41	0.19	-0.6	-0.44
$\text{CaHPO}_4 \cdot 2\text{H}_2\text{O}$	0.02	0.11	-0.12	-0.91	-0.75
$\text{Ca}_5(\text{PO}_4)_3\text{OH}$	6.00	6.88	5.32	1.34	3.9
$\text{MgHPO}_4 \cdot 3\text{H}_2\text{O}$	0.22	0.12	0.22	0.22	-0.35
MnHPO_4	4.08	4.59	2.78	2.25	2.16
$\text{Fe}_3(\text{PO}_4)_2 \cdot 8\text{H}_2\text{O}$	0.61	2.65	-2.38	-3.98	-3.33

the majority of the phosphate source or the TE to the feed solution. The SI of Design 4 and 5 indicate that either choice will affect the supersaturation, though the SI of $\text{MgHPO}_4 \cdot 3\text{H}_2\text{O}$ and MnHPO_4 does not change significantly in either case. The SI of $\text{Ca}_5(\text{PO}_4)_3\text{OH}$ does not decrease equally for both designs, which indicates that even the phosphate required for the batch phase is more likely to precipitate.

The above considerations suggest that Design 4 is the most suitable design for the proposed media. Although the design satisfies most of the points considered above, it is not a perfect design. A few compounds are still supersaturated and some minor elements do not meet the calculated minimal requirement. However, it satisfies sufficiently without compromising on the major elements required and the fed-batch type fermentation. The final medium design contains per liter: 7.04 g K_2HPO_4 , 3.84 g $\text{NaH}_2\text{PO}_4 \cdot 2\text{H}_2\text{O}$, 5 g $(\text{NH}_4)_2\text{SO}_4$, 40 mg EDTA, 0.7 g $\text{MgCl}_2 \cdot 6\text{H}_2\text{O}$, 4 mg $\text{ZnSO}_4 \cdot 7\text{H}_2\text{O}$, 6 mg $\text{CaCl}_2 \cdot 2\text{H}_2\text{O}$, 20 g $\text{FeSO}_4 \cdot 7\text{H}_2\text{O}$, 0.4 mg $\text{Na}_2\text{MoO}_4 \cdot 2\text{H}_2\text{O}$, 2 mg $\text{CuSO}_4 \cdot 5\text{H}_2\text{O}$, 0.8 mg $\text{CoCl}_2 \cdot 6\text{H}_2\text{O}$ and 2.44 mg $\text{MnCl}_2 \cdot 4\text{H}_2\text{O}$. The missing minor elements would be added to the feed at 40 mL TE·L⁻¹ and Mg as 6.5 g·L⁻¹ $\text{MgCl}_2 \cdot 6\text{H}_2\text{O}$.

Growth inhibition of $(\text{NH}_4)_2\text{SO}_4$ and NH_4Cl

Industrial fermentation processes usually use cheap nitrogen sources such as complex corn steep liquor [26]. However, *P. putida* is incapable of secreting proteases to readily utilize protein-rich nitrogen sources. Therefore, more defined nitrogen sources such as ammonia, ammonium salts or urea should be used [27, 28]. Urea contains carbon and may act as a base, complicating the use of the compound. Furthermore, special equip-

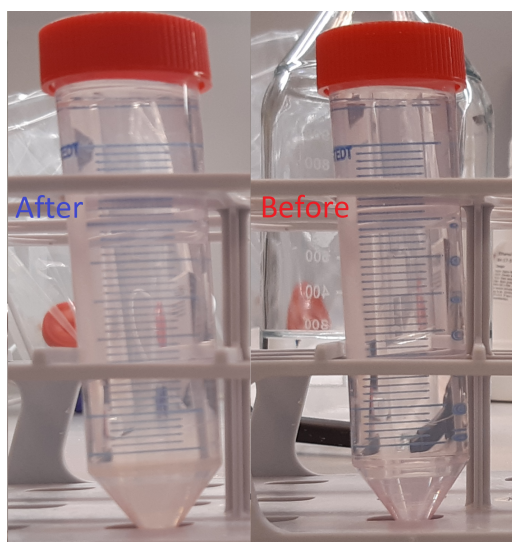


Figure 4.1: Precipitation of Design 1 after 18 h incubation at room temperature.

ment is required to safely handle pure ammonia, leaving the ammonium salts as the only option for the nitrogen source [26]. The two ammonium salts $(\text{NH}_4)_2\text{SO}_4$ and NH_4Cl were investigated as potential nitrogen sources for *P. putida* KT2440 fermentations. As an added benefit, the pure compounds facilitate analysis.

Inhibition of $(\text{NH}_4)_2\text{SO}_4$ on the growth of *P. putida* KT2440 is readily apparent in Figure 4.2a and Figure 4.2b, where an increasing concentration of the ammonium salt decreases growth. Both the backscatter biomass signal (Figure 4.2a) and the dissolved oxygen (DO) signal show good agreement with each other, as up to at least a concentration of 0.242 M nitrogen, inhibition is only minor. This is also apparent from Figure 4.3, which shows the average time to reach the minimum DO, indicating the point of glucose depletion. At 0.484 M nitrogen, a significant reduction in growth is observed, which is only aggravated at higher concentrations as growth is almost absent at 0.969 M nitrogen and completely absent at 2.2 M nitrogen. Supplying all the $(\text{NH}_4)_2\text{SO}_4$ in the batch phase would require 1.12 mol nitrogen equal to 0.86 M nitrogen according to the calculated minimal requirement for a biomass concentration of $55 \text{ g}\cdot\text{L}^{-1}$. Such a concentration would evidently inhibit growth already in the batch phase, suggesting that either the nitrogen should be added through the feed or through another source.

The backscatter and DO profiles of cultivations with increasing NH_4Cl concentration il-

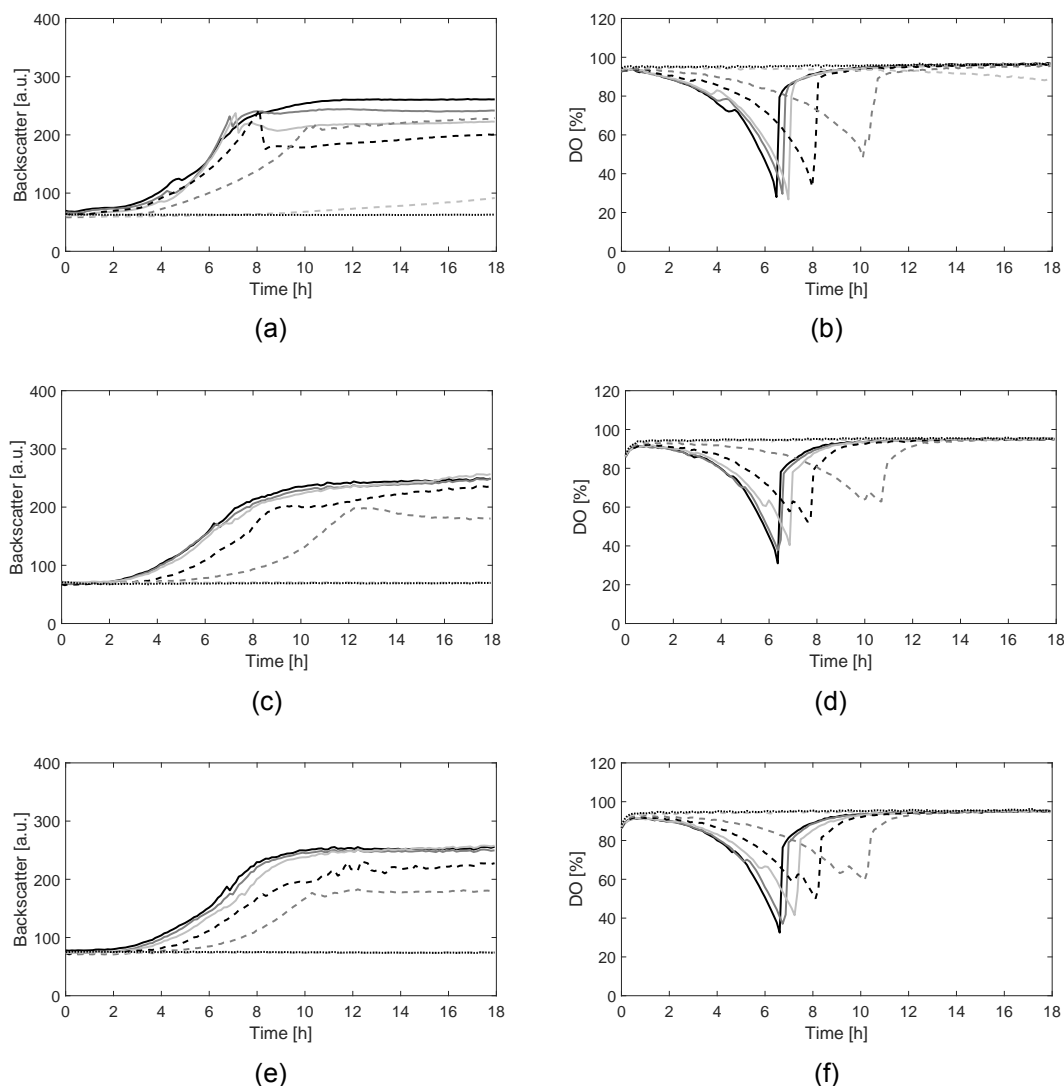


Figure 4.2: *P. putida* KT2440 Biolector experiments at different concentrations of $(\text{NH}_4)_2\text{SO}_4$, (a) and (b), NH_4Cl , (c) and (d), NaCl, (e) and (f). Biomass as backscatter, (a), (c) and (e). Dissolved oxygen as a percentage of saturation, (b), (d) and (f). Concentrations expressed as either M nitrogen or M chloride: 0.030 M, black line, 0.061 M, dark grey line, 0.121 M, light grey line, 0.242 M, black dashed line, 0.484 M, dark grey dashed line, 0.969 M, light grey dashed line, 2.2 M, black dotted line.

illustrated in Figure 4.2c and Figure 4.2d, respectively, show a trend similar to that of increasing $(\text{NH}_4)_2\text{SO}_4$. The inhibition on the backscatter profiles at 0.242 M nitrogen and 0.484 are slightly stronger, though the same observation can't be made on the DO profile. In addition, growth at 0.969 M nitrogen is completely absent, unlike with $(\text{NH}_4)_2\text{SO}_4$ where minor growth is observed. The results show that neither compound is a perfect nitrogen source. The choice of nitrogen source here would likely also affect other media compounds, such as the Mg source, to meet the Cl or S requirements. However, as

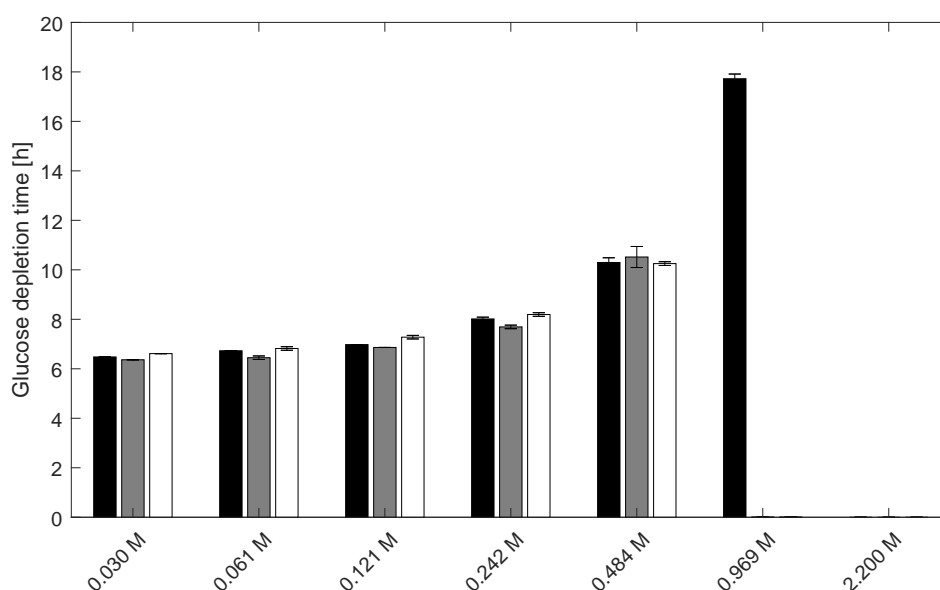


Figure 4.3: Time required for *P. putida* KT2440 cultivations to reach the minimum DO, the time point associated with glucose depletion. (NH₄)₂SO₄, black, NH₄Cl, grey and NaCl, white.

the average times to reach glucose depletion are comparable for both compounds, the choice of nitrogen source, in this case, is based on its compatibility with the construction material of the bioreactor. Most benchtop bioreactors consist of a glass vessel and a stainless steel headplate, whereas most pilot or industrial-scale bioreactors are manufactured entirely from stainless steel. Chloride is a powerful oxidizer of stainless steel and high concentrations may lead to corrosion [29]. If the aim is to scale-up a process (NH₄)₂SO₄ is the superior choice over NH₄Cl.

The similar growth inhibition trend of either increasing (NH₄)₂SO₄ or NH₄Cl concentration suggests that ammonium might be the inhibiting factor in either experiment. Suzuki et al. (1986) found similar inhibition patterns for *Pseudomonas* sp. regardless of the ammonium compound and observed severe inhibition at 0.055 M nitrogen, at this concentration *P. putida* KT2440 showed no growth inhibition [30]. Another study of the *P. putida* relative, *Pseudomonas aeruginosa*, showed no growth inhibition on solid medium up to 1.21 M nitrogen of (NH₄)₂SO₄. Neither gives clear evidence that the ammonium is inhibitory, but the latter shows that a *P. putida* relative can survive similar (NH₄)₂SO₄ concentrations. To investigate if ammonium is inhibitory, an experiment similar to the previous two

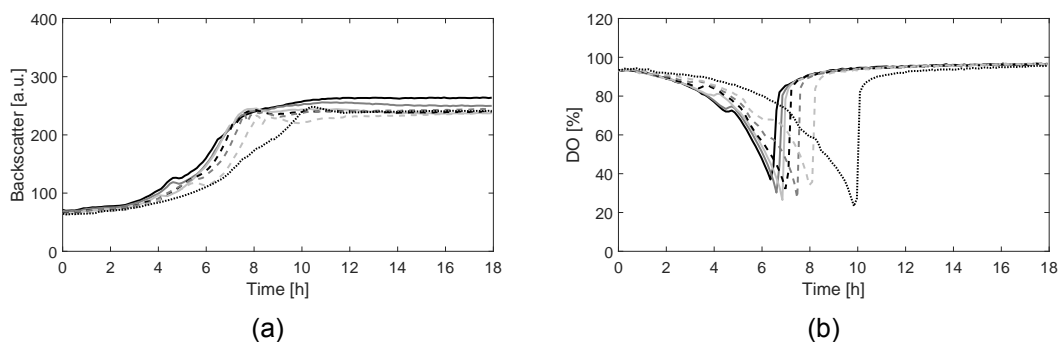


Figure 4.4: *P. putida* KT2440 Biolector experiments at different concentrations of phosphate buffer. Biomass backscatter, (a) and dissolved oxygen as a percentage of saturation, (b). Concentrations: 0.036 M phosphorous, black line, 0.054 M phosphorous, dark grey line, 0.072 M phosphorous, light grey line, 0.090 M phosphorous, black dashed line, 0.108 M phosphorous, dark grey dashed line, 0.143 M phosphorous, light grey dashed line, 0.179 M phosphorous, black dotted line.

was performed, where instead of NH_4Cl , the same amount of NaCl was added to reach equivalent chloride concentrations. The resulting backscatter and DO profiles are presented in Figure 4.2e and Figure 4.2f, respectively. Growth profiles of *P. putida* KT2440 with increasing NaCl concentrations show highly similar inhibition patterns compared to the NH_4Cl cultivations. This similarity indicates that the chloride of the NH_4Cl cultivations was the major inhibitor and consequently that the sulfate of the $(\text{NH}_4)_2\text{SO}_4$ to be such as well rather than the ammonium.

Phosphate inhibition of *P. putida* KT2440 cultivations

In smaller cultivation vessels such as shake flasks, the phosphate source often serves two purposes, P source and pH buffer [26]. In the case of a larger cultivation, such as a fed-batch in a bioreactor, the phosphate buffer will be insufficient to control the pH without possibly inhibiting the organism. Kampen (2014) reported that bacteria can, in general, endure up to $5 \text{ g}\cdot\text{L}^{-1}$ potassium phosphate corresponding to 36.8 mM phosphorous [26]. However, others have reported concentrations of up to 367 mM phosphorous, though neither were for *P. putida* [31, 32]. The designed medium would require 84.5 mmol phosphorous or 65 mM phosphorous in the batch phase to reach $55 \text{ g}\cdot\text{L}^{-1}$ biomass, almost twice the general tolerable concentration reported by Kampen (2014) [26]. Nevertheless, Sun et al. (2006) applied 96.9 mM phosphorous and Poblete-Castro et al. (2014) 69.8

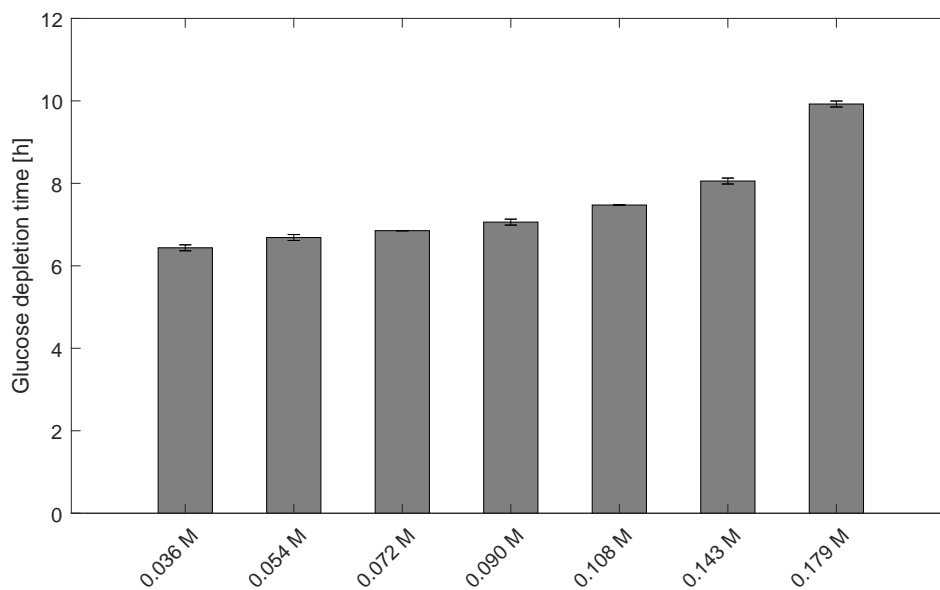


Figure 4.5: Time required for *P. putida* KT2440 cultivations with increasing phosphate concentration to reach the minimum DO, the time point associated with glucose depletion.

mM phosphorous for fed-batch bioreactor cultivations of *P. putida* KT2440, indicating that such concentrations were, in fact, tolerable by the bacterium [12, 18]. To investigate tolerable levels of phosphate, an experiment with increasing phosphate concentration starting at 36 mM phosphorous, equivalent to the concentration of P in the preculture medium used in this study, to 179 mM phosphorous was performed.

Figure 4.4a shows that increasing the phosphate concentration up to 179 mM phosphorous has no significant effect on the accumulated biomass. It does, however, have an inhibitory effect on the growth as evident from Figure 4.4 and Figure 4.5 where reaching glucose depletion with 179 mM phosphorous takes 54.17% longer compared to 36 mM phosphorous. Reaching glucose depletion at 72 mM phosphorous only takes 6.45% longer time compared to standard conditions, implying that including all required P as a phosphate buffer in the batch phase would not significantly inhibit the cultivation. Such a minor phosphate inhibition would likely disappear over the course of cultivation as the phosphate is consumed. The use of just a single phosphate salt rather than two might reduce the inhibitory effect, indicated by the much higher phosphate tolerance of *Lactococcus lactis* reported by de Vuyst and Vandamme (1993) [31]. Otherwise, the use of either

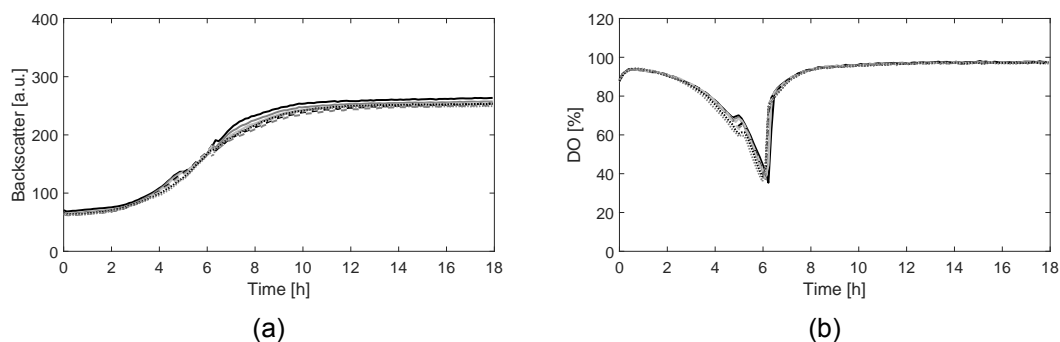


Figure 4.6: *P. putida* KT2440 Biolector experiments at different TE concentrations. Biomass backscatter, (a) and dissolved oxygen as a percentage of saturation, (b). TE concentration: 1 mL·L⁻¹, black line, 1.5 mL·L⁻¹, dark grey line, 2 mL·L⁻¹, light grey line, 4 mL·L⁻¹, black dashed line, 10 mL·L⁻¹, dark grey dashed line, 15 mL·L⁻¹, light grey dashed line, 20 mL·L⁻¹, black dotted line, 40 mL·L⁻¹, dark grey dotted line.

sodium or potassium phosphates could likely be an avenue for further improvement as de Vuyst and Vandamme (1993) showed different growth behavior on the individual mono- and dihydrogen phosphate salts [31].

Effect of increased trace element concentration on *P. putida* KT2440 cultivation

The trace element requirement increases with increasing biomass concentration and might not cause inhibitory issues at low concentrations [26, 30]. However, EDTA has been shown to be inhibitory towards cell growth, for which reason the effect of increased TE concentration on *P. putida* KT2440 growth was investigated [25]. Both the backscatter and DO profiles illustrated in Figure 4.6 show highly similar growth profiles. Only a very slight decrease in the time to reach glucose depletion from 6.27 ± 0.07 to 6.02 ± 0.07 h at 1 mL TE·L⁻¹ and 40 mL TE·L⁻¹ (Figure 4.7), respectively. The lack of inhibition by the TE solution within the concentrations investigated suggests that EDTA in the TE solution does not present an issue. The slight increase in growth by increasing the TE concentration could indicate that certain elements of the TE solution could be increased to optimize growth marginally. Such an optimization would require similar experiments with each compound in the TE, which is out of the scope of this study.

Glucose inhibition of *P. putida* KT2440

Several studies have reported the use of elevated glucose concentration in *P. putida* strains KT2440 and BM01 cultivations but do not supply detailed or conclusive information

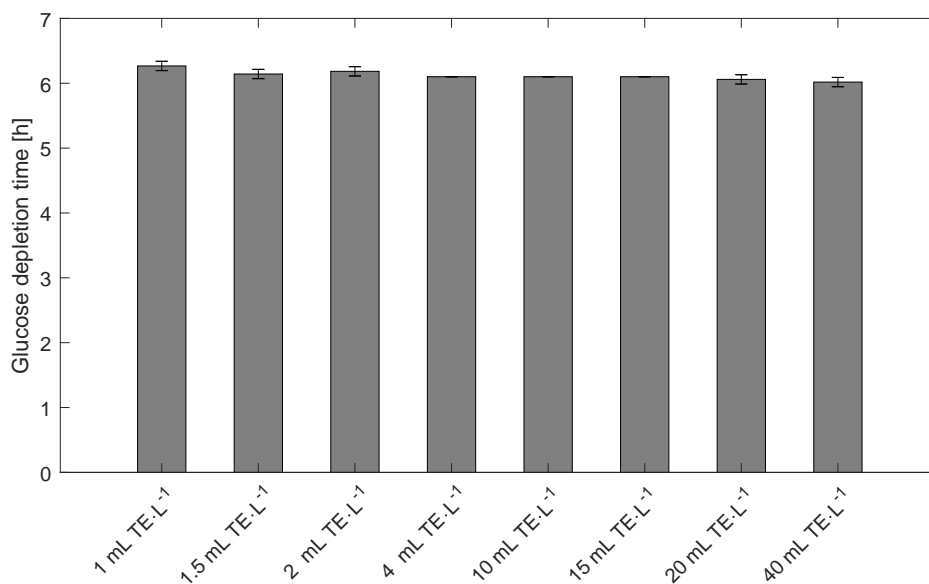


Figure 4.7: Time required for *P. putida* KT2440 cultivations to reach the minimum DO, the time point associated with glucose depletion, at different TE concentrations.

on substrate inhibition [33]. Patil et al. (2016) considered a concentration above $30 \text{ g}\cdot\text{L}^{-1}$ glucose to be substrate inhibition as the enzyme titer did not increase with higher concentrations of glucose but did not investigate the effect on other cultivation parameters [34]. In another study, Hofer et al. (2002) investigated glucose concentrations between $11 \text{ g}\cdot\text{L}^{-1}$ and $60 \text{ g}\cdot\text{L}^{-1}$ observing a reduction in the yield of biomass on the supplied glucose [35]. However, as only endpoint measurements of OD_{600} were available, it was not possible to determine if the reduced yield originated from another source. A study on high cell concentration *P. putida* BM01 fed-batch cultivation conducted by Kim et al. (1996) reported no significant inhibition below $40 \text{ g}\cdot\text{L}^{-1}$, but no data was shown [36]. Lastly, a study by Kakimoto et al. (1971) showed an increase in the final biomass after 24 h for glucose concentrations of up to $20 \text{ g}\cdot\text{L}^{-1}$ but a decrease in the biomass concentration at higher glucose concentrations [37]. To further investigate the substrate inhibition of glucose on *P. putida* KT2440 cultivations, an experiment with increasing glucose concentration from $4 \text{ g}\cdot\text{L}^{-1}$ to $300 \text{ g}\cdot\text{L}^{-1}$ was conducted.

Figure 4.8a shows that glucose inhibition occurs already between 25 and $50 \text{ g}\cdot\text{L}^{-1}$ glucose, but exceeding $125 \text{ g}\cdot\text{L}^{-1}$ glucose leads to complete inhibition of growth. The Biolector was,

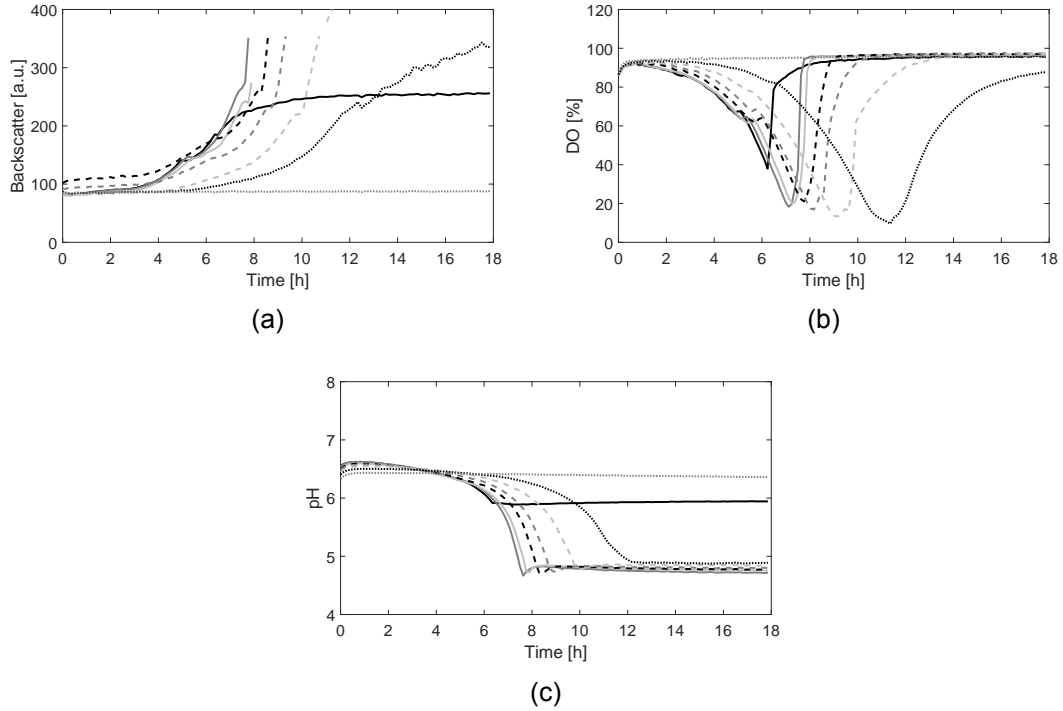


Figure 4.8: *P. putida* KT2440 Biolector experiments at increasing glucose concentration up to $150 \text{ g}\cdot\text{L}^{-1}$. Results with glucose concentrations above $150 \text{ g}\cdot\text{L}^{-1}$ are not shown as no growth was observed. Biomass backscatter, (a), dissolved oxygen as a percentage of saturation, (b), pH, (c). Glucose concentration: $4 \text{ g}\cdot\text{L}^{-1}$, black line, $10 \text{ g}\cdot\text{L}^{-1}$, dark grey line, $25 \text{ g}\cdot\text{L}^{-1}$, light grey line, $50 \text{ g}\cdot\text{L}^{-1}$, black dashed line, $75 \text{ g}\cdot\text{L}^{-1}$, dark grey dashed line, $100 \text{ g}\cdot\text{L}^{-1}$, light grey dashed line, $125 \text{ g}\cdot\text{L}^{-1}$, black dotted line, $150 \text{ g}\cdot\text{L}^{-1}$, dark grey dotted line.

at the applied filter settings, only able to record backscatter up to around 350 a.u. resulting in cut of graphs. The DO profiles illustrated in Figure 4.8b show similar patterns as the backscatter profiles, though an apparent glucose depletion occurs for all growing cultures. However, considering that the base medium is designed for shake flask cultivation, it is more likely another nutrient being depleted. Another possible explanation can be found in the pH profiles presented in Figure 4.8c and Figure 4.9, where the time point of minimum DO and pH are comparable. This could indicate that growth halts not due to nutrient depletion but due to a decrease in pH. Based on the $Y_{X/S}$ reported by Sun et al. (2006), the $4 \text{ g}\cdot\text{L}^{-1}$ glucose cultivation should be able to produce $1.64 \text{ g}\cdot\text{L}^{-1}$ biomass without consuming all $(\text{NH}_4)_2\text{SO}_4$ [18]. The $10 \text{ g}\cdot\text{L}^{-1}$ glucose cultivation should be able to produce $4.1 \text{ g}\cdot\text{L}^{-1}$ biomass based on the glucose supply, but only $2.97 \text{ g}\cdot\text{L}^{-1}$ biomass based on the $(\text{NH}_4)_2\text{SO}_4$ supply, indicating that all cultivations, except for $4 \text{ g}\cdot\text{L}^{-1}$ glucose, would even-

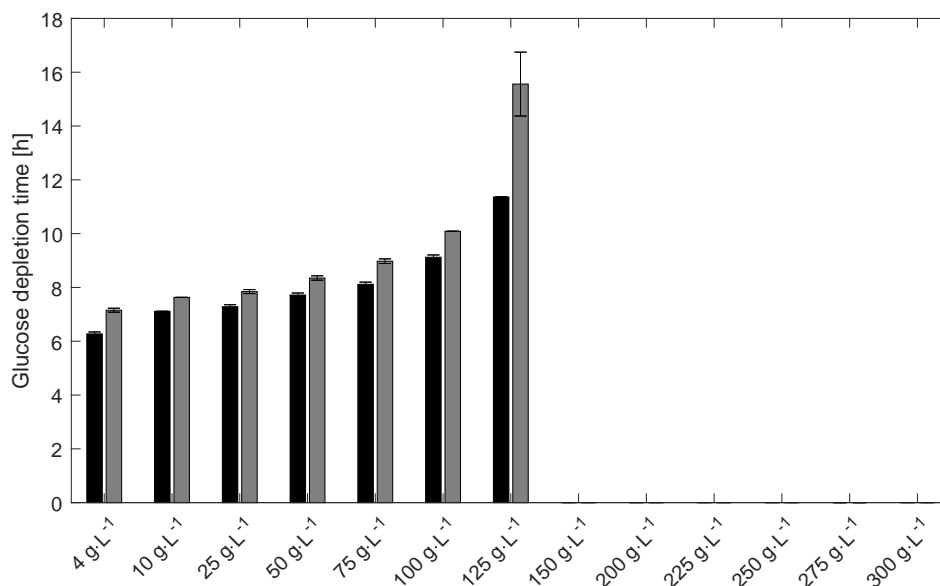


Figure 4.9: Time required for *P. putida* KT2440 cultivations to reach the end of growth at increasing glucose concentrations. The time point where the minimum DO is reached is illustrated in black, whereas the time point where the minimum pH is reached is illustrated in gray. No growth between 150 g·L⁻¹ and 300 g·L⁻¹ glucose was observed.

usually be nitrogen limited and reach a biomass concentration out of the measuring range of the Biolector. Assuming (NH₄)₂SO₄ assimilation is the main acidifier of the cultures, the origin of the growth halt can not be determined [26, 38]. Regardless of what causes growth to cease, the growth curves indicate that increasing glucose concentration leads to inhibition.

The presented results of increasing glucose concentration on *P. putida* KT2440 cultivations are in good agreement with data available from other *P. putida* strains. The concentration at which glucose inhibition occurs agrees well with the reported ranges of 30 g·L⁻¹ to 40 g·L⁻¹ [34, 36, 37]. The concentration intervals applied were too broad to capture either the onset of inhibition or complete inhibition more accurately. Nevertheless, the results indicate that batch cultivations of up to 25 g·L⁻¹ glucose are feasible and higher concentrations should be used with caution. Fed-batch cultivation does show to be the best mode of operation if industrially relevant biomass concentrations are to be reached, as 25 g·L⁻¹ will only yield approximately 10 g·L⁻¹ biomass.

Kakimoto et al. (1971) observed a decrease in the biomass growth at glucose concentra-

tions up to $100 \text{ g}\cdot\text{L}^{-1}$, followed by the absence of growth at $200 \text{ g}\cdot\text{L}^{-1}$ glucose [37]. These results are in good agreement with the results presented in Figure 4.8 where inhibition is observed at glucose concentrations exceeding $25 \text{ g}\cdot\text{L}^{-1}$ and growth is completely absent at glucose concentrations exceeding $125 \text{ g}\cdot\text{L}^{-1}$. Contrary to the data presented by Kakimoto et al. (1971), the data presented in this study relies on time course data rather than just endpoint measurements [37]. The time course data of the pH profiles with a plateau combined with the biomass profiles, showing a reduction in growth rate, support the interpretation that it is, in fact, glucose inhibition and not an artifact created by low pH or nutrient depletion. Based on the endpoint measurements performed by Kakimoto et al. (1971) [37], the latter possibilities cannot be rejected.

Influence of pH on *P. putida* KT2440 cultivation

The medium pH is of great importance to most, if not all, microorganisms, including *P. putida* [39]. Many studies report an optimal pH for *P. putida* cultivations, however, they range from biomass production to enzyme production and aromatics degradation with a range of carbon sources. In addition, common themes among the studies are that the optimum is reported, but no data is shown, or it is a design of experiment with a specific objective function [11, 34, 40, 41]. To fill the gap of knowledge, an experiment with pH ranging from pH 5.8 to 8.0, in 0.2 pH intervals, was conducted. The pH range was partially selected based on the reported optimum and partially on the feasible range of a set of phosphate buffers [15, 41].

Growth profiles of backscatter presented in Figure 4.10a show abnormal trends for the curves below pH 7.0. The trends did not appear in the DO profiles in Figure 4.10b which, from experience, are more reliable. Therefore, the backscatter profiles were not considered in this case. If one inspects the DO profiles in Figure 4.10b, it is apparent that cultivations at pH between 5.8 and 6.6 do not reach a minimum DO similar to pH 7.0, whereas cultivations between pH 6.8 and 8.0 show similar DO profiles indicating uninhibited growth. Figure 4.11 gives a good overview at which pH cultures were uninhibited, though the time points at lower pH reached a minimum earlier.

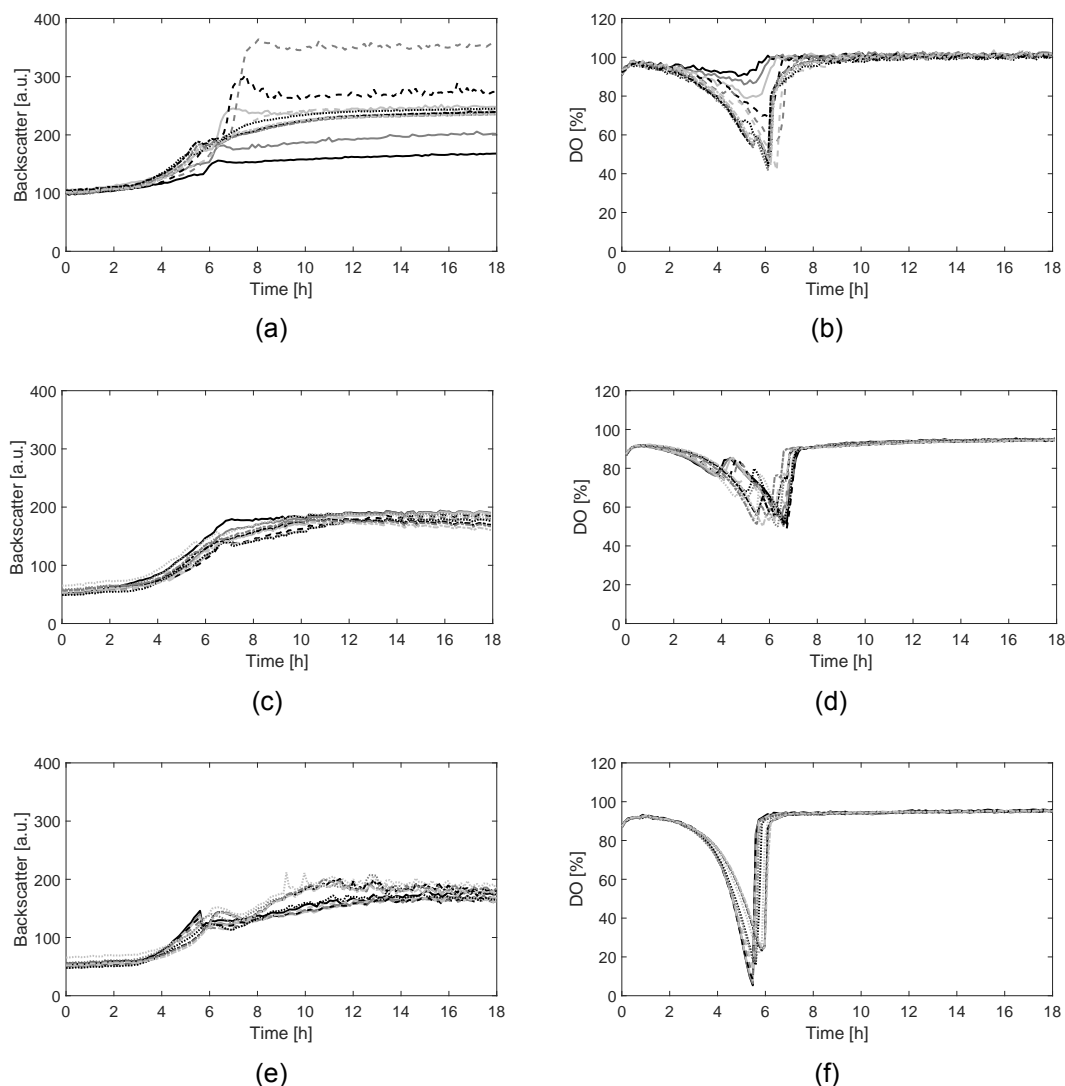


Figure 4.10: *P. putida* KT2440 Biolector experiments at an initial pH ranging from 5.8 to 8.0. Carbon source: Glucose, (a) and (b), gluconate, (c) and (d), succinate, (e) and (f). Biomass, (a), (c) and (e), DO, (b), (d) and (f). Range of pH: 5.8, black line, 6.0, dark grey line, 6.2, light grey line, 6.4, black dashed line, 6.6, dark grey dashed line, 6.8, light grey dashed line, 7.0, black dotted line, 7.2, dark grey dotted line, 7.4, light grey dotted line, 7.6, black dot-dashed line, 7.8, dark grey dot-dashed line, 8.0, light grey dot-dashed line.

The experiment showed a clear trend that growth was optimal at or above pH 7.0 which is in line with other reported values [34, 41]. Whether the inhibition is related to the growth on glucose is not clear from this experiment but could be associated with another factor. Hudcovae et al. (2011) identified a similar range (pH 7.0 - 7.4) for growth on aromatic compounds. Another study discussed that inhibition at low pH could be correlated to inhibition of glucose dehydrogenase (*gcd*), the enzyme responsible for the oxidation of glucose to gluconate in the periplasm [42]. Such inhibition could be significant as *P. putida* me-

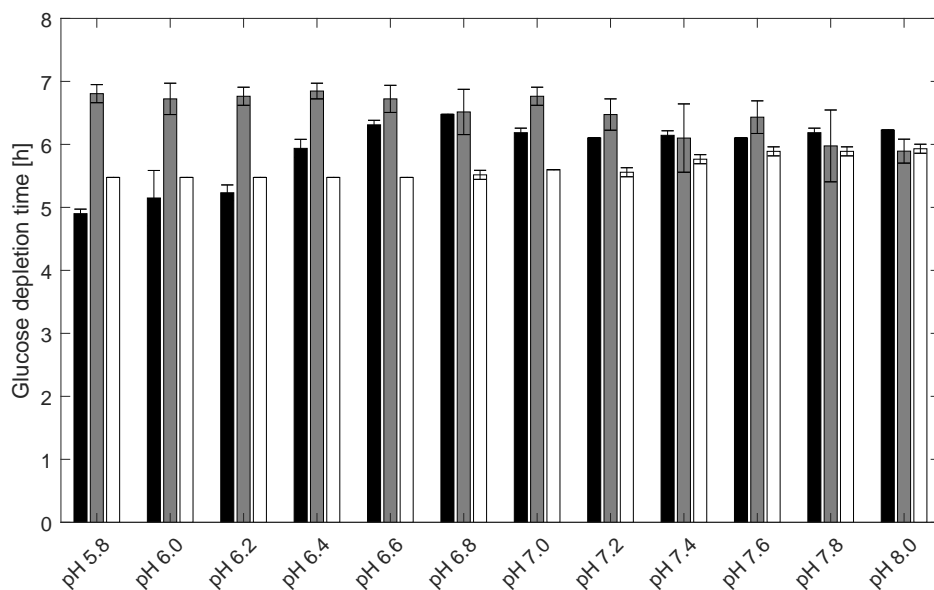


Figure 4.11: Time required for *P. putida* KT2440 cultivations to reach the minimum DO, the time point associated with glucose depletion, at initial pH values ranging from 5.8 to 8.0. Carbon sources: Glucose, black, gluconic acid, grey, succinic acid, white.

tabolizes the majority of glucose through the oxidative pathway [7, 43]. To investigate the relation of pH inhibition to glucose assimilation, two further experiments were performed at the given pH range, one with gluconate and one with succinate as the sole carbon source. The alternative carbon sources were added in the same c-mol amount as glucose.

Growth of *P. putida* on succinate presented in Figure 4.10f and Figure 4.11 show no inhibition over the tested pH range, neither does growth on gluconate as illustrated in Figure 4.10d and Figure 4.11, thus indicating that the inhibition is correlated to the uptake or conversion of glucose. Deletion of *gcd* showed 20-27% loss of the maximum specific growth rate and 16% loss of the biomass yield on glucose [44, 45]. Nevertheless, such reduction in growth seems modest compared to the reduction observed at the lowest pH, which indicates that the bacterium is inhibited in other aspects besides *gcd*. The presented data is not sufficient to determine whether *gcd* is in fact inhibited by the pH level or what other effect pH has on the assimilation of glucose.

The DO profiles of both growth on glucose and gluconate show bumps, at which the culture seems to change its metabolism, presumably from one substrate of the oxidative pathway to another. The bump is apparent in most cultivations presented so far and is

a general trend observed for *P. putida* growth on glucose as the oxygen requirement of glucose is higher than that of gluconate, and the requirement of gluconate is higher than that of 2-ketogluconate [19]. Larger bumps are presumably due to the shift from glucose to gluconate as carbon source, thereby skipping a conversion step.

Comparison of KT2440 and SEM10

The previously tested conditions were also applied to the genome reduced *P. putida* strain SEM10 to investigate if the strain was more susceptible compared to the wild type strain KT2440 [6]. KT2440 reached a minimum DO concentration faster than the SEM10 strain in most cases, as is visible in Figure 4.12. However, flagellar-less strains of KT2440, similar to SEM10, have been shown to grow poorly in microwell plates on minimal glucose medium compared to KT2440 due to sedimentation [46]. Figure 4.13 illustrates the time required to reach the DO minimum relative to the base medium, thus making the effect of conditions on each strain comparable considering the growth deficiency of SEM10 in micro cultivation systems.

Figure 4.13 shows that the strains observe similar relative DO minima times with increasing concentrations of $(\text{NH}_4)_2\text{SO}_4$, NH_4Cl , NaCl and glucose. Increasing the concentration of phosphate buffer or the pH showed different results. Martínez-García et al. (2014) showed that a flagellar-less mutant, a predecessor of SEM10, was more susceptible to acidic pH, which agrees well with the lower relative times of SEM10 in Figure 4.13g that indicates poor growth at lower pH. Increasing pH, however, seems to benefit SEM10 as it reaches DO minimum faster compared to KT2440. The flagellar-less mutant did not show improved growth at higher pH, though the difference here might be due to the pH change over cultivation time. Extending to the cultivation of increasing phosphate buffer concentration, we see a significantly lower relative time to reach the DO minimum. SEM10 requires 30.70% longer time to reach the DO minimum at maximum buffer concentration, whereas KT2440 requires 54.16% longer compared to standard conditions. This indicated that SEM10 endures higher phosphate concentrations better than KT2440. Another explanation for this is that the pH drop experienced in these cultivations is smaller, thus benefiting the acid-susceptible SEM10 strain [46]. SEM10 might not endure higher

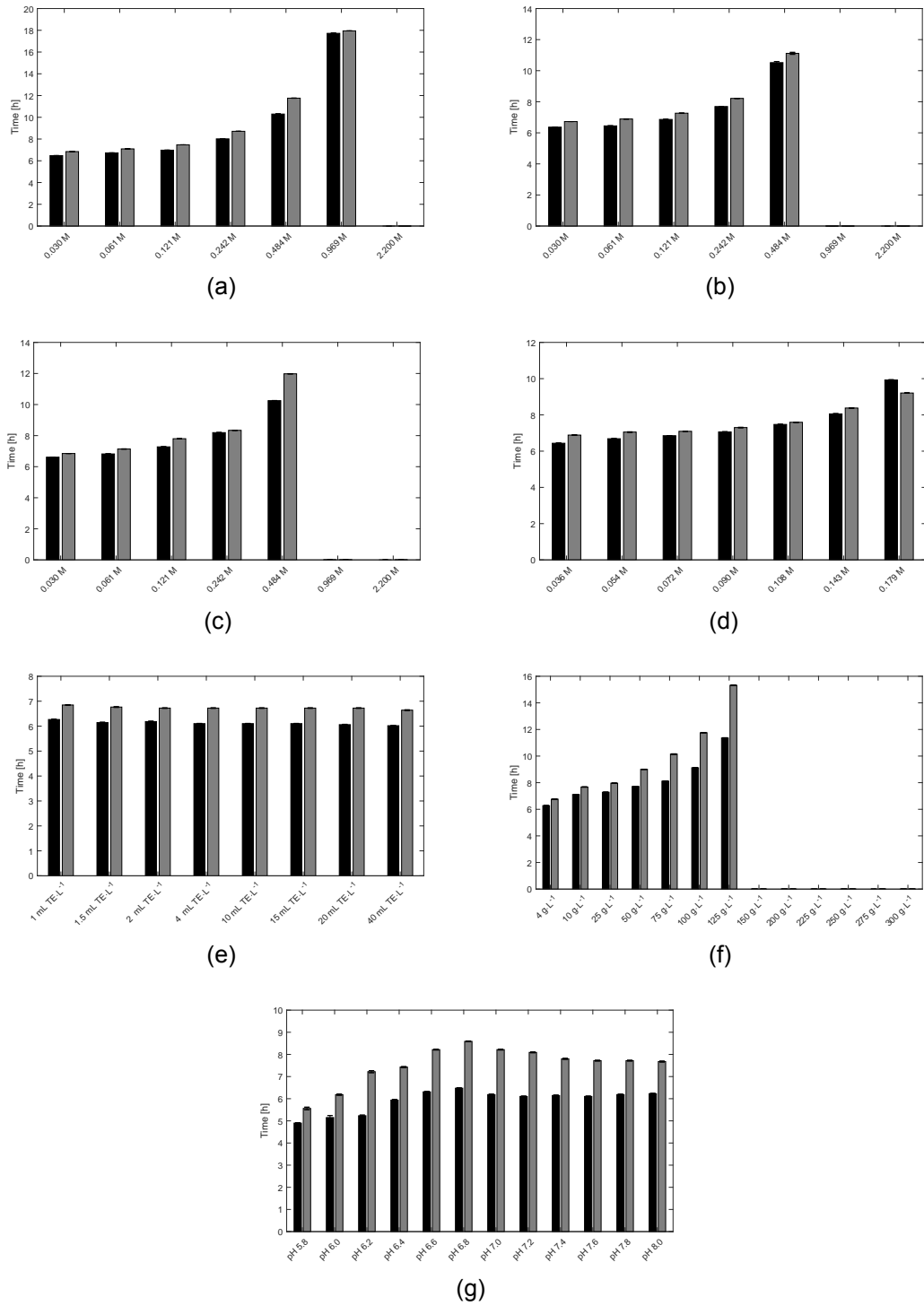


Figure 4.12: Biolector experiments cultivated at different nutrient concentrations and pH, illustrating the time point to reach minimum DO, associated with glucose depletion. KT2440, black bars and SEM10, grey bars. Ammonium sulfate (a), ammonium chloride (b), sodium chloride (c), phosphate buffer (d), TE (e), glucose (f) and pH (g).

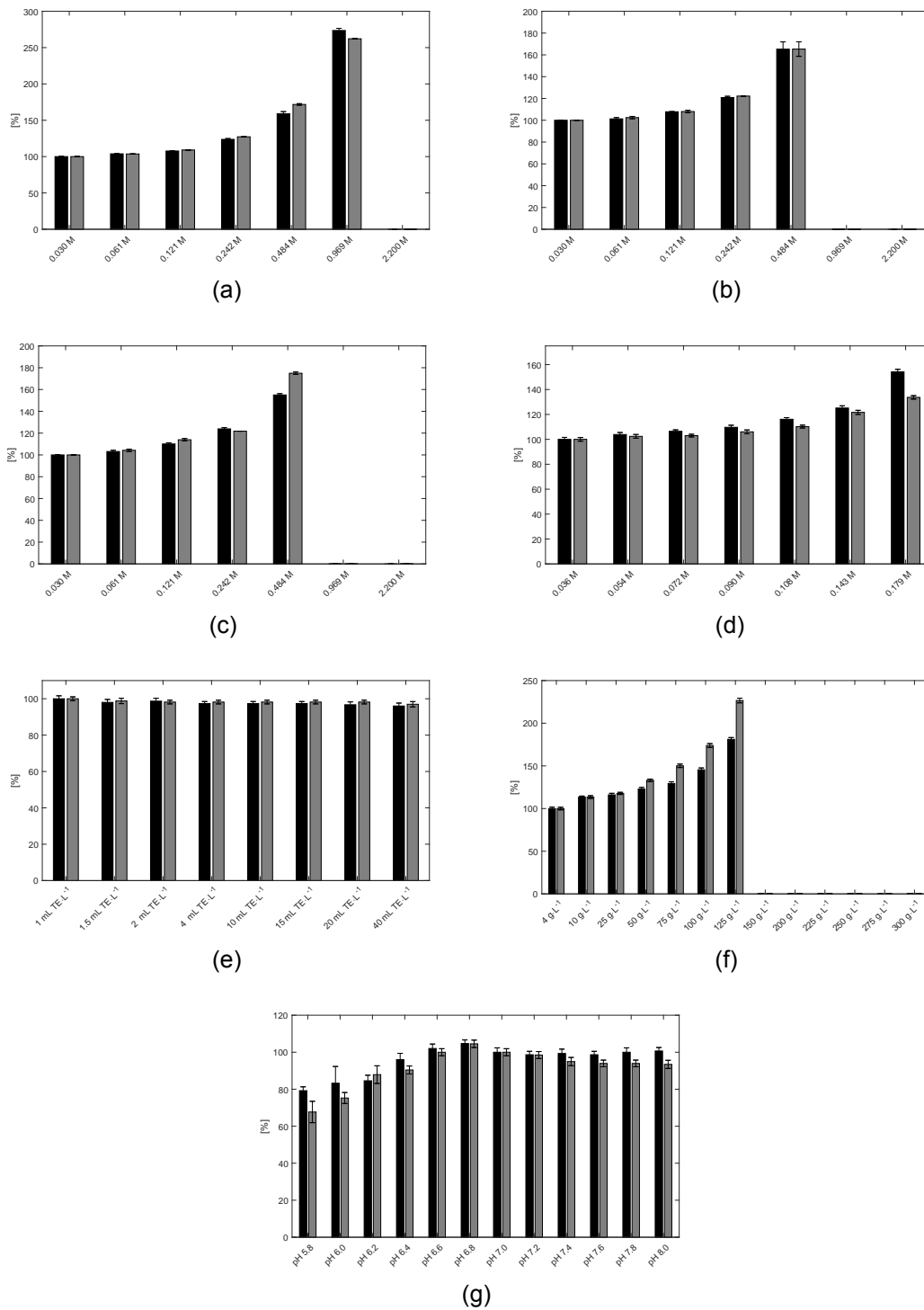


Figure 4.13: Biolector experiments cultivated at different nutrient concentrations and pH, illustrating the time to reach minimum DO as a percentage relative to the standard condition. KT2440, black bars and SEM10, grey bars. Ammonium sulfate (a), ammonium chloride (b), sodium chloride (c), phosphate buffer (d), TE (e), glucose (f) and pH (g).

concentrations of phosphate buffer or elevated pH better than KT2440 but is merely benefiting from an artifact created by the varying pH profiles. As illustrated in Figure 4.13f, growth at increased glucose concentrations shows the most significant difference between the two strains as SEM10 grows slower than KT2440 at glucose concentrations above $25 \text{ g}\cdot\text{L}^{-1}$. However, this discrepancy might come down to the acidity of the culture as well, rather than the glucose concentration. With elevated glucose concentrations and associated inhibition resulting in prolonged exposure to lower pH, an even lower growth rate must be expected from SEM10.

4.4 Conclusions

This study showed that media applied for *P. putida* cultivations in literature were diverse in their composition and nutrient concentration. On this basis, a medium was developed based on nutritional requirements as well as potential chemical and equipment constraints. The different compounds of the developed medium were tested for inhibitory effects towards the wild type *P. putida* KT2440 strain as well as the genome reduced platform strain SEM10. Especially the N source showed inhibitory effects at relevant concentrations. Both $(\text{NH}_4)_2\text{SO}_4$ and NH_4Cl showed significant inhibition at 0.484 M nitrogen and 0.969 M nitrogen, which indicated that such N source must be supplied through the feed of a fed-batch cultivation. In addition, the other major component, phosphorous, in the form of phosphate buffer, showed both inhibition at higher phosphate concentrations and a tendency to cause precipitation. Therefore, to avoid the phosphate-associated obstacles, the phosphate concentration should be adjusted carefully to avoid precipitation and TE should be present in the feed to avoid precipitation. The study further elaborated on the observed glucose inhibition, indicating that the glucose concentrations exceeding $25 \text{ g}\cdot\text{L}^{-1}$ to be inhibitory, which emphasizes the advantage of the industrially favored fed-batch type cultivation. Lastly, the study showed that the optimum pH for cultivations with glucose as the carbon source is between pH 7.0 and 8.0. In contrast, cultivations with carbon sources other than glucose may successfully utilize a broader pH range.

Cultivation of the genome reduced strain SEM10 at the tested concentrations and con-

ditions did not show any apparent increased susceptibility compared to the wild type KT2440. Unfortunately, the cultivation method applied might have masked any advantages of SEM10 under the tested conditions leaving the comparison inconclusive.

Ultimately this showed that a medium appropriate for *P. putida* fed-batch cultivations should be carried out at pH 7.0 with no more than 25 g·L⁻¹ glucose in the batch phase. The phosphate concentration should be maintained at such a level that the nutritional requirements are met but inhibition and precipitation minimized. Due to significant inhibitory effects, nitrogen should preferably be added as ammonium sulfate through a separate feed.

References

- [1] Becker, J. and Wittmann, C. "Advanced biotechnology: Metabolically engineered cells for the bio-based production of chemicals and fuels, materials, and health-care products". In: *Angewandte Chemie - International Edition* 54 (11 2015), pp. 3328–3350. DOI: 10.1002/anie.201409033.
- [2] Park, S. Y., Yang, D., Ha, S. H., and Lee, S. Y. "Metabolic Engineering of Microorganisms for the Production of Natural Compounds". In: *Advanced Biosystems* 2 (1 2018). DOI: 10.1002/adbi.201700190.
- [3] Nikel, P. I. and Lorenzo, V. de. "Pseudomonas putida as a functional chassis for industrial biocatalysis: From native biochemistry to trans-metabolism". In: *Metabolic Engineering* 50 (May 2018), pp. 142–155. DOI: 10.1016/j.ymben.2018.05.005.
- [4] Calero, P. and Nikel, P. I. "Chasing bacterial chassis for metabolic engineering: a perspective review from classical to non-traditional microorganisms". In: *Microbial Biotechnology* 12 (1 2019), pp. 98–124. DOI: 10.1111/1751-7915.13292.
- [5] Martínez-García, E., Nikel, P. I., Aparicio, T., and Lorenzo, V. de. "Pseudomonas 2.0: Genetic upgrading of *P. putida* KT2440 as an enhanced host for heterologous gene expression". In: *Microbial Cell Factories* 13 (1 2014), pp. 1–15. DOI: 10.1186/s12934-014-0159-3.

- [6] Volke, D. C., Friis, L., Wirth, N. T., Turlin, J., and Nikel, P. I. "Synthetic control of plasmid replication enables target- and self-curing of vectors and expedites genome engineering of *Pseudomonas putida*". In: *Metabolic Engineering Communications* 10 (January 2020), e00126. DOI: 10.1016/j.mec.2020.e00126.
- [7] Nikel, P. I., Chavarría, M., Fuhrer, T., Sauer, U., and Lorenzo, V. de. "Pseudomonas putida KT2440 Strain Metabolizes Glucose through a Cycle Formed by Enzymes of the Entner-Doudoroff, Embden-Meyerhof-Parnas, and Pentose Phosphate Pathways". In: *Journal of Biological Chemistry* 290 (43 2015), pp. 25920–25932. DOI: 10.1074/jbc.M115.687749.
- [8] Ankenbauer, A., Schäfer, R. A., Viegas, S. C., Pobre, V., Voß, B., Arraiano, C. M., and Takors, R. "Pseudomonas putida KT2440 is naturally endowed to withstand industrial-scale stress conditions". In: *Microbial Biotechnology* 13 (4 2020), pp. 1145–1161. DOI: 10.1111/1751-7915.13571.
- [9] Demling, P., Ankenbauer, A., Klein, B., Noack, S., Tiso, T., Takors, R., and Blank, L. M. "Pseudomonas putida KT2440 endures temporary oxygen limitations". In: *Biotechnology and Bioengineering* 118 (12 2021), pp. 4735–4750. DOI: 10.1002/bit.27938.
- [10] Kuepper, J., Dickler, J., Biggel, M., Behnken, S., Jäger, G., Wierckx, N., and Blank, L. M. "Metabolic engineering of *Pseudomonas putida* KT2440 to produce anthranilate from glucose". In: *Frontiers in Microbiology* 6 (NOV 2015). DOI: 10.3389/fmicb.2015.01310.
- [11] Hudcova, T., Halecky, M., Kozliak, E., Stiborova, M., and Paca, J. "Aerobic degradation of 2,4-dinitrotoluene by individual bacterial strains and defined mixed population in submerged cultures". In: *Journal of Hazardous Materials* 192 (2 2011), pp. 605–613. DOI: 10.1016/j.jhazmat.2011.05.061.
- [12] Poblete-Castro, I., Rodriguez, A. L., Lam, C. M. C., and Kessler, W. "Improved production of medium-chain-length polyhydroxyalkanoates in glucose-based fed-batch cultivations of metabolically engineered *Pseudomonas putida* strains". In: *Journal*

- of *Microbiology and Biotechnology* 24 (1 2014). Look at cites, pp. 59–69. DOI: 10.4014/jmb.1308.08052.
- [13] Tiso, T., Ihling, N., Kubicki, S., Biselli, A., Schonhoff, A., Bator, I., Thies, S., Karmainski, T., Kruth, S., Willenbrink, A. L., Loeschcke, A., Zapp, P., Jupke, A., Jaeger, K. E., Büchs, J., and Blank, L. M. “Integration of Genetic and Process Engineering for Optimized Rhamnolipid Production Using *Pseudomonas putida*”. In: *Frontiers in Bioengineering and Biotechnology* 8 (2020). DOI: 10.3389/fbioe.2020.00976.
 - [14] Kampers, L. F., Volkers, R. J., and Santos, V. A. M. dos. “*Pseudomonas putida* KT2440 is HV1 certified, not GRAS”. In: *Microbial Biotechnology* (635536 2019), pp. 10–13. DOI: 10.1111/1751-7915.13443.
 - [15] Gomori, G. “Preparation of Buffers for Use in Enzyme Studies”. In: *Methods in Enzymology* 1 (1955), pp. 138–146.
 - [16] Parkhurst, D. L. and Appelo, C. A. J. “Description of Input and Examples for PHREEQC Version 3-A Computer Program for Speciation, Batch-Reaction, One-Dimensional Transport, and Inverse Geochemical Calculations”. In: *U.S. Geological Survey Techniques and Methods, Book 6*. 2013, p. 497.
 - [17] Parkhurst, D. L. and Apello, C. A. J. *PHREEQC*. <https://www.usgs.gov/software/phreeqc-version-3>. Accessed 21/02/2023. 2021.
 - [18] Sun, Z., Ramsay, J. A., Guay, M., and Ramsay, B. A. “Automated feeding strategies for high-cell-density fed-batch cultivation of *Pseudomonas putida* KT2440”. In: *Applied Microbiology and Biotechnology* 71 (4 2006), pp. 423–431. DOI: 10.1007/s00253-005-0191-7.
 - [19] Tlemçani, L. L., Corroler, D., Barillier, D., and Mosrati, R. “Physiological states and energetic adaptation during growth of *Pseudomonas putida* mt-2 on glucose”. In: *Archives of Microbiology* 190 (2 2008), pp. 141–150. DOI: 10.1007/s00203-008-0380-8.
 - [20] Lieder, S., Jahn, M., Koepff, J., Müller, S., and Takors, R. “Environmental stress speeds up DNA replication in *Pseudomonas putida* in chemostat cultivations”. In: *Biotechnology Journal* 11 (1 2016), pp. 155–163. DOI: 10.1002/biot.201500059.

- [21] Follonier, S., Henes, B., Panke, S., and Zinn, M. "Putting cells under pressure: A simple and efficient way to enhance the productivity of medium-chain-length polyhydroxyalkanoate in processes with *Pseudomonas putida* KT2440". In: *Biotechnology and Bioengineering* 109 (2 2012), pp. 451–461. DOI: 10.1002/bit.23312.
- [22] Duuren, J. B. van, Puchalka, J., Mars, A. E., Bücker, R., Eggink, G., Wittmann, C., and Santos, V. A. dos. "Reconciling in vivo and in silico key biological parameters of *Pseudomonas putida* KT2440 during growth on glucose under carbon-limited condition". In: *BMC Biotechnology* 13 (2013). Elemental biomass composition for *P. putida* K2440. DOI: 10.1186/1472-6750-13-93.
- [23] Plugge, C. M. "Anoxic media design, preparation, and considerations". In: *Methods in Enzymology* 397 (2005), pp. 3–16. DOI: 10.1016/S0076-6879(05)97001-8.
- [24] Beskæftigelsesministeriet. *Bekendtgørelse om foranstaltninger til forebyggelse af kræfttrikoen ved arbejde med stoffer og materialer*. 2015.
- [25] Krujatz, F., Haarstrick, A., Nörtemann, B., and Greis, T. "Assessing the toxic effects of nickel, cadmium and EDTA on growth of the plant growth-promoting rhizobacterium *Pseudomonas brassicacearum*". In: *Water, Air, and Soil Pollution* 223 (3 2012), pp. 1281–1293. DOI: 10.1007/s11270-011-0944-0.
- [26] Kampen, W. H. "Nutritional Requirements in Fermentation Processes". In: Third. Elsevier Inc., 2014, pp. 37–57. DOI: <https://doi.org/10.1016/C2011-0-05779-4>.
- [27] Joshi, H., Dave, R., and Venugopalan, V. P. "Protein as chemical cue: Non-nutritional growth enhancement by exogenous protein in *Pseudomonas putida* KT2440". In: *PLoS ONE* 9 (8 2014). DOI: 10.1371/journal.pone.0103730.
- [28] "Comparative genomics and functional analysis of niche-specific adaptation in *Pseudomonas putida*". In: *FEMS Microbiology Reviews* 35 (2 2011), pp. 299–323. DOI: 10.1111/j.1574-6976.2010.00249.x.
- [29] Xie, J. J., Ningyu, H., Sun, X., and Zhan, J. Y. "Corrosion behavior of 316L stainless Steel under Cl⁻ corrosion medium". In: vol. 711. Institute of Physics Publishing, 2020. DOI: 10.1088/1757-899X/711/1/012058.

- [30] Suzuki, T., Yamane, T., and Shimizu, S. "Applied Microbiology Biotechnology Mass production of poly- β -hydroxybutyric acid by fully automatic fed-batch culture of methylophilus". In: *Applied Microbiology and Biotechnology* 23 (1986), pp. 322–329.
- [31] Vuyst, L. D. and Vandamme, E. J. "Applied Microbiology Biotechnology Influence of the phosphorus and nitrogen source on nisin production in *Lactococcus lactis* subsp. *lactis* batch fermentations using a complex medium". In: *Applied Microbiology and Biotechnology* 40 (1993), pp. 17–22.
- [32] Kim, M. H., Kong, Y. J., Baek, H., and Hyun, H. H. "Optimization of culture conditions and medium composition for the production of micrococcin GO5 by *Micrococcus* sp. GO5". In: *Journal of Biotechnology* 121 (1 2006), pp. 54–61. DOI: 10.1016/j.jbiotec.2005.06.022.
- [33] Davis, R., Duane, G., Kenny, S. T., Cerrone, F., Guzik, M. W., Babu, R. P., Casey, E., and O'Connor, K. E. "High cell density cultivation of *Pseudomonas putida* KT2440 using glucose without the need for oxygen enriched air supply". In: *Biotechnology and Bioengineering* 112 (4 2015), pp. 725–733. DOI: 10.1002/bit.25474.
- [34] Patil, M. D., Shinde, K. D., Patel, G., Chisti, Y., and Banerjee, U. C. "Use of response surface method for maximizing the production of arginine deiminase by *Pseudomonas putida*". In: *Biotechnology Reports* 10 (2016), pp. 29–37. DOI: 10.1016/j.btre.2016.03.002.
- [35] Hofer, H., Mandl, T., and Steiner, W. "Acetopyruvate hydrolase production by *Pseudomonas putida* O1 - Optimization of batch and fed-batch fermentations". In: *Applied Microbiology and Biotechnology* 60 (3 2002), pp. 293–299. DOI: 10.1007/s00253-002-1133-2.
- [36] Kim, G. J., In Young, L., Choi, D. K., Yoon, S. C., and Park, Y. H. "High Cell Density Cultivation of *Pseudomonas putida* BM01 Using Glucose". In: *Journal of Microbiology and Biotechnology* 6 (3 1996), pp. 221–224.
- [37] Kakimoto, T., Shibatani, T., and Nishimura, N. "Enzymatic Production of L-Citrulline by *Pseudomonas putida*". In: *APPLIED MICROBIOLOGY* 22 (6 1971), pp. 992–999.

- [38] Hahn-hägerdal, B., Karhumaa, K., Larsson, C. U., Gorwa-Grauslund, M., Görgens, J., and Zyl, W. H. van. "Role of cultivation media in the development of yeast strains for large scale industrial use". In: *Microbial Cell Factories* 4 (1 2005), p. 31. DOI: 10.1186/1475-2859-4-31.
- [39] Clarke, K. G. "Microbial kinetics during batch, continuous and fed-batch processes". In: Elsevier, 2013, pp. 97–146. DOI: 10.1533/9781782421689.97.
- [40] Schulte, M. F., Tozakidis, I. E., and Jose, J. "Autotransporter-Based Surface Display of Hemicellulases on *Pseudomonas putida*: Whole-Cell Biocatalysts for the Degradation of Biomass". In: *ChemCatChem* 9 (20 2017), pp. 3955–3964. DOI: 10.1002/cctc.201700577.
- [41] Bonilla, M., Olivaro, C., Corona, M., Vazquez, A., and Soubes, M. "Production and characterization of a new bioemulsifier from *Pseudomonas putida* ML2". In: *Journal of Applied Microbiology* 98 (2 2005), pp. 456–463. DOI: 10.1111/j.1365-2672.2004.02480.x.
- [42] "Metabolic engineering of *Pseudomonas putida* for production of the natural sweetener 5-ketofructose from fructose or sucrose by periplasmic oxidation with a heterologous fructose dehydrogenase". In: *Microbial Biotechnology* 14 (6 2021), pp. 2592–2604. DOI: 10.1111/1751-7915.13913.
- [43] Kohlstedt, M. and Wittmann, C. "GC-MS-based ¹³ C metabolic flux analysis resolves the parallel and cyclic glucose metabolism of *Pseudomonas putida* KT2440 and *Pseudomonas aeruginosa* PAO1". In: *Metabolic Engineering* 54 (January 2019), pp. 35–53. DOI: 10.1016/j.ymben.2019.01.008.
- [44] Castillo, T. D., Ramos, J. L., Rodríguez-Herva, J. J., Fuhrer, T., Sauer, U., and Duque, E. "Convergent peripheral pathways catalyze initial glucose catabolism in *Pseudomonas putida*: Genomic and flux analysis". In: *Journal of Bacteriology* 189 (14 2007), pp. 5142–5152. DOI: 10.1128/JB.00203-07.
- [45] Sánchez-Pascuala, A., Fernández-Cabezón, L., Lorenzo, V. de, and Nikel, P. I. "Functional implementation of a linear glycolysis for sugar catabolism in *Pseudomonas*

- putida". In: *Metabolic Engineering* 54 (January 2019), pp. 200–211. DOI: 10.1016/j.jymben.2019.04.005.
- [46] Martínez-García, E., Nickel, P. I., Chavarría, M., and Lorenzo, V. de. "The metabolic cost of flagellar motion in *Pseudomonas putida*KT2440". In: *Environmental Microbiology* 16 (1 2014), pp. 291–303. DOI: 10.1111/1462-2920.12309.

5 Application of a genome reduced *Pseudomonas putida* strain in fed-batch cultivation

Abstract

The emergence of *Pseudomonas putida* as an alternative production host and the development of streamlined genome reduced strains requires additional insights into industrially relevant conditions. Streamlined *P. putida* strains are characterized by their improved growth, efficient carbon utilization and susceptibility to genetic engineering in comparison to the wild type KT2440. This study sought to apply the wildtype KT2440 and the genome reduced SEM10 strains in a high cell concentration fed-batch cultivation to evaluate the genome reduced strain under industrially relevant conditions. The genome reduced variant grew faster and more efficiently during the initial 6 h of the feeding phase compared to KT2440 before growth halted, achieving similar final biomass concentrations, $26.15 \pm 1.04 \text{ g} \cdot \text{L}^{-1}$ and $28.15 \pm 0.39 \text{ g} \cdot \text{L}^{-1}$, respectively. However, results indicated that the genome reduced strain experienced dual limitation of both glucose and oxygen in the later stage of the feeding phase, which eliminated its advantageous growth characteristics. The SEM10 strain thus showed promise in the early feeding phase, indicating that the strain can be a valuable *P. putida* platform strain when the cultivation process avoids continuous dual limitation of glucose and oxygen.

5.1 Introduction

Chemicals derived from non-renewable feedstocks, such as oil, have been an integral part of everyday products throughout the past century and continue to be so [1]. In an effort to move to renewable feedstocks in chemical production, fermentation-based manufacturing has been intensively explored over the past decades. As such, the market for bio-based chemicals has been steadily increasing and was estimated to amount to USD 127 billion in 2014 [2]. Research has often been carried out with a traditional set of mi-

microorganisms such as *Escherichia coli* and *Saccharomyces cerevisiae* though other less common microorganisms have also been applied in for example, organic acid production [3]. Utilizing alternative microorganisms as platforms for bio-based production, depending on the product and production environment has emerged as an option over the traditional microorganisms [4, 5].

The bacterium *Pseudomonas putida* has gained interest as an alternative host for bio-based chemical production due to its native robustness and versatile metabolism [6, 7]. As the bacterium is equipped with a metabolism that allows for adaptation to cope with high demands of reducing power, it becomes well suited for the production of highly reduced or toxic chemicals [8]. This is also reflected in the broad scope of applications explored in research, ranging from biosurfactants and biopolymers to conversion of aromatic compounds [9–11]. Consequently, research also focused on exploring the industrially relevant conditions to which end *P. putida* showed to be endowed with a natural ability to endure glucose starvation and repeated short-term oxygen limitation [12, 13].

Furthermore, the wildtype strain KT2440 has been streamlined by genome reduction to yield more efficient platform strains to further the potential of *P. putida* [14, 15]. The first genome reduced variant, EM383, had its genome reduced by 4.3% compared to KT2440. The genome reduction focused on increasing genetic stability, removing prophage DNA and reducing futile energy spending. The latter was achieved by deletion of the flagellar operon as the flagellar was deemed unnecessary in an agitated bioreactor environment. Compared to the wild type KT2440, EM383 showed improved growth characteristics like higher biomass yields, lower maintenance demand and increased viability [14, 16]. The genome of EM383 was further reduced by an additional 0.5%, compared to KT2440, to yield the SEM10 strain. The genome reduction of SEM10 focused on the strain's susceptibility towards genetic engineering by, for example, reducing *P. putida* KT2440's natural resistance to antibiotics [15].

Both, the wildtype strain KT2440 and the genome reduced strain EM383, have been explored in the bioreactor setting. However, whereas KT2440 has been applied in high cell

concentration fed-batch cultivations, the genome reduced strains have only been tested in low cell concentration batch and chemostat cultivations [10, 14, 16–18]. In this study, we apply a range of online and offline analysis methods to evaluate the application of the genome reduced SEM10 strain in the industrially relevant fed-batch cultivation [15]. In addition, the study aims to elucidate if the genome reduced strain possesses traits that will be advantageous in potentially demanding high cell concentration cultivations.

5.2 Materials and Methods

Bacterial Strains and Medium

Bacterial strains, *Pseudomonas putida* KT2440 and SEM10, were used in this study and stored at -80°C in 50 % (w/w) glycerol. Lysogeny broth (LB) agar medium contained per liter: 10 g tryptone, 5 g yeast extract and 10 g NaCl and 20 g agar. The defined basis medium contained per liter: 7.76 g K_2HPO_4 , 4.24 g $\text{NaH}_2\text{PO}_4 \cdot 2\text{H}_2\text{O}$, 4 g $(\text{NH}_4)_2\text{SO}_4$ (VWR, USA), 20 mL TE1 and 8 g glucose (VWR, USA). The initial fed-batch medium contained per liter: 7.04 g K_2HPO_4 , 3.84 g $\text{NaH}_2\text{PO}_4 \cdot 2\text{H}_2\text{O}$, 5 g $(\text{NH}_4)_2\text{SO}_4$ (VWR, USA), 2 mL trace element solution 2 (TE2), 1.54 mL trace element booster solution (TEB), 43 mg $\text{MgCl}_2 \cdot 6\text{H}_2\text{O}$ (VWR, USA) and 10 g glucose (VWR, USA). The TE1 solution contained per liter: 1 g EDTA, 10 g $\text{MgCl}_2 \cdot 6\text{H}_2\text{O}$ (VWR, USA), 0.2 g $\text{ZnSO}_4 \cdot 7\text{H}_2\text{O}$, 0.1 g $\text{CaCl}_2 \cdot 2\text{H}_2\text{O}$, 0.5 g $\text{FeSO}_4 \cdot 7\text{H}_2\text{O}$, 0.02 g $\text{Na}_2\text{MoO}_4 \cdot 2\text{H}_2\text{O}$, 0.02 g $\text{CuSO}_4 \cdot 5\text{H}_2\text{O}$, 0.04 g $\text{CoCl}_2 \cdot 6\text{H}_2\text{O}$ and 0.122 mg $\text{MnCl}_2 \cdot 4\text{H}_2\text{O}$. The TE2 solution contained per liter: 10 g EDTA, 2 g $\text{ZnSO}_4 \cdot 7\text{H}_2\text{O}$, 1 g $\text{CaCl}_2 \cdot 2\text{H}_2\text{O}$, 5 g $\text{FeSO}_4 \cdot 7\text{H}_2\text{O}$, 0.2 g $\text{Na}_2\text{MoO}_4 \cdot 2\text{H}_2\text{O}$, 0.2 g $\text{CuSO}_4 \cdot 5\text{H}_2\text{O}$, 0.4 g $\text{CoCl}_2 \cdot 6\text{H}_2\text{O}$ and 1.22 g $\text{MnCl}_2 \cdot 4\text{H}_2\text{O}$. The TEB solution contained per liter: 13 g EDTA (VWR, USA), 2.6 g $\text{CaCl}_2 \cdot 2\text{H}_2\text{O}$, 3.25 g $\text{FeSO}_4 \cdot 7\text{H}_2\text{O}$ (VWR, USA) and 1.04 g $\text{CuSO}_4 \cdot 5\text{H}_2\text{O}$. All chemicals were purchased from Merck, USA, unless otherwise stated.

Shake Flask Cultivations

Precultures were prepared in three steps: First, glycerol stocks were activated by streaking on LB agar plates and incubating at 30°C for 18 h. Second, a 14 mL cultivation tube (Falcon, Corning, Mexico) filled with 5 mL of basis medium, was inoculated with 3 colonies

from a fresh LB agar plate and incubated at 30°C and 180 rpm for 8 h in a rotary shaker (Ecotron, Infors HT, Switzerland). Third, a final liquid preculture was inoculated to an initial cell dry weight (CDW) concentration of 4.59 mg·L⁻¹ in 500 mL baffled shake flasks (DWK Life Sciences, United Kingdom) containing 50 mL basis medium and incubated at 30°C and 180 rpm for 18 h in a rotary shaker (Ecotron, Infors HT, Switzerland). Precultures for bioreactor fed-batch experiments used basis medium.

Fed-batch Cultivations

Fed-batch cultivations were performed in a BioBench bioreactor (Biostream, the Netherlands) with 2 L working volume and 3 L total volume. The starting volume was set to 1.3 L to avoid splashing during the batch phase. The fed-batch cultivation was inoculated with a 2% (v/v) shake flask preculture. Cultivation conditions were controlled by the BioBench control tower (Biostream, the Netherlands). Agitation, aeration and temperature were maintained at 1000 rpm, 2 l air·min⁻¹ and 30°C, respectively, throughout the cultivation. The pH was controlled at 7.0 by the addition of 4 M NaOH or 2 M H₂SO₄. Antifoam agent, Antifoam 204 (Sigma Aldrich, USA), was added as required by a built-in online foam sensor. The feed contained 300 g·L⁻¹ glucose, 4.875 g·L⁻¹, MgCl₂ · 6H₂O (VWR, USA), 30 mL·L⁻¹ TE 2, 23.08 mL·L⁻¹ TEB and 100 g·L⁻¹ (NH₄)₂SO₄. The feed was autoclaved separately from the bioreactor and (NH₄)₂SO₄ was autoclaved separately from the remaining main feed solution. The main feed solution and (NH₄)₂SO₄ solution were combined aseptically before the final feed solution was attached to the bioreactor.

Online Analytics

Off-gas composition of O₂ and CO₂ was measured online by BlueInOne Cell (BlueSens, Germany). Dissolved oxygen (DO) concentration was measured relative to ambient air and pressure with a Visiferm optical DO sensor (Hamilton, USA). Cell dry weight (CDW) was estimated online by light backscatter with a fiber optic BE3000 Biomass sensor (Buglab, USA). The sensor was calibrated with offline measurements of CDW at the sampling points of the fed-batch cultivations.

Offline Analytics

Samples for high pressure liquid chromatography (HPLC) analysis were, immediately after sample withdrawal, spiked with 1:100 volume of 2 M H₂SO₄ to adjust the pH and stop reactions. Subsequently, the samples were centrifuged (Centrifuge 5430 R, Eppendorf, Germany) at 10,000 x g at 4°C for 2 min before being filtered through a 0.2 µm cellulose acetate syringe filter (Phenomenex, USA). The filtered samples were stored at - 18°C prior to analysis. Glucose, gluconate and 2-ketogluconate were measured by HPLC. Analysis was performed in an Ultimate 3000 HPLC system (Thermo Scientific, USA) with a built-in ultraviolet (UV) detector and equipped with a RefractoMax 520 (Thermo Scientific, USA) refractive index (RI) detector. Separation was achieved with an Aminex HPX-87H ion exchange column (Bio-Rad, USA). Operation settings were 30°C column temperature, 5 mM H₂SO₄ mobile phase, 0.6 mL·min⁻¹ flow rate, detection in the RI and UV channel at 210 nm. Glucose and gluconate co-elute but their concentrations were correlated with their differential contribution in the refractive index and UV channel.

Total biomass concentration was measured as cell dry weight (CDW). An appropriately diluted sample was filtered through a 0.2 µm polyethersulfone filter membrane (Sartorius Stedim Biotech, Germany) and the filter was flushed twice with 5 mL of deionized water. The filter was then dried in a microwave oven for 30 min at 180 W and cooled for 48 h in a desiccator before weighing. Viable and total cells were measured with a BactoBox® (SBT Instruments, Denmark) using impedance flow cytometry. Samples were diluted appropriately with a 1:9 PBS buffer prior to analysis to obtain a sample conductivity between 1,700-2,100 µS·cm⁻¹ and a total cell count between 10,000-5,000,000 total cells·mL⁻¹. Colony-forming units (CFU) were estimated by plate counts on LB agar. Samples were diluted in 0.9% (w/v) NaCl and 100 µl were spread on an LB agar plate. The plate was incubated overnight at 30°C before CFU was counted (Infors HT, Switzerland).

Samples for protein analysis were centrifuged (Centrifuge 5430 R, Eppendorf, Germany) at 10,000 x g at 4°C for 5 min and the supernatant was withdrawn and centrifuged. The resulting supernatant was withdrawn and used for analysis. Total extracellular protein

concentration was estimated by Bradford bovine serum albumin (BSA) assay (BioRad, USA.). Samples were diluted in MilliQ water to reach a concentration range of 1.25-20 $\mu\text{g}\cdot\text{mL}^{-1}$, the linear range of the BSA microassay protocol. In a 2 mL microcentrifuge tube (Sarsted, Germany), 0.5 mL diluted sample and 0.5 mL dye reagent were mixed and incubated for 15 min. The absorbance was measured at 595 nm in an UV-1800 UV-spectrophotometer (Shimadzu, Japan) and total protein concentration was calculated based on a BSA standard.

Distribution of extracellular protein according to size was performed by lithium dodecyl sulfate–polyacrylamide gel electrophoresis (LDS-PAGE). Samples of supernatant were mixed with 4x lithium dodecyl sulfate (LDS) sample buffer, reduced by adding 10x reducing agent, and incubated at 70°C for 10 min. Samples were loaded on a gradient 4-12% Bis-Tris gel and separated for 50 min at 200 V (PowerEase 90W, Thermo Fisher, USA). The running buffer was a 3-(N-morpholino)propanesulfonic acid-sodium dodecyl sulfate buffer supplemented with 2.5 mL antioxidant per liter of buffer. Each well was loaded with 10 μL sample mix and a separate well was loaded with SeeBlue™ Plus2 Pre-stained Protein Standard as molecular weight standard. Following electrophoresis, the gel was washed with DI water and stained for an hour with Simply Blue™ SafeStain. The gel was destained with DI water and an image was taken with a GelDoc Go Gel Imaging System (Bio-Rad, USA). All reagents were obtained from Invitrogen (Thermo Fisher Scientific, USA).

5.3 Mathematical Model

A kinetic model that describes the cultivation process was developed to aid the feed control design as well as the data analysis. The applied kinetic equations were adapted from Davis et al. (2015) [18]. The model was developed to describe growth as well as the evolution of major components related to growth, like substrate consumption and CO_2 production in both the liquid and the gas phase. In addition, the limitation of glucose and oxygen was also accounted for:

$$\mu = \mu_{max} \cdot \frac{c_S}{c_S + K_S} \cdot \frac{c_{O_2}}{c_{O_2} + K_{O_2}} \quad (5.1)$$

Where μ_{\max} (h^{-1}) is the maximum specific growth rate, c_S ($\text{g}\cdot\text{L}^{-1}$) is the glucose concentration, K_S ($\text{g}\cdot\text{L}^{-1}$) is the glucose affinity constant, c_{O_2} ($\text{g}\cdot\text{L}^{-1}$) is the dissolved oxygen concentration, K_{O_2} ($\text{g}\cdot\text{L}^{-1}$) is the oxygen affinity constant.

Biomass-specific uptake rates of glucose, dissolved oxygen and ammonium in addition to the production of CO_2 were modeled as yield-based Monod equations:

$$q_S = \frac{\mu}{Y_{X/S}} \quad (5.2)$$

$$q_{O_2} = \frac{\mu}{Y_{X/O_2}} \quad (5.3)$$

$$q_{CO_2} = \frac{\mu}{Y_{X/CO_2}} \quad (5.4)$$

$$q_{NH_4} = \frac{\mu}{Y_{X/NH_4}} \quad (5.5)$$

Where q_S ($\text{g S}\cdot(\text{g X}\cdot\text{h})^{-1}$) is the biomass-specific glucose uptake rate, q_{O_2} ($\text{g O}_2\cdot(\text{g X}\cdot\text{h})^{-1}$) is the biomass-specific oxygen uptake rate, q_{CO_2} ($\text{g CO}_2\cdot(\text{g X}\cdot\text{h})^{-1}$) is the biomass-specific CO_2 production rate, q_{NH_4} ($\text{g NH}_4\cdot(\text{g X}\cdot\text{h})^{-1}$) is the biomass-specific ammonium uptake rate, $Y_{X/S}$ ($\text{g X}\cdot(\text{g S})^{-1}$) is the biomass yield on glucose, Y_{X/O_2} ($\text{g X}\cdot(\text{g O}_2)^{-1}$) is the biomass yield on oxygen, Y_{X/CO_2} ($\text{g X}\cdot(\text{g CO}_2)^{-1}$) is the biomass yield on CO_2 and Y_{X/NH_4} ($\text{g X}\cdot(\text{g NH}_4)^{-1}$) is the biomass yield on ammonium.

The oxygen transfer from the gas phase to the liquid phase was calculated according to eq. (5.6). The solubility of oxygen in the medium was calculated using Henry's law at 1 atm and the solubility constant associated with water at 30°C . Solubility was continuously calculated based on the off gas-composition. The transfer of CO_2 from the liquid phase to the gas phase was modeled in a similar fashion, though the volumetric mass transfer coefficient ($k_L a$) was assumed to be equal to that of oxygen:

$$OTR = k_L a \cdot (c_{O_2}^* - c_{O_2}) \quad (5.6)$$

$$CTR = k_L a \cdot (c_{CO_2} - c_{CO_2}^*) \quad (5.7)$$

Where OTR ($g\ O_2 \cdot (L \cdot h)^{-1}$) is the oxygen transfer rate, $k_L a$ (h^{-1}) is the volumetric mass transfer coefficient, $c_{O_2}^*$ ($g \cdot L^{-1}$) is the solubility of oxygen in water, CTR ($g\ O_2 \cdot (L \cdot h)^{-1}$) is the CO_2 transfer rate, $c_{CO_2}^*$ ($g \cdot L^{-1}$) is the solubility of CO_2 in water.

The above rate equations were used to formulate the mass balances of the liquid phase described below. Each mass balance contains a consumption/production term, a feed term and a dilution term to adjust for the incoming feed:

$$\frac{dc_X}{dt} = \mu \cdot c_X - \frac{F_{in}}{V} \cdot c_X \quad (5.8)$$

$$\frac{dc_S}{dt} = -q_S \cdot c_X + \frac{F_{in} \cdot c_{S,feed}}{V} - \frac{F_{in}}{V} \cdot c_S \quad (5.9)$$

$$\frac{dc_{O_2}}{dt} = -q_{O_2} + OTR + \frac{F_{in} \cdot c_{O_2,feed}}{V} - \frac{F_{in}}{V} \cdot c_{O_2} \quad (5.10)$$

$$\frac{dc_{CO_2}}{dt} = q_{CO_2} - CTR + \frac{F_{in} \cdot c_{CO_2,feed}}{V} - \frac{F_{in}}{V} \cdot c_{CO_2} \quad (5.11)$$

$$\frac{dc_{NH_4}}{dt} = -q_{NH_4} + \frac{F_{in} \cdot c_{NH_4,feed}}{V} - \frac{F_{in}}{V} \cdot c_{NH_4} \quad (5.12)$$

Where c_X ($g \cdot L^{-1}$) is the biomass concentration, c_S ($g \cdot L^{-1}$) is the glucose concentration, c_{O_2} ($g \cdot L^{-1}$) is the dissolved oxygen concentration, c_{CO_2} ($g \cdot L^{-1}$) is the dissolved CO_2 concentration, c_{NH_4} ($g \cdot L^{-1}$) is the ammonium concentration, F_{in} ($L \cdot h^{-1}$) is the feed flow rate and V (L) is the reactor liquid volume.

The volume change was modeled as described in Equation (5.13) by the addition of feed and withdrawal of sample volume:

$$\frac{dV}{dt} = F_{in} - F_{sample} \quad (5.13)$$

Where F_{sample} is the sample withdrawal.

The gas phase was modeled for O_2 and CO_2 using equations 4.14-4.16.

$$n_{total} = \frac{p \cdot V_{gas}}{R \cdot T} \quad (5.14)$$

$$\frac{dn_{O_2}}{dt} = F_{gas,in} \cdot \gamma_{O_2,in} - F_{gas,out} \cdot \frac{n_{O_2}}{n_{total}} - OTR \quad (5.15)$$

$$\frac{dn_{CO_2}}{dt} = F_{gas,in} \cdot \gamma_{CO_2,in} - F_{gas,out} \cdot \frac{n_{CO_2}}{n_{total}} + CTR \quad (5.16)$$

Where n_{total} (mol) is the amount of gas, R ($L \cdot atm \cdot (K \cdot mol)^{-1}$) is the ideal gas constant, T (K) is the temperature, n_{O_2} (mol) is the amount of O_2 , $F_{gas,in}$ ($mol \cdot h^{-1}$) is the flow rate of gas into the bioreactor, $\gamma_{O_2,in}$ is the mole fraction of O_2 in the inlet gas, $F_{gas,out}$ ($mol \cdot h^{-1}$) is the flow rate of gas out of the bioreactor, n_{CO_2} (mol) is the amount of CO_2 and $\gamma_{CO_2,in}$ is the mole fraction of CO_2 in the inlet gas.

The bioreactor feed rate was based on a basic proportional–integral (PI) control function, illustrated in Equation (5.17) with the error function described in Equation (5.18). The PI controller was set up to control the DO of the cultivation by adjusting the feed flow rate.

$$F_{in} = F_{in,0} + K_c \cdot \epsilon(t) + K_i \cdot \int_0^t \epsilon(t) dt \quad (5.17)$$

$$\epsilon(t) = c_{O_2} - c_{O_2,set} \quad (5.18)$$

Where $F_{in,0}$ ($L \cdot h^{-1}$) is the initial feed flow rate, K_c is the proportional gain, K_i (h^{-1}) is the integral gain, ϵ is the control error and $c_{O_2,set}$ ($g \cdot L^{-1} O_2$) is the control set point.

The presented model is a simplification of the cultivation and thus comes with certain constraints: The $k_L a$ was measured in water, not medium and without cells. Changes in viscosity and its effect on mass transfer was not considered. The solubility of O_2 and CO_2 is calculated based on the Henry constants for pure water. The gas phase is only considered to contain three species, O_2 , CO_2 and N_2 . The latter being considered constant and accounts for the remaining species of atmospheric air. No inhibition is considered, except for glucose and oxygen limitations. The pH was assumed to be constant and no addition of acid or base was considered. Evaporation during the cultivation is neglected due to off-gas cooling at 4°C.

5.4 Results and Discussion

The wild type *P. putida* KT2440 and the genome reduced SEM10 strains were cultivated in fed-batch mode to compare the performance in an industrially relevant setting. A general representation of the cultivation phases is illustrated in Figure 5.1. Figure 5.2 shows the general cultivation profiles of KT2440 and SEM10. Figure 5.2 (a) and (b) show the evolution of the added glucose and the bioreactor volume, which were controlled by a PI controller, adjusting the feed rate to control the DO concentration at 20%. However, the PI controller did not function as expected and immediately reached the feed rate's upper boundaries, unable to maintain the set DO concentration. In order to provide longevity of the experiment, the upper boundary was reduced after approximately two hours from 57.5 mL·h⁻¹ to 28.8 mL·h⁻¹. The PI controller failed to properly control the DO over the course of the fermentation, as visible in Figure 5.2 (c) and (d) and the feed rate remained constant at the upper boundaries.

The batch phases of both KT2440 and SEM10 were comparable to those presented in

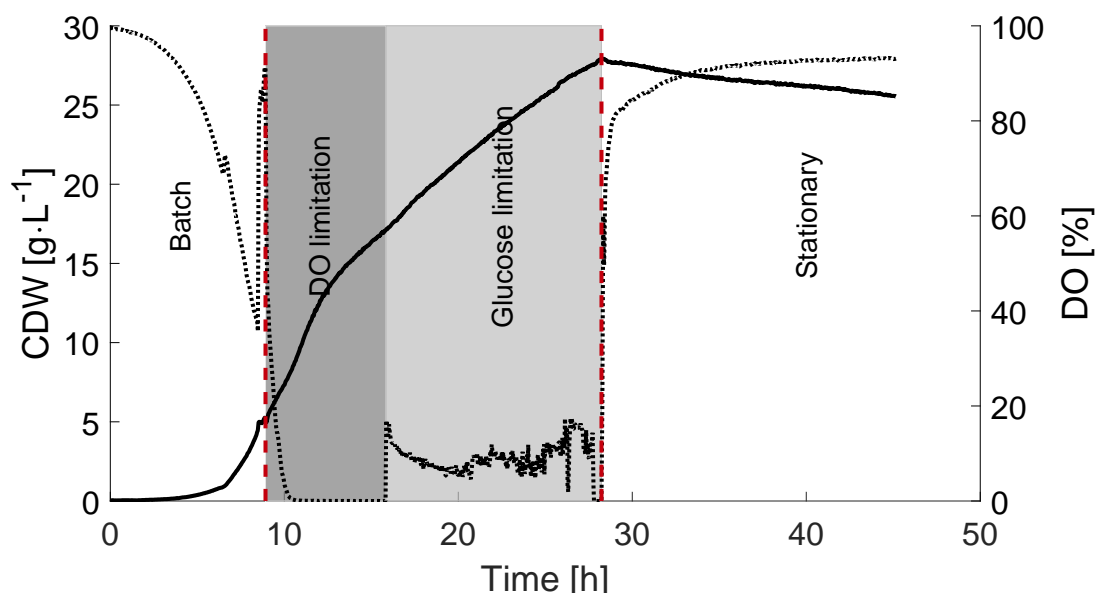


Figure 5.1: Phases of cultivation exemplified by one KT2440 fed-batch replicate represented by the CDW concentration (-) and DO (·). The initial batch phase was followed by a feeding phase (dark and light grey) and a stationary phase. The feeding phase is divided into a DO (dark grey) and glucose (light grey) limiting phases. The red dashed lines represent the onset and end of the feeding.

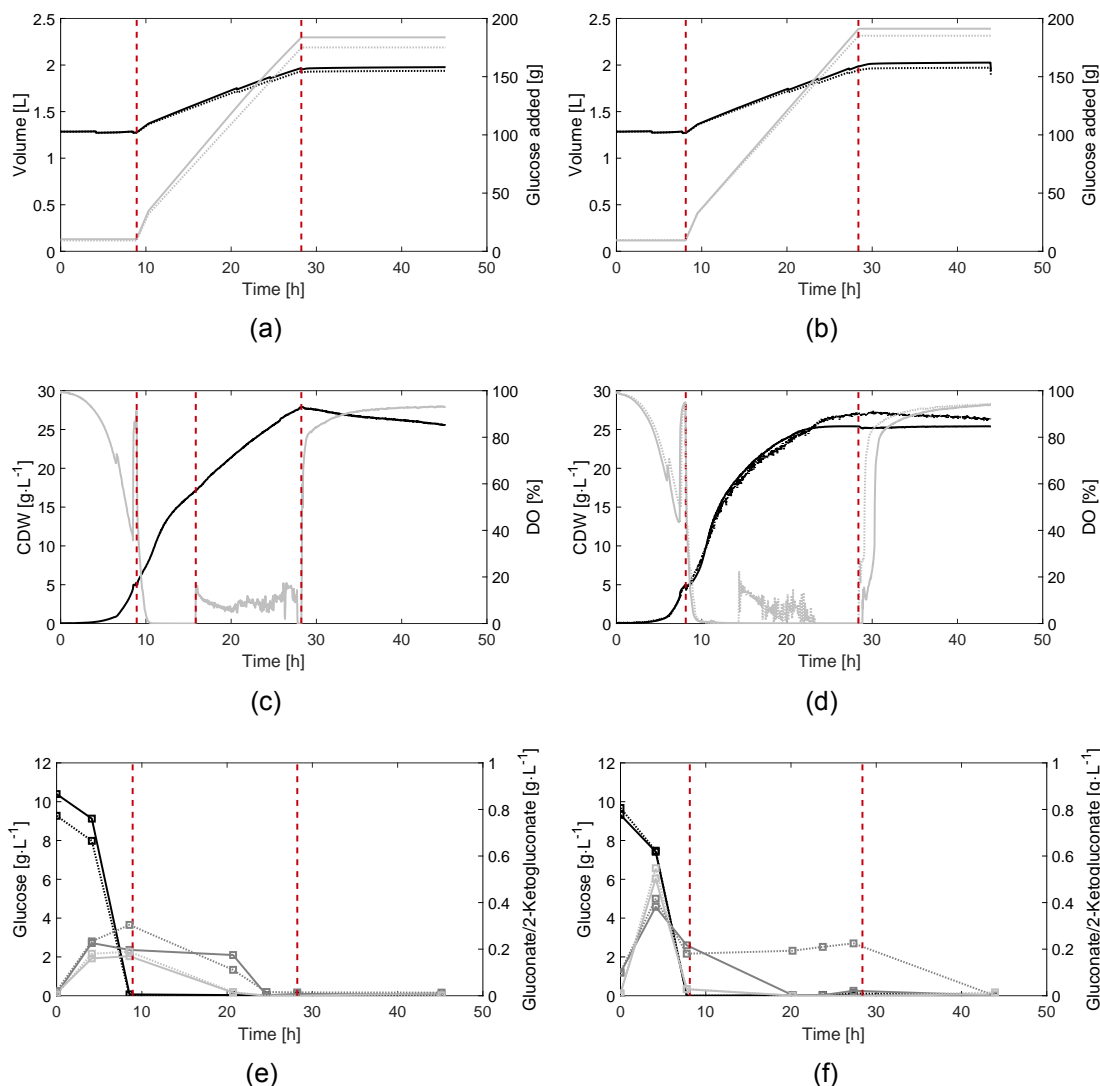


Figure 5.2: General cultivation profiles of *P. putida* KT2440 and SEM10 fed-batch cultivations. The first column represents the KT2440 strain (subfigures (a), (c) and (e)) and the second column the SEM10 strain (subfigures (b), (d) and (f)). **(e)** and **(f)** represent the cultivation volume (black) and added glucose (light grey). **(c)** and **(d)** represent CDW (black) and DO (light grey) profiles. **(e)** and **(f)** show the evolution of glucose (black \square), gluconate (dark grey \square) and 2-ketogluconate (light grey \square). Full and dashed lines represent individual replicates. The red dashed lines in all figures represent the onset and the end of the feeding phase.

Chapter 3. However, none of the KT2440 replicates managed to consume all gluconate and 2-ketogluconate prior to the onset of the feeding phase. Figure 5.2 (c) and (d) illustrate the biomass accumulation and DO profiles of the KT2440 and SEM10 fed-batch cultivations, respectively. Biomass accumulated fastest initially before a shift in growth diminished the accumulation rate after approximately 15 h. The DO was depleted at the

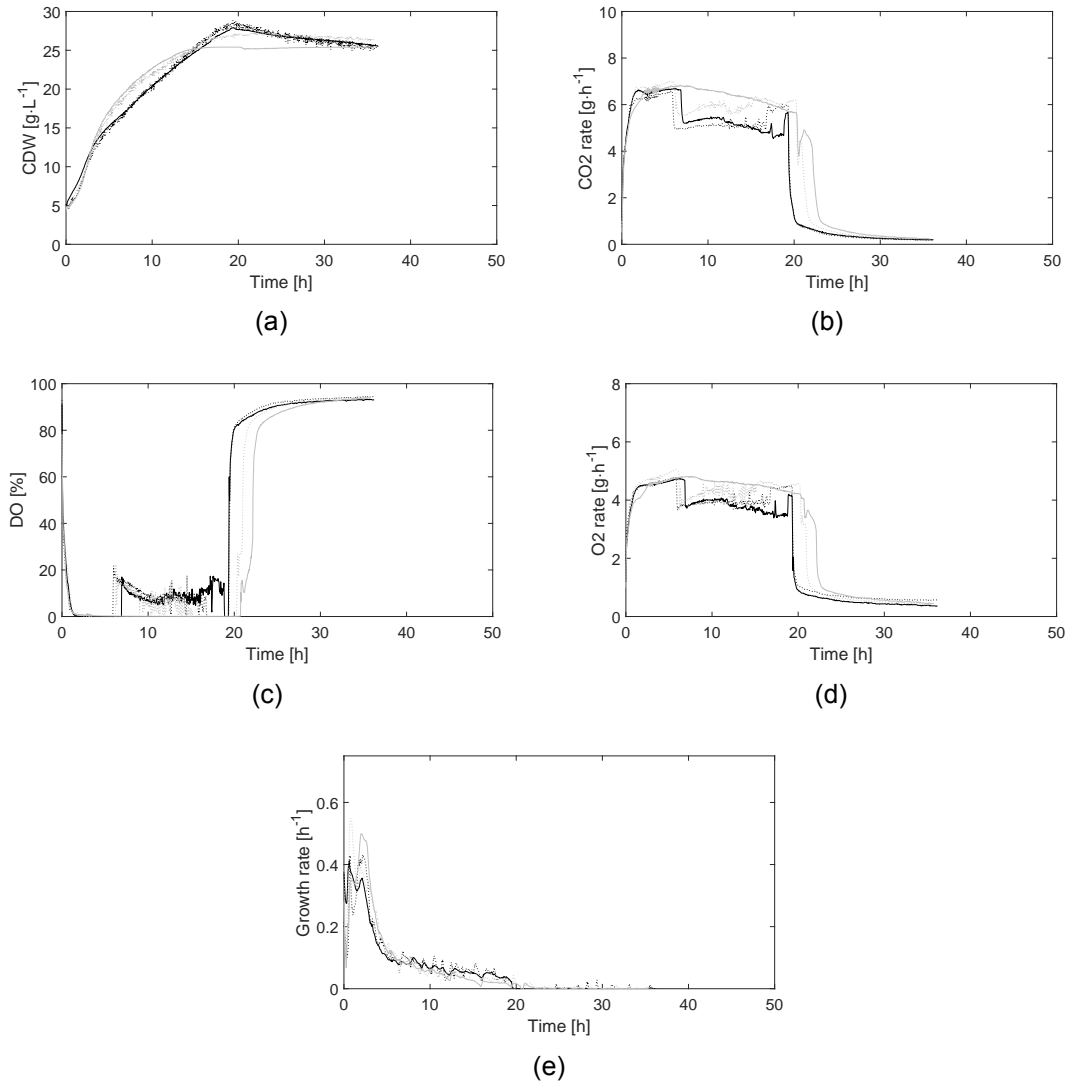


Figure 5.3: Comparison of CDW concentration, DO, gas rates and growth rate of the feeding and stationary phases. Time 0 h is the beginning of the feeding phase. KT2440 is illustrated as black and SEM10 as light grey, line type denotes different replicates. Subfigures illustrate: (a), CDW concentration, (b), CO₂ emission rate (CER), (c), DO, (d), O₂ uptake rate (OUR) and (e), specific growth rate calculated over 10 min. The feeding was stopped after 19.3 h and 20.3 h for KT2440 and SEM10, respectively.

beginning of the feeding phase, before an abrupt increase in the DO was observed around 15 h as presented in Figure 5.2 (c) and (d). After 23 h, both SEM10 strains observed DO limitation, whereas KT2440 did not observe any further DO depletion during the cultivation.

The shift in biomass accumulation and increase in DO, after approximately 6 h of feeding, was accompanied by a drop in oxygen uptake rate (OUR) and CO₂ emission rate (CER)

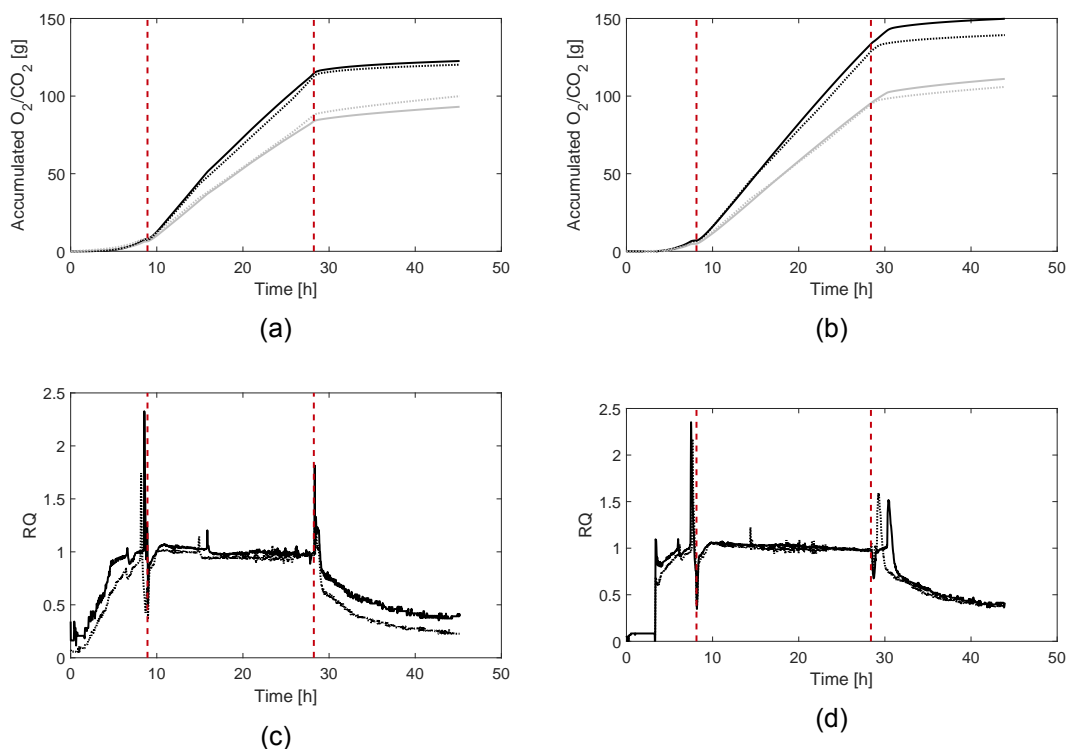


Figure 5.4: Profiles of accumulated gases and the respiratory quotient for *P. putida* KT2440 and SEM10 fed-batch cultivations. The first column represents the KT2440 strain (subfigures (a) and (c)) and the second column the SEM10 strain (subfigures (b) and (d)). **(a)** and **(b)** produced CO₂ (black) and consumed O₂ (light grey) profiles. **(c)** and **(d)** show the evolution of the respiratory quotient (RQ). Full and dashed lines indicate individual replicates.

as presented in Figure 5.3 (b) and (d). This indicated that for the first 6 h of the feeding phase, the cultivation was limited by the oxygen transfer capabilities of the bioreactor. The following increase in DO and reduction of OUR and CER after 6 h indicated that the cultivation was now limited by glucose addition rather than oxygen transfer. Furthermore, it is plausible to assume that glucose had been accumulating for the first 6 h of feeding, as indicated by the DO limitation and the high growth rate in this period. An interesting point to note was the respiratory quotient (RQ) illustrated in Figure 5.4 (c) and (d), which remains mostly constant throughout the feed phase, implying that the switch in limitations and the excess of either oxygen or glucose did not have an apparent effect on the metabolism. The absence of change in the RQ showed that the cultivation was in a pseudo-steady state concerning the conversion of glucose in the periplasm, as *P. putida* mt-2 has different O₂ requirements depending on which of glucose gluconate and 2-ketogluconate is the

primary metabolite to enter the cell [19]. Furthermore, the RQ-value of 1 suggests that no fermentation occurs but only respiration, agreeing with the lack of fermentative pathways of *P. putida* KT2440 [20].

The biomass-specific rates and yields presented in Figure 5.5 were calculated for the feed phase. The biomass-specific rates, presented in Figure 5.5, showed good agreement with the increasing biomass concentration and the decreasing specific growth rate going from oxygen limited to glucose limited cultivation. Furthermore, the q_{O_2} and q_{CO_2} showed a steep increase initially in the feeding phase, indicating that the bacteria required a short adaptation period between the batch and the feeding phase.

The biomass yields on glucose ($Y_{X/S}$) of KT2440 and SEM10 presented in Figure 5.5 were low and did not peak as Y_{X/O_2} and Y_{X/CO_2} as it was calculated based on added glucose rather than actually consumed glucose. The glucose consumption rate was calculated on the feed rate, a method that is only reliable during glucose limitation. In addition, the maximum $Y_{X/S}$ of KT2440 and SEM10 only reaches $0.304 \pm 0.018 \text{ g} \cdot \text{g}^{-1}$ and $0.361 \pm 0.023 \text{ g} \cdot \text{g}^{-1}$, respectively, during the feeding phase. These values are significantly lower than those reported in the literature for KT2440 of $0.41 \text{ g} \cdot \text{g}^{-1}$ (Sun et al. (2006)) and $0.45 \pm 0.02 \text{ g} \cdot \text{g}^{-1}$ (Davis et al. (2015)) [17, 18]. Had $Y_{X/S}$ been calculated on actually consumed glucose, the trend might have looked more similar to the biomass yields on O_2 and CO_2 . The observed decrease seen for all three biomass yields could be related to the biomass yields not being true yields but rather apparent yields. The apparent yield coefficient $Y_{X/S}$ is described as follows by the Herbert-Pirt relation [21]:

$$Y_{X/S} = \frac{\mu}{\frac{\mu}{Y_{X/S}^{true}} + m_S} \quad (5.19)$$

Where $Y_{X/S}$ is the apparent biomass yield coefficient, μ is the specific growth rate, $Y_{X/S}^{true}$ is the true biomass yield coefficient and $m_S \text{ (g S} \cdot \text{(g X} \cdot \text{h)}^{-1})$ is the maintenance coefficient. This correlation shows that the apparent biomass yield on substrate decreases at low specific growth rates, as is the case after glucose limitation occurs.

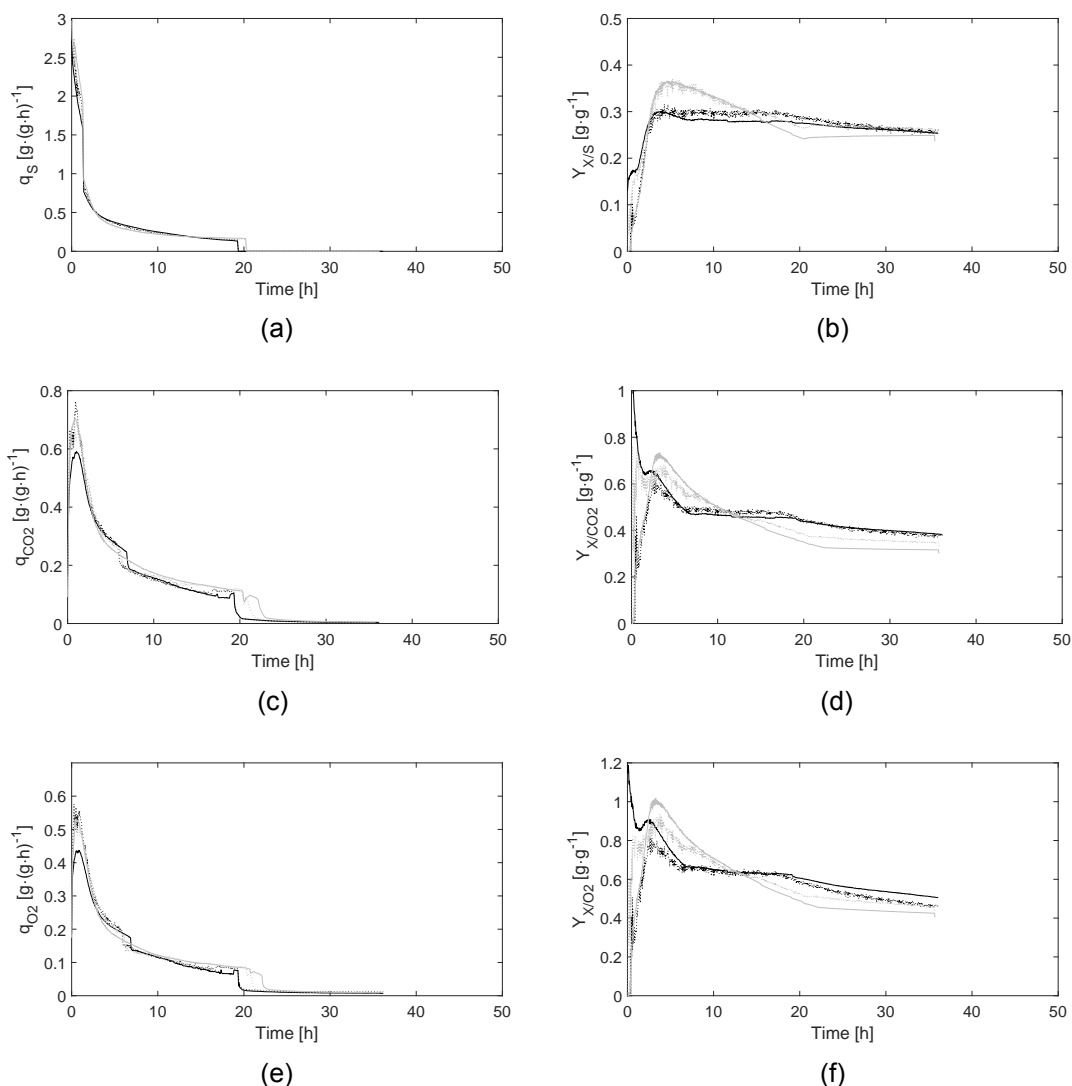


Figure 5.5: Comparison of yields and biomass-specific rate during the feeding and stationary phase. Time 0 h is the beginning of the feeding phase. KT2440 is illustrated as black and SEM10 as light grey, line type denotes different replicates. Subfigures illustrate: (a), q_S , (b), $Y_{X/S}$, (c), q_{CO_2} , (d), Y_{X/CO_2} , (e), q_{O_2} and (f), Y_{X/O_2} . The feeding was stopped after 19.3 h and 20.3 h for KT2440 and SEM10, respectively.

SEM10 performance suffers from dual limitation

Fed-batch cultivation of *P. putida* KT2440 and SEM10 grew similarly, however, a few differences were readily observable. SEM10 accumulated biomass faster initially compared to KT2440, but growth reached a plateau late in the feeding phase as exemplified by the CDW profiles in Figure 5.3 (a) and the growth rate in Figure 5.3 (e). At the same time, KT2440 and SEM10 achieved a maximum $Y_{X/S}$ of $0.304 \pm 0.018 \text{ g} \cdot \text{g}^{-1}$ and $0.361 \pm 0.023 \text{ g} \cdot \text{g}^{-1}$, respectively, during the DO limited growth phase. The better growth of SEM10 ini-

Table 5.1: Cultivation yields and viability of the fed-batches at sampling points during the feeding phase. The noted values are the average and standard deviation of two replicates.

Strain	Time (h)	$Y_{X/S}$ (g·g ⁻¹)	Y_{X/CO_2} (g·g ⁻¹)	Y_{X/O_2} (g·g ⁻¹)	Viability (%)
KT2440	20.70	0.287±0.019	0.637±0.023	0.468±0.026	23.43±3.35
	24.62	0.289±0.015	0.633±0.016	0.468±0.019	26.62±11.03
	28.22	0.284±0.011	0.612±0.024	0.454±0.007	24.11±1.22
SEM10	20.18	0.317±0.012	0.656±0.023	0.470±0.024	31.10±3.44
	23.73	0.290±0.007	0.587±0.012	0.421±0.018	28.57±4.22
	27.33	0.261±0.010	0.520±0.016	0.375±0.016	29.41±10.57

tially, during the period of glucose excess, can be attributed to the genome reduction of the strain, as already described elsewhere for its predecessors EM42 and EM383 in batch cultures [14, 16]. The advantageous growth of SEM10 disappears as the culture endures an apparent dual limitation of both DO and glucose after approximately 6 h of feeding.

The biomass yields on glucose, O₂ and CO₂ followed a similar pattern to the biomass evolution. The yield profiles presented in Figure 5.5 showed that strains saw the highest yield initially in the feeding phase when glucose was accumulating and decreased over the course of the cultivation. However, the yield decrease was more notable for SEM10, which continuously decreased over the feeding phase. SEM10 saw biomass yields decrease by 18-20% between the sample points at 20.2 h and 27.3 h (Table 5.1), whereas KT2440 observed no reduction. In contrast, the biomass-specific rates of the feeding phase presented in Table 5.2 show that SEM10 sees an 18-21% decrease in biomass-specific rates, whereas the biomass-specific rates of KT2440 are reduced by 32-35% between the first and last sample of the feed phase. This shows that while KT2440 continues to grow throughout the feeding phase, SEM10 does not. However, as evident from this and the continued high OUR and CER illustrated in Figure 5.3, the strain showed continued metabolic activity by converting all glucose (Figure 5.2 (f)). *P. putida* KT2440 has been shown to endure repeated short term glucose starvation and retain the intracellular energy levels [12]. Furthermore, it has been shown to endure short term dual glucose and oxygen starvation but not retain intracellular energy levels during starvation [13]. In both

Table 5.2: Biomass-specific rates of the fed-batches at sampling points during the feeding phase. The noted values are the average and standard deviation of two replicates.

Strain	Time (h)	CDW (g·L ⁻¹)	μ (h ⁻¹)	q_s (g·(g·h) ⁻¹)	q_{O_2} (g·(g·h) ⁻¹)	q_{CO_2} (g·(g·h) ⁻¹)
KT2440	20.70	21.99±0.15	0.15±0.02	0.245±0.016	0.110±0.004	0.150±0.008
	24.62	25.64±0.51	0.11±0.01	0.190±0.010	0.087±0.002	0.117±0.005
	28.22	28.15±0.39	0.05±0.00	0.160±0.006	0.075±0.003	0.101±0.001
SEM10	20.18	23.71±0.40	0.08±0.02	0.223±0.008	0.108±0.003	0.150±0.007
	23.73	25.66±0.52	0.15±0.01	0.192±0.004	0.095±0.002	0.132±0.006
	27.33	26.15±1.04	0.05±0.00	0.175±0.004	0.088±0.001	0.122±0.005

studies, the starvation was only temporary and the bacteria could recuperate between periods of starvation. In contrast, during the fed-batch cultivation of SEM10, both glucose and oxygen were limited for a prolonged time, not allowing the strain the opportunity to recuperate. The prolonged exposure to the dual limitation might have triggered the stringent response, seizing growth in SEM10. This was further supported by the finding of Vogeleer and L  tisse (2022) that *P. putida* KT2440 was still metabolically active during stringent response induction [22]. The above highly suggests that *P. putida* SEM10 was not able to withstand prolonged dual limitation of glucose and oxygen.

Inspection of the DO, OUR and CER in Figure 5.4 showed that SEM10 was still metabolically active for 1-2 h after the feed had been stopped, even though the cultivation was glucose limited. This phenomenon could be explained by the accumulation of polyhydroxyalkanoates (PHA) as *P. putida* KT2440 has been shown to accumulate PHA under nutrient limitation and stressful conditions [7, 13]. As such, SEM10 might have accumulated some amount of PHA during the continued glucose and oxygen limitation that was thus consumed after the end of the feeding phase explaining the extended metabolic activity of SEM10.

Culture viability decreases during the feeding phase

Figure 5.6 (c) and (d) showed that the viability of both KT2440 and SEM10 were higher during the batch phase compared to the feeding phase. Mid-batch phase SEM10 observed a viability of 69.48±8.14% and a maximum viability of 31.10±3.44% during the feeding phase (Table 5.1). Similarly, KT2440 observed a viability of 45.46±6.43% mid-

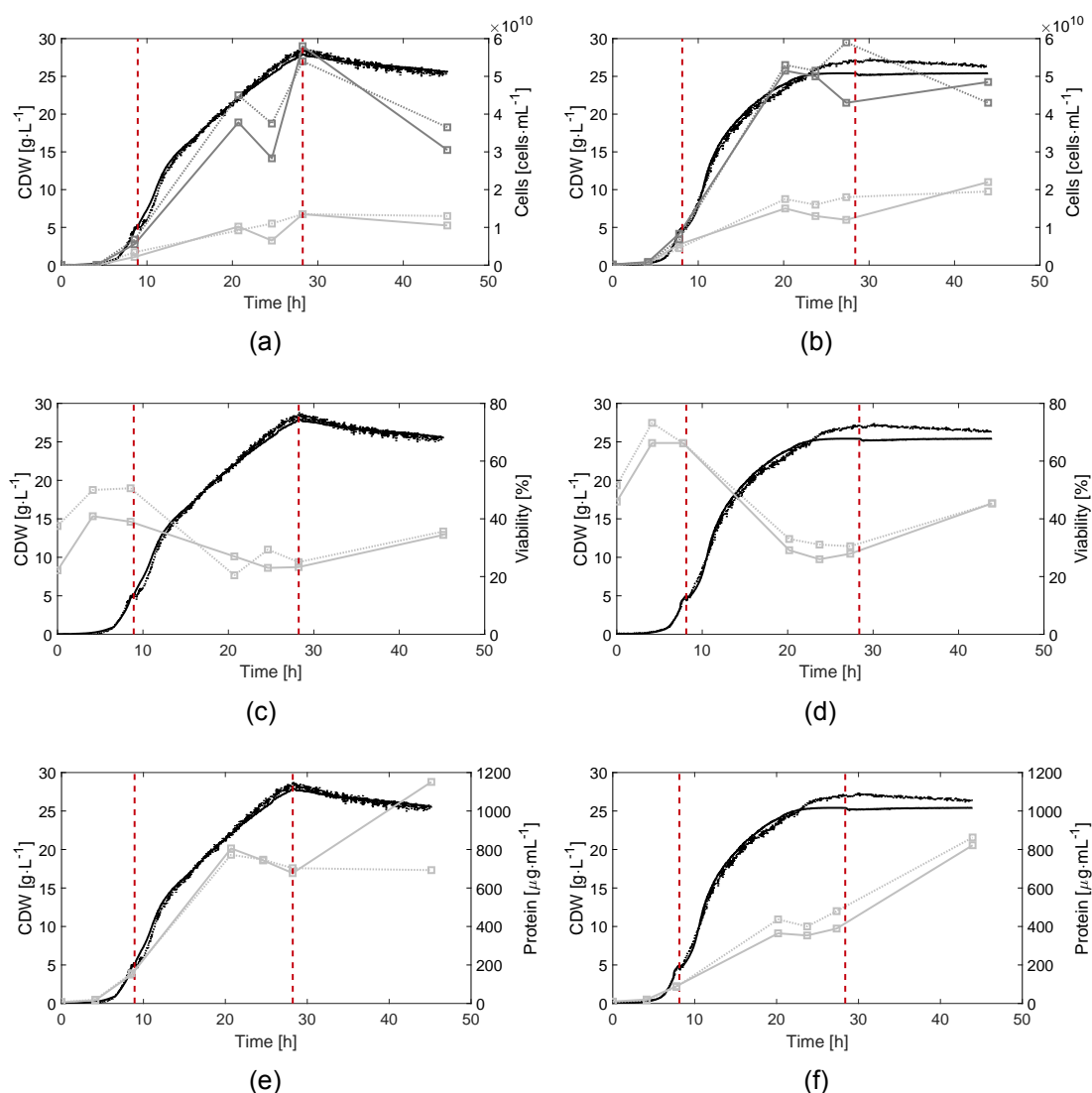


Figure 5.6: Culture viability and extracellular protein accumulation of *P. putida* KT2440 and SEM10 fed-batch cultivations. The first column represents the KT2440 strain (sub-figures (a), (c) and (e)) and the second column the SEM10 strain (subfigures (b), (d) and (f)). **(a)** and **(b)** represent CDW concentration (black) total cell concentration (dark grey \square) and live cell concentration (light grey \square). **(c)** and **(d)** CDW concentration (black) and relative viability (light grey \square). **(e)** and **(f)** CDW concentration (black) and extracellular protein concentration (light grey \square). Full and dashed lines represent individual replicates. The red dashed lines in all figures represent the onset and the end of the feeding phase.

batch phase and a maximum viability of $26.62 \pm 11.03\%$ during the feeding phase (Table 5.1). The superior viability of SEM10 compared to KT2440 during the batch phase agreed with the reported higher viability of EM383 (a SEM10 predecessor) compared to KT2440 in shake flask cultivations [14, 16]. In addition, the reduction in viability from the batch to the feeding phase is most likely a result of either the glucose or the oxy-

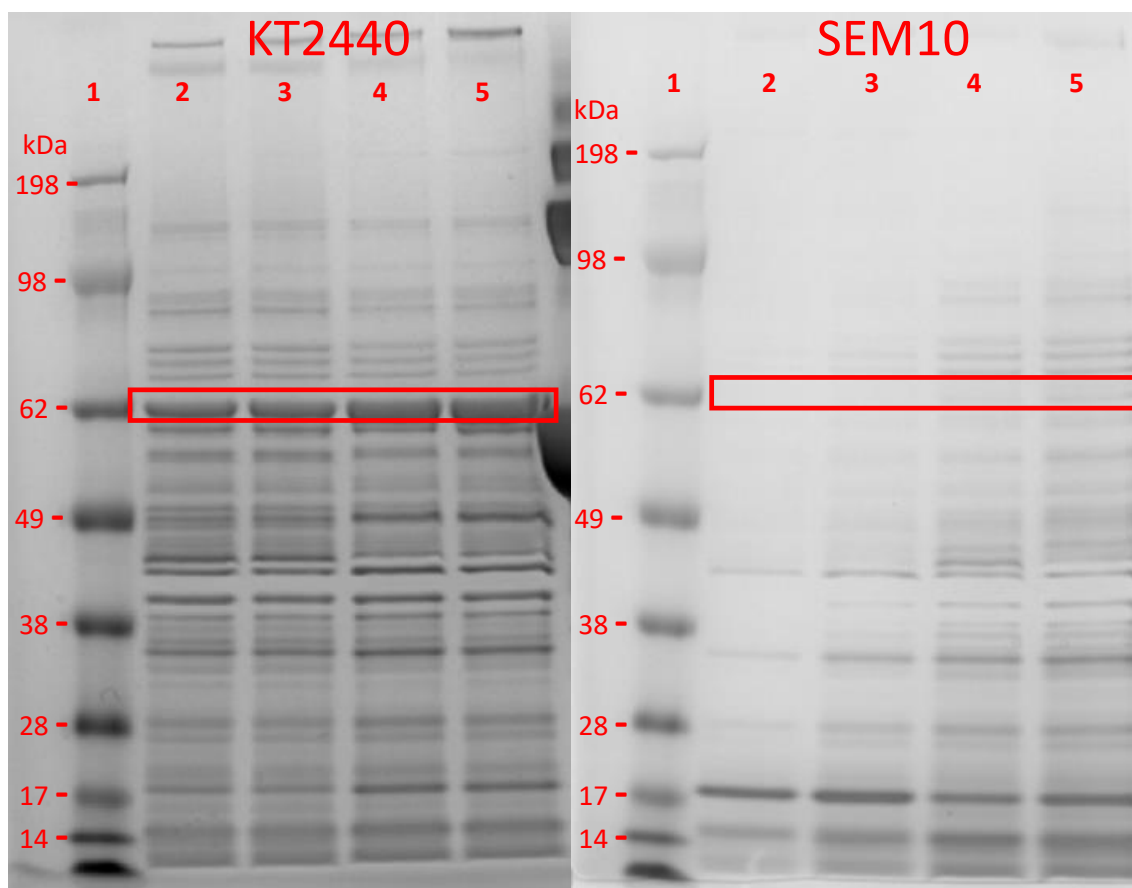


Figure 5.7: LDS-page of the extracellular protein of fed-batch cultivations of KT2440 and SEM10. The left gel shows the samples of KT2440: Column 1 is the protein standard, columns 2 and 3 are samples withdrawn after 28.22 h at the end of the feeding phase and columns 4 and 5 are samples withdrawn after 45.15 h at the end of the cultivation. The right gel shows the samples of SEM10: Column 1 is the protein standard, columns 2 and 3 are samples withdrawn after 27.33 h at the end of the feeding phase and columns 4 and 5 are samples withdrawn after 43.93 h at the end of the cultivation.

gen limitation in this case. Such a decrease in viability during the feeding phase has been reported for *E. coli* in a glucose limited fed-batch [23]. However, the similar viability of KT2440 and SEM10 during the feeding phase agreed with the previous finding that SEM10 was enduring a demanding dual glucose and oxygen limitation during the feeding phase. This further emphasizes the need to ensure sufficient oxygen availability to leverage the genome reduced strain as a *P. putida* platform strain.

Lack of flagellar reduces extracellular protein concentration

Figure 5.6 (e) and (f) showed that KT2440 accumulated more extracellular protein than SEM10 during the feeding phase. KT2440 had accumulated $690.18 \pm 18.14 \mu\text{g} \cdot \text{mL}^{-1}$ protein in the cultivation broth at the end of the feeding phase compared to 479.78 ± 64.14

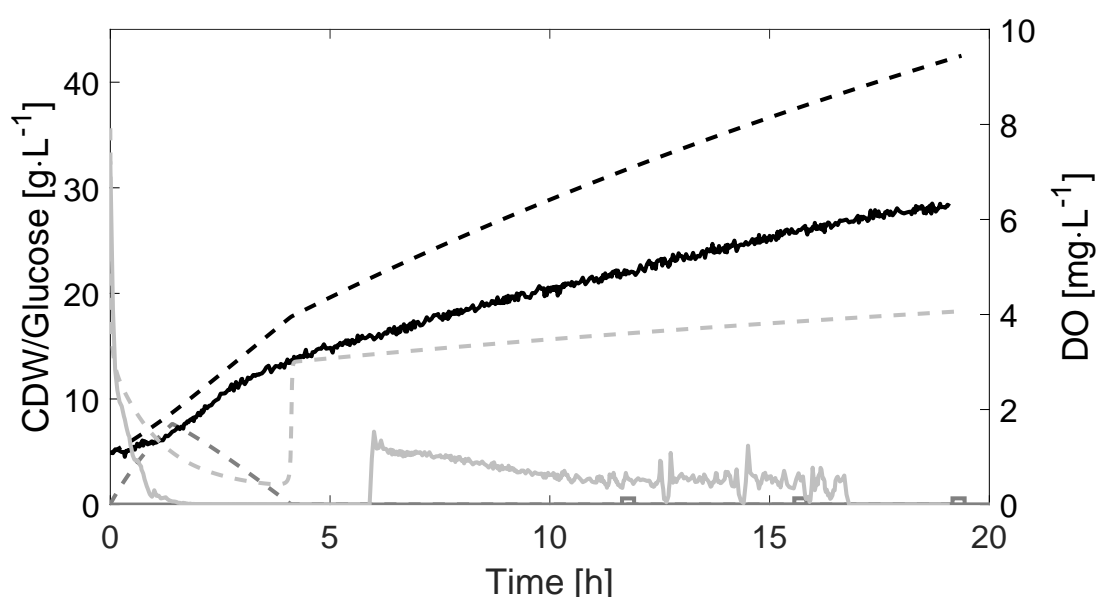


Figure 5.8: Comparison of model prediction and experimental data of the feeding phase, illustrated with a single KT2440 replicate as an example. Experimental data (-) and model prediction (- -). Biomass (black), glucose (dark grey \square) and DO (light grey).

$\mu\text{g}\cdot\text{mL}^{-1}$ by SEM10. LDS-PAGE analysis of samples at the end of the feeding phase and the end of the cultivation was performed to identify the source of the extracellular protein. The wide distribution of the protein sizes for KT2440 and SEM10 presented in Figure 5.7 suggested that the extracellular protein originates from cell lysis. However, as the viability at both sample points were similar (Figure 5.6 (c) and (d)), cell lysis might only partially explain the difference between KT2440 and SEM10. Figure 5.7 shows a missing band around 62 kDa (red box) for SEM10, indicating a distinct difference between the strains protein composition. The size of the missing band is similar to the reported size of 67 kDa for the flagellar of *P. putida* KT442 [24]. This suggested that deletion of the flagellar operon in SEM10 reduced not only futile energy spending but also protein accumulation in the cultivation broth. The reduced protein content in the cultivation broth can be a key advantage of the SEM10 strain as it may facilitate downstream processing.

Model Prediction

The fed-batch model presented in this study was used to tune the PI controller by a manual tuning procedure. The resulting PI parameters were able to control the DO at 20% in the model but not during the actual fed-batch, indicating limitations of either the PI tuning or

the fed-batch model. Calculating the apparent $k_L a$ showed it to be, on average, 465 h^{-1} at the beginning of the feeding phase, 3.5 fold higher than the experimentally determined value (130 h^{-1}) applied for PI tuning. Applying the calculated $k_L a$ to the model resulted in a DO limitation similar to the experiments, indicating that the model input impaired the PI tuning.

By replacing the PI controlled feed rates with the actual feed rates and the experimentally measured $k_L a$ with the calculated, it was possible to evaluate the fed-batch model. The model prediction of *P. putida* KT2440 presented in Figure 5.8 showed biomass, DO and glucose concentration trends similar to the experimental data during the feeding phase. However, it was clear that the model did not sufficiently predict the fed-batch as the model accumulated 52.5% more biomass and DO was never limiting. The higher biomass accumulation predicted by the model could be attributed to the constant yields assumed by the model. A glucose limited fed-batch with a constant feed rate will observe a continuously decreasing specific growth rate as biomass increases, which eventually reduces the apparent biomass yields as described by the Heber-Pirt relation in equation 5.19. Furthermore, including a maintenance term would account for the nutrients allocated for non-growth-related maintenance of the cell. The maintenance demand at the end of the feeding phase would account for a significant 16.9% of the glucose consumption (based on the maintenance glucose demand reported by Lieder et al. (2015)) [16].

The $k_L a$ is known to decrease with increasing viscosity [25, 26]. However, the model applied in this study did not consider the change in viscosity and its effect on $k_L a$. A study by Blunt et al. (2019) with *P. putida* LS46 showed that at $25.3 \text{ g}\cdot\text{L}^{-1}$ of biomass, the viscosity had increased 9 fold and the $k_L a$ decreased by almost 50%, compared to the start of the cultivation [27]. This suggests that assuming a constant $k_L a$ over the course of a high cell concentration cultivation will lead to an overestimation of the oxygen transfer capacity. Together with the constant biomass yields, it clearly showed that for the model to predict the *P. putida* KT2440 fed-batch sufficiently, it must take into account the changing rheology of the cultivation broth in addition to a more dynamic representation of biomass

growth.

5.5 Conclusions

Fed-batch cultivation of the genome reduced SEM10 strain showed promise as anticipated based on previous studies of the SEM10 predecessor in batch cultivations [14, 16]. The strain showed similar growth patterns compared to the wild type KT2440 strain, though improved performance was observed during the first 6 h of the feeding phase. Here SEM10 showed slightly faster growth and obtained a higher maximum $Y_{X/S}$ of $0.361 \pm 0.023 \text{ g} \cdot \text{g}^{-1}$ compared to $0.304 \pm 0.018 \text{ g} \cdot \text{g}^{-1}$ for KT2440 before enduring continuous oxygen limitation later in the feeding phase. Furthermore, SEM10 showed improved characteristics in the batch phase, where especially a higher viability of $69.48 \pm 8.14\%$ was apparent compared to $45.46 \pm 6.43\%$ for KT2440. However, a continuous limitation of both glucose and oxygen seemingly impaired the growth of SEM10 during the later part of the feeding phase. It highlighted the importance of supplying sufficient nutrients to maintain a healthy bacterial population.

The extracellular protein content of the cultivation broth was shown to be lower when cultivating SEM10 rather than KT2440. A feature attributed to either less cell lysis or the lack of flagellar on SEM10 cells. As such, the genome reduced strain showed industrial advantages by reducing the futile energy spending and reducing the impact on downstream processing.

The developed model was able to predict the beginning of the feeding phase but was unable to do so for the later parts of the feeding phase. However, the model failed to capture the dynamics of high cell concentrations where the increased biomass concentration leads to changes in the hydrodynamics and the cell growth. This showed that, for the model to predict a high cell concentration *P. putida* fed-batch sufficiently, it had to consider the dynamics of increased cell concentration.

Ultimately the application of SEM10 in the industrially relevant fed-batch cultivation showed promise, though the performance suffered from sub-optimal cultivation conditions. Further

application of the strain requires additional investigation of the cultivation conditions, such as continued oxygen limitation. In addition, the development of an appropriate control and cultivation strategy should be explored to harness the potential of *P. putida* genome reduced strains. Both facets could be facilitated by an improved fed-batch model, which fits the experimental environment and elaborates on deeper cellular interactions.

References

- [1] Burk, M. J. and Dien, S. V. “Biotechnology for Chemical Production: Challenges and Opportunities”. In: *Trends in Biotechnology* 34 (3 2016), pp. 187–190.
- [2] Lokko, Y., Heijde, M., Schebesta, K., Scholtès, P., Montagu, M. V., and Giacca, M. “Biotechnology and the bioeconomy—Towards inclusive and sustainable industrial development”. In: *New Biotechnology* 40 (2018), pp. 5–10. DOI: 10.1016/j.nbt.2017.06.005.
- [3] Becker, J., Lange, A., Fabarius, J., and Wittmann, C. “Top value platform chemicals: Bio-based production of organic acids”. In: *Current Opinion in Biotechnology* 36 (2015), pp. 168–175. DOI: 10.1016/j.copbio.2015.08.022.
- [4] Calero, P. and Nikel, P. I. “Chasing bacterial chassis for metabolic engineering: a perspective review from classical to non-traditional microorganisms”. In: *Microbial Biotechnology* 12 (1 2019), pp. 98–124. DOI: 10.1111/1751-7915.13292.
- [5] Nikel, P. I. and Lorenzo, V. de. “Pseudomonas putida as a functional chassis for industrial biocatalysis: From native biochemistry to trans-metabolism”. In: *Metabolic Engineering* 50 (May 2018), pp. 142–155. DOI: 10.1016/j.ymben.2018.05.005.
- [6] Poblete-Castro, I., Acuña, J. M. B.-d., Nikel, P. I., Kohlstedt, M., and Wittmann, C. “Host Organism: Pseudomonas putida”. In: Wiley-VCH Verlag GmbH & Co. KGaA, 2016, pp. 299–326. DOI: 10.1002/9783527807796.ch8.
- [7] Weimer, A., Kohlstedt, M., Volke, D. C., Nikel, P. I., and Wittmann, C. “Industrial biotechnology of Pseudomonas putida: advances and prospects”. In: *Applied Microbiology and Biotechnology* 104 (18 2020), pp. 7745–7766. DOI: 10.1007/s00253-020-10811-9.

- [8] Nikel, P. I., Chavarría, M., Danchin, A., and Lorenzo, V. de. "From dirt to industrial applications: *Pseudomonas putida* as a Synthetic Biology chassis for hosting harsh biochemical reactions". In: *Current Opinion in Chemical Biology* 34 (2016), pp. 20–29. DOI: 10.1016/j.cbpa.2016.05.011.
- [9] Tiso, T., Ihling, N., Kubicki, S., Biselli, A., Schonhoff, A., Bator, I., Thies, S., Karmainski, T., Kruth, S., Willenbrink, A. L., Loeschcke, A., Zapp, P., Jupke, A., Jaeger, K. E., Büchs, J., and Blank, L. M. "Integration of Genetic and Process Engineering for Optimized Rhamnolipid Production Using *Pseudomonas putida*". In: *Frontiers in Bioengineering and Biotechnology* 8 (2020). DOI: 10.3389/fbioe.2020.00976.
- [10] Poblete-Castro, I., Rodriguez, A. L., Lam, C. M. C., and Kessler, W. "Improved production of medium-chain-length polyhydroxyalkanoates in glucose-based fed-batch cultivations of metabolically engineered *Pseudomonas putida* strains". In: *Journal of Microbiology and Biotechnology* 24 (1 2014). Look at cites, pp. 59–69. DOI: 10.4014/jmb.1308.08052.
- [11] Hudcova, T., Halecky, M., Kozliak, E., Stiborova, M., and Paca, J. "Aerobic degradation of 2,4-dinitrotoluene by individual bacterial strains and defined mixed population in submerged cultures". In: *Journal of Hazardous Materials* 192 (2 2011), pp. 605–613. DOI: 10.1016/j.jhazmat.2011.05.061.
- [12] Ankenbauer, A., Schäfer, R. A., Viegas, S. C., Pobre, V., Voß, B., Arraiano, C. M., and Takors, R. "*Pseudomonas putida* KT2440 is naturally endowed to withstand industrial-scale stress conditions". In: *Microbial Biotechnology* 13 (4 2020), pp. 1145–1161. DOI: 10.1111/1751-7915.13571.
- [13] Demling, P., Ankenbauer, A., Klein, B., Noack, S., Tiso, T., Takors, R., and Blank, L. M. "*Pseudomonas putida* KT2440 endures temporary oxygen limitations". In: *Biotechnology and Bioengineering* 118 (12 2021), pp. 4735–4750. DOI: 10.1002/bit.27938.
- [14] Martínez-García, E., Nikel, P. I., Aparicio, T., and Lorenzo, V. de. "Pseudomonas 2.0: Genetic upgrading of *P. putida* KT2440 as an enhanced host for heterologous gene

- expression". In: *Microbial Cell Factories* 13 (1 2014), pp. 1–15. DOI: 10.1186/s12934-014-0159-3.
- [15] Volke, D. C., Friis, L., Wirth, N. T., Turlin, J., and Nikel, P. I. "Synthetic control of plasmid replication enables target- and self-curing of vectors and expedites genome engineering of *Pseudomonas putida*". In: *Metabolic Engineering Communications* 10 (January 2020), e00126. DOI: 10.1016/j.mec.2020.e00126.
- [16] Lieder, S., Nikel, P. I., Lorenzo, V. de, and Takors, R. "Genome reduction boosts heterologous gene expression in *Pseudomonas putida*". In: *Microbial Cell Factories* 14 (1 2015), pp. 1–14. DOI: 10.1186/s12934-015-0207-7.
- [17] Sun, Z., Ramsay, J. A., Guay, M., and Ramsay, B. A. "Automated feeding strategies for high-cell-density fed-batch cultivation of *Pseudomonas putida* KT2440". In: *Applied Microbiology and Biotechnology* 71 (4 2006), pp. 423–431. DOI: 10.1007/s00253-005-0191-7.
- [18] Davis, R., Duane, G., Kenny, S. T., Cerrone, F., Guzik, M. W., Babu, R. P., Casey, E., and O'Connor, K. E. "High cell density cultivation of *Pseudomonas putida* KT2440 using glucose without the need for oxygen enriched air supply". In: *Biotechnology and Bioengineering* 112 (4 2015), pp. 725–733. DOI: 10.1002/bit.25474.
- [19] Tlemçani, L. L., Corroler, D., Barillier, D., and Mosrati, R. "Physiological states and energetic adaptation during growth of *Pseudomonas putida* mt-2 on glucose". In: *Archives of Microbiology* 190 (2 2008), pp. 141–150. DOI: 10.1007/s00203-008-0380-8.
- [20] Nikel, P. I. and Lorenzo, V. de. "Engineering an anaerobic metabolic regime in *Pseudomonas putida* KT2440 for the anoxic biodegradation of 1,3-dichloroprop-1-ene". In: *Metabolic Engineering* 15 (1 2013). AEC ATP/ADP, pp. 98–112. DOI: 10.1016/j.ymben.2012.09.006.
- [21] Pirt, S. J. "The maintenance energy of bacteria in growing cultures". In: *Proceedings of the Royal Society of London. Series B. Biological Sciences* 163 (991 1965), pp. 224–231. DOI: 10.1098/rspb.1965.0069.

- [22] Vogeleeer, P. and Létisse, F. “Dynamic Metabolic Response to (p)ppGpp Accumulation in *Pseudomonas putida*”. In: *Frontiers in Microbiology* 13 (Apr. 2022). DOI: 10.3389/fmicb.2022.872749.
- [23] Hewitt, C. J., Caron, G. N.-V., Nienow, A. W., and McFarlane, C. M. “The use of multi-parameter flow cytometry to compare the physiological response of *Escherichia coli* W3110 to glucose limitation during batch, fed-batch and continuous culture cultivations”. In: *Journal of Biotechnology* 75 (1999), pp. 251–264.
- [24] Wang, J., Ma, W., Wang, Y., Lin, L., Wang, T., Wang, Y., Li, Y., and Wang, X. “Deletion of 76 genes relevant to flagella and pili formation to facilitate polyhydroxyalkanoate production in *Pseudomonas putida*”. In: *Applied Microbiology and Biotechnology* 102 (24 2018), pp. 10523–10539. DOI: 10.1007/s00253-018-9439-x.
- [25] Villadsen, J., Nielsen, J., and Lidén, G. *Bioreaction Engineering Principles*. Springer US, 2011. DOI: 10.1007/978-1-4419-9688-6.
- [26] Martín, M., Montes, F. J., and Galán, M. A. “Mass transfer rates from bubbles in stirred tanks operating with viscous fluids”. In: *Chemical Engineering Science* 65 (12 2010), pp. 3814–3824. DOI: 10.1016/j.ces.2010.03.015.
- [27] Blunt, W., Gaugler, M., Collet, C., Sparling, R., Gapes, D. J., Levin, D. B., and Cicek, N. “Rheological behavior of high cell density *pseudomonas putida* ls46 cultures during production of medium chain length polyhydroxyalkanoate (PHA) polymers”. In: *Bioengineering* 6 (4 Dec. 2019). DOI: 10.3390/bioengineering6040093.

6 Conclusions

This thesis sought to advance *P. putida* as a production host by evaluating the genome reduced SEM10 strain under industrially relevant conditions. This was achieved by (1) cultivating the *P. putida* wild type strain KT2440 and the genome reduced strain SEM10 on glucose at low oxygen supply to mimic mass transfer limitations at industrial scale, (2) developing and evaluating a fed-batch medium based on nutritional requirements and (3) applying said medium in a fed-batch cultivation.

Variation in oxygen supply by altering either power input (agitation) or the oxygen partial pressure (pO_2), showed significant effects on both the wild type (KT2440) and genome reduced (SEM10) strains. In *P. putida* KT2440 shake flask cultivations, different agitation speeds did not result in any distinct difference in the biomass profiles. However, the μ_{max} was significantly reduced at low (80 rpm) and high (280 rpm) agitation speeds by 4.32% and 11.53%, respectively, compared to $0.694 \pm 0.11 \text{ h}^{-1}$ at the intermediate agitation speed of 180 rpm. This suggests that both low oxygen transfer rates and mechanical stress could affect the growth of *P. putida* KT2440. The Biolector system allowed for control of the pO_2 in the cultivation chamber, which enabled investigation of the variation in the oxygen supply without changing the power input. However, cultivation of *P. putida* KT2440 and SEM10 at a high pO_2 of 0.21 atm, corresponding to ambient air, and a medium pO_2 of 0.105 atm showed a small increase in cultivation time. Moreover, it was suggested that the Biolector system was not a suitable system to investigate the effect of reduced oxygen availability on genome reduced SEM10 strain as it appeared to suffer from a growth deficiency. This growth deficiency might be attributed to sedimentation due to the lack of flagellar on the genome reduced strain.

To avoid sedimentation-associated issues, the two strains were cultivated in a bioreactor with 2 L working volume in batch mode cultivations with a high pO_2 of 0.21 atm and a low pO_2 of 0.0525 atm. At high pO_2 , during exponential growth, the genome reduced SEM10 strain grew faster and more efficiently as visible from the 6.38% and 9.93% higher μ_{max}

and $Y_{X/S}$, respectively, compared to the wild type KT2440 ($\mu_{\max} = 0.596 \pm 0.007 \text{ h}^{-1}$ and $Y_{X/S} = 0.413 \pm 0.011 \text{ g} \cdot \text{g}^{-1}$). The superior growth characteristics agreed with previously reported findings for the SEM10 predecessor EM383. During exponential growth at low $p\text{O}_2$ both strains showed an increase in biomass yields on glucose, O_2 and CO_2 compared to growth at high $p\text{O}_2$, but not μ_{\max} as that parameter decreased. Under these conditions, SEM10 showed higher biomass yields compared to KT2440 as exemplified by the 7.72% higher $Y_{X/S}$ of $0.492 \pm 0.016 \text{ g} \cdot \text{g}^{-1}$ and $0.454 \pm 0.017 \text{ g} \cdot \text{g}^{-1}$, respectively. However, when faced with DO limitation at low $p\text{O}_2$, both strains suffered reductions in their overall yields, reaching values similar to growth at high $p\text{O}_2$. Overall, KT2440 reached $Y_{X/S}$ of $0.383 \pm 0.016 \text{ g} \cdot \text{g}^{-1}$ and $0.352 \pm 0.027 \text{ g} \cdot \text{g}^{-1}$ at high and low $p\text{O}_2$, respectively. Similarly, SEM10 achieved overall $Y_{X/S}$ of $0.432 \pm 0.015 \text{ g} \cdot \text{g}^{-1}$ and $0.434 \pm 0.008 \text{ g} \cdot \text{g}^{-1}$ at high and low $p\text{O}_2$, respectively. These findings showed that regardless of the $p\text{O}_2$, the genome reduced strain grew more efficiently compared to the wild type strain. Furthermore, the reduced maintenance requirement of SEM10 was suggested to support growth at DO limitation, which added to the advantageous growth characteristics of genome reduced *P. putida* strains.

A medium for high cell concentration *P. putida* fed-batch cultivations was developed. The nutrient concentrations were based on available nutritional requirements of *P. putida* in literature and the potential process constraints. Major components were investigated for inhibitory effects of *P. putida* strains KT2440 and SEM10. Comparable inhibitory effects were observed for the two tested nitrogen sources, $(\text{NH}_4)_2\text{SO}_4$ and NH_4Cl , which showed significant inhibitory effects at concentrations of 0.484 M nitrogen. As chloride is a strong oxidizer of stainless steel, a regular material of larger bioreactors, it was suggested to use ammonium sulfate as the nitrogen source, considering that both compounds displayed similar inhibition profiles. Furthermore, inhibition by glucose was observed at concentrations exceeding $25 \text{ g} \cdot \text{L}^{-1}$, emphasizing the need to establish a fed-batch cultivation at industrial scale. Thus, the two strong inhibitors, ammonium sulfate and glucose, were suggested to be fed separately. Another significant medium component, phosphorous, showed both inhibitory effects and a tendency to precipitate other media components,

mainly of the TE solution. Therefore, the phosphate buffer concentration should be adjusted to a bare minimum to avoid these effects, and most of the TE should be added through the feed. Lastly, the study showed that the growth on glucose was inhibited at lower pH resulting in a pH optimum between pH 7.0 and 8.0. Neither the wild type KT2440 strain nor the genome reduced SEM10 strain showed considerably better tolerance towards the inhibitory effects of the tested conditions. However, cultivation in the Biolector system might have concealed potential advantages of the genome reduced strain due to sedimentation.

The developed medium was subsequently applied in a fed-batch cultivation of the SEM10 and KT2440 strains. Overall, the strains did not perform too differently, achieving similar final biomass concentrations of $28.15 \pm 0.39 \text{ g} \cdot \text{L}^{-1}$ and $26.15 \pm 1.04 \text{ g} \cdot \text{L}^{-1}$ for KT2440 and SEM10, respectively. However, a difference was observable at the beginning of the feeding phase, where DO was limiting and glucose was in excess, the genome reduced strain more efficiently than the wild type strain, showing a higher growth rate and biomass yield on glucose. Later in the feeding phase, both DO and glucose became limiting for the SEM10 strain and it observed longer continuous periods of substrate limitation. Whereas KT2440 did not observe a continued DO limitation and subsequent growth impairment. Nevertheless, the genome reduced strain showed increased viability in both the batch ($69.48 \pm 8.14\%$) and stationary ($45.35 \pm 0.36\%$) phases compared to the batch ($45.46 \pm 6.43\%$) stationary ($35.08 \pm 6.90\%$) phases for KT2440. The findings indicated that SEM10 performed superior to KT2440 during single limitation of oxygen in the early feeding phase. Lastly, during the fed-batch cultivation, SEM10 accumulated less extracellular protein compared to KT2440, presumably due to the lack of the flagellar on the genome reduced strain. This trait could facilitate the downstream processing of future processes applying the genome reduced strain.

The above highly suggests that the genome reduced *P. putida* strain, SEM10, is superior to the wild type strain, KT2440, under industrially relevant conditions considering the superior growth characteristics at low oxygen availability identified during both batch

and fed-batch cultivations. This highlights the importance of further development of the *P. putida* genome reduced strains and continued research on how *P. putida* endures conditions relevant to industrial applications.

7 Future work

This work on the glucose metabolism of *P. putida* at varying oxygen availability, presents a decent overview of how the species behave under such conditions. However, the conversion of glucose through the oxidative pathway in the periplasm has been reported to be DO dependent, changing the extent to which glucose, gluconate and 2-ketogluconate accumulate [1, 2]. In addition, the growth rate and biomass yields depend on whether glucose, gluconate or 2-ketogluconate are the dominant entry point to the metabolism [3]. These observations suggest that glucose metabolism could be affected by potential gradients in an industrial-scale bioreactor. Studies by Ankenbauer et al. (2020) and Demling et al. (2021) have shown that *P. putida* KT2440 can endure temporal glucose and DO limitation of 2.6 minutes. However, they do not elaborate on the specific conversion in the periplasm [2, 4]. To gain further insights into how glucose is metabolized in the periplasm, one could resolve the fluxes with ^{13}C labeling at known DO concentrations. This would estimate the conversion and uptake fluxes of glucose, gluconate and 2-ketogluconate. This could be coupled with, or replaced by, measurements of the activity and concentrations of the catalytic enzymes in batch or chemostat cultivations, enabling the calculation of the conversion rates at distinct time points and conditions. The latter could provide insights into the dynamics of glucose metabolism rather than a single time point, which is typical for ^{13}C labeling experiments [5, 6]. DO dependent glucose conversion would affect the energy and redox states of cells, which should be measured concurrently with the enzyme assays [2, 5]. Such measurements enable evaluation of how the co-factor supply is affected by DO concentration and facilitate the development of appropriate cultivation control strategies.

The above only represents the behavior in a well-defined environment that is not similar to the expected heterogeneous environment at industrial-scale. Two options are available to investigate the transient effects of gradients on the glucose metabolism of *P. putida*: (1) coupling kinetics to a computational fluid dynamic (CFD) model or (2) applying the bac-

terium in a scale-down system. The latter has been performed for *P. putida* KT2440 in a system, operating at a steady state, consisting of a stirred tank bioreactor connected to a plug flow bioreactor (PFR). Along the PFR, there was no addition of oxygen or glucose inducing temporary dual glucose and DO starvation. During the induced dual starvation, the energy charge was shown to drop [2]. However, the study did not investigate if or how the periplasmic glucose conversion changed as a result of the limitations. The former option, coupling a kinetic model to Lagrangian lifelines of a CFD model, enables a more detailed investigation of how the uptake and conversion of glucose through the oxidative pathway in the periplasm might change and affect the cell as a consequence of its cultivation history [7, 8].

Further development and benchmarking of the genome reduced strain would be paramount for the maturation of *P. putida* as an industrial production host. To ensure that the genetic streamlining of SEM10 is, in fact, advantageous in an industrial environment, it will be necessary to further benchmark the strain against the wild type KT2440 under industrially relevant conditions. Accordingly, evaluation of SEM10 under both glucose and DO limitation in scale-down systems, as reported elsewhere for KT2440, will provide a solid foundation to assess the characteristics of SEM10 under industrially relevant conditions [2, 4]. SEM10 has already been upgraded from a safety and genetic engineering perspective in addition to optimization of the energy spending [9, 10]. Identifying additional genes that are unnecessary in a cultivation environment and are potentially futile energy sinks can help reduce the energy demand of *P. putida* and increase substrate conversion efficiency. Either rational selection of targets or randomized deletions could be applied to achieve this goal [9, 11]. However, it will be essential to ensure that an increased implementation of deletions does not affect the cell fitness, especially in a bioreactor environment [12].

The genome reduced strain has a lower DNA content and does not produce flagellar, which both contain phosphorous and/or nitrogen, reducing the potential requirement of those elements. The nutritional requirement of SEM10 for phosphorous and nitrogen

should be determined for the strain to facilitate medium optimization. A potential reduction in consumption of the two major medium components can be an additional advantage combined with the more efficient use of glucose in order to reduce medium costs. This is an important aspect in the production of low-value products, where medium costs are often the major contributor to the overall production price. Further investigation of the requirement for the TE solution's individual elements could reveal these elements' critical concentration limits. The critical concentration limits can serve as a foundation for further development of a reliable cultivation medium for application in research centered around *P. putida*. In addition, it would provide a guideline to ensure sufficient minor elements are supplied to industrial production.

References

- [1] Choi, W. J., Lee, E. Y., and Choi, C. Y. "Effect of dissolved oxygen concentration on the metabolism of glucose in *Pseudomonas putida* BM014". In: *Biotechnology and Bioprocess Engineering* 3 (2 1998), pp. 109–111. DOI: 10.1007/BF02932512.
- [2] Demling, P., Ankenbauer, A., Klein, B., Noack, S., Tiso, T., Takors, R., and Blank, L. M. "*Pseudomonas putida* KT2440 endures temporary oxygen limitations". In: *Biotechnology and Bioengineering* 118 (12 2021), pp. 4735–4750. DOI: 10.1002/bit.27938.
- [3] Tlemçani, L. L., Corroler, D., Barillier, D., and Mosrati, R. "Physiological states and energetic adaptation during growth of *Pseudomonas putida* mt-2 on glucose". In: *Archives of Microbiology* 190 (2 2008), pp. 141–150. DOI: 10.1007/s00203-008-0380-8.
- [4] Ankenbauer, A., Schäfer, R. A., Viegas, S. C., Pobre, V., Voß, B., Arraiano, C. M., and Takors, R. "*Pseudomonas putida* KT2440 is naturally endowed to withstand industrial-scale stress conditions". In: *Microbial Biotechnology* 13 (4 2020), pp. 1145–1161. DOI: 10.1111/1751-7915.13571.
- [5] Nikel, P. I., Chavarría, M., Fuhrer, T., Sauer, U., and Lorenzo, V. de. "*Pseudomonas putida* KT2440 Strain Metabolizes Glucose through a Cycle Formed by Enzymes

- of the Entner-Doudoroff, Embden-Meyerhof-Parnas, and Pentose Phosphate Pathways". In: *Journal of Biological Chemistry* 290 (43 2015), pp. 25920–25932. DOI: 10.1074/jbc.M115.687749.
- [6] Kohlstedt, M. and Wittmann, C. "GC-MS-based ¹³ C metabolic flux analysis resolves the parallel and cyclic glucose metabolism of *Pseudomonas putida* KT2440 and *Pseudomonas aeruginosa* PAO1". In: *Metabolic Engineering* 54 (January 2019), pp. 35–53. DOI: 10.1016/j.ymben.2019.01.008.
- [7] Wang, J., Ma, W., Wang, Y., Lin, L., Wang, T., Wang, Y., Li, Y., and Wang, X. "Deletion of 76 genes relevant to flagella and pili formation to facilitate polyhydroxyalkanoate production in *Pseudomonas putida*". In: *Applied Microbiology and Biotechnology* 102 (24 2018), pp. 10523–10539. DOI: 10.1007/s00253-018-9439-x.
- [8] Haringa, C., Tang, W., Wang, G., Deshmukh, A. T., Winden, W. A. van, Chu, J., Gulik, W. M. van, Heijnen, J. J., Mudde, R. F., and Noorman, H. J. "Computational fluid dynamics simulation of an industrial *P. chrysogenum* fermentation with a coupled 9-pool metabolic model: Towards rational scale-down and design optimization". In: *Chemical Engineering Science* 175 (2018), pp. 12–24. DOI: 10.1016/j.ces.2017.09.020.
- [9] Martínez-García, E., Nikel, P. I., Aparicio, T., and Lorenzo, V. de. "Pseudomonas 2.0: Genetic upgrading of *P. putida* KT2440 as an enhanced host for heterologous gene expression". In: *Microbial Cell Factories* 13 (1 2014), pp. 1–15. DOI: 10.1186/s12934-014-0159-3.
- [10] Volke, D. C., Friis, L., Wirth, N. T., Turlin, J., and Nikel, P. I. "Synthetic control of plasmid replication enables target- and self-curing of vectors and expedites genome engineering of *Pseudomonas putida*". In: *Metabolic Engineering Communications* 10 (January 2020), e00126. DOI: 10.1016/j.mec.2020.e00126.
- [11] Vernyik, V., Karcagi, I., Tímár, E., Nagy, I., Györkei, Á., Papp, B., Györfy, Z., and Pósfai, G. "Exploring the fitness benefits of genome reduction in *Escherichia coli* by a selection-driven approach". In: *Scientific Reports* 10 (1 2020). DOI: 10.1038/s41598-020-64074-5.

- [12] Karcagi, I., Draskovits, G., Umenhoffer, K., Fekete, G., Kovács, K., Méhi, O., Balikó, G., Szappanos, B., Györfy, Z., Fehér, T., Bogos, B., Blattner, F. R., Pál, C., Pósfai, G., and Papp, B. “Indispensability of Horizontally Transferred Genes and Its Impact on Bacterial Genome Streamlining”. In: *Molecular Biology and Evolution* 33 (5 2016), pp. 1257–1269. DOI: 10.1093/molbev/msw009.

PROSYS

Department of Chemical and Biochemical Engineering

Technical University of Denmark

Søltofts Plads, Building 228A

2800 Kgs. Lyngby

Tlf. +45 4525 2822

www.kt.dtu.dk